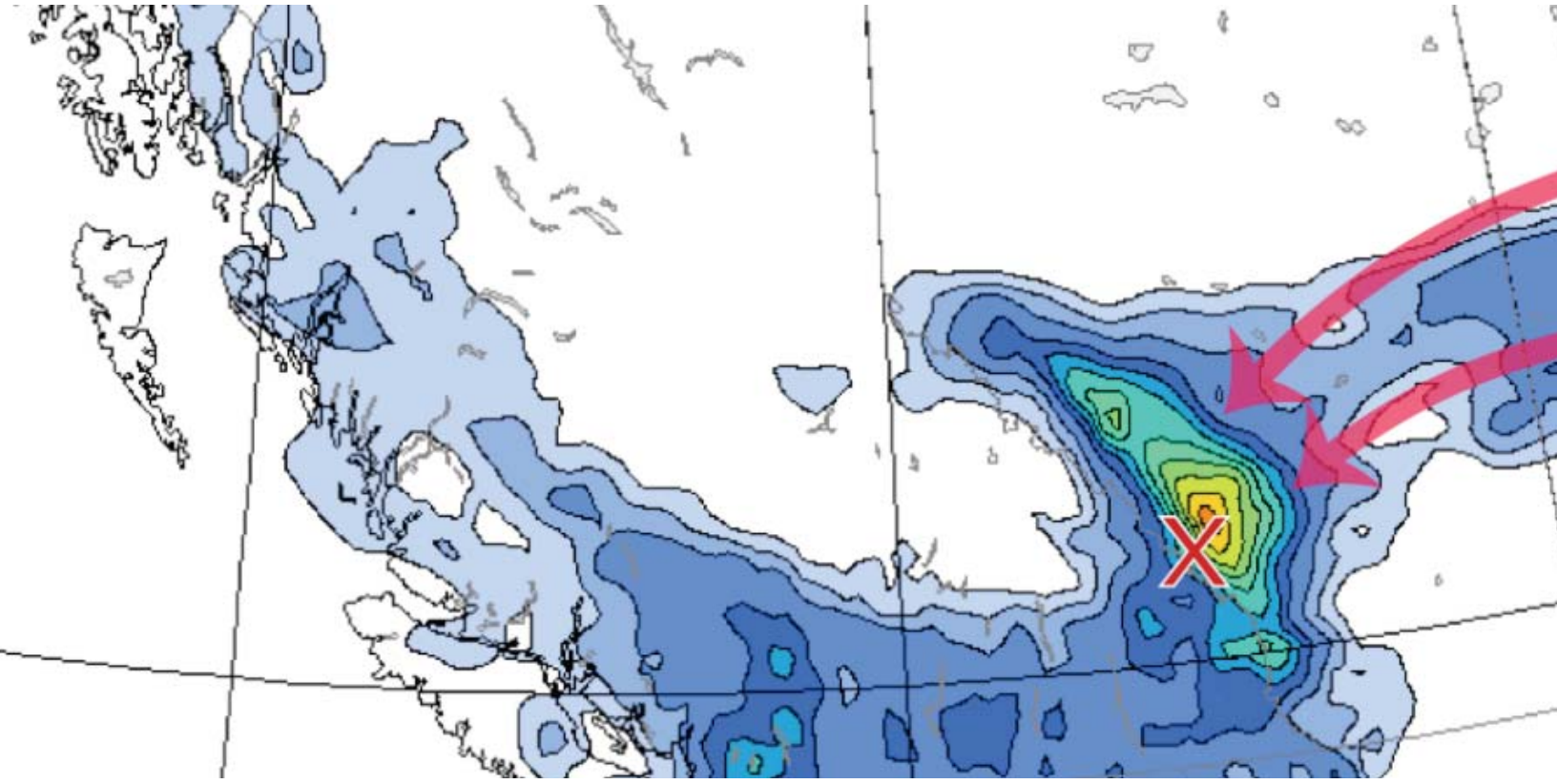

# COUGAR CREEK FORENSIC ANALYSIS, HYDROCLIMATIC ANALYSIS OF THE JUNE 2013 STORM

FINAL REPORT

PROJECT No: 1261-001

Document No: TC13-005

August 1, 2014

BGC ENGINEERING INC.
AN APPLIED EARTH SCIENCES COMPANY

# TOWN OF CANMORE

# COUGAR CREEK FORENSIC ANALYSIS

# HYDROCLIMATIC ANALYSIS OF THE JUNE 2013 STORM

## FINAL

| | | | |
|---|---|---|---|
| PROJECT NO.: | 1261-001-04 | DISTRIBUTION: | |
| DATE: | August 1, 2014 | RECIPIENT: | 3 copies |
| DOCUMENT NO.: | TC13-005 | BGC: | 2 copies |

BGC ENGINEERING INC.
AN APPLIED EARTH SCIENCES COMPANY
Suite 800 - 1045 Howe Street
Vancouver, BC Canada V6Z 2A9
Telephone (604) 684-5900
Fax (604) 684-5909

August 1, 2014
Project No.: 1261-001-04

Mr. Andy Esarte, P.Eng.
Engineering Services, Town of Canmore
902 7th Avenue
Canmore, AB, T1W 3K1

Dear Andy,

**Re: Cougar Creek Hydroclimatic Analysis of the June 2013 Storm – FINAL**

Please find attached the above referenced final report. It has been a pleasure to prepare this information and we look forward to continuing work with the Town of Canmore.

Yours sincerely,

**BGC ENGINEERING INC.**
**per:**

ISSUED AS DIGITAL DOCUMENT.
SIGNED HARDCOPY ON FILE WITH
BGC ENGINEERING INC.

Matthias Jakob, Ph.D., P.Geo.
Senior Geoscientist and Project Manager

# EXECUTIVE SUMMARY

On June 19 to 21, 2013, heavy rainfall in the Canmore area, combined with snowmelt at higher elevations, initiated flooding, debris floods and debris flows on the Bow River and its tributaries. BGC has been retained for forensic analyses of ten creeks within the Town boundary, as well as a detailed hazard and risk assessment for Cougar Creek. As part of the forensic analyses, the Town requested that BGC summarize the hydroclimatic conditions of the June 2013 flood event.

The Meteorological Service of Canada Kananaskis climate station has the longest data record in the region. Record-breaking 1-day, 2-day and 3-day rainfall values were measured at this station during the storm. The 1-day maximum rainfall was 75% greater than the long-term average rain for the month of June. Frequency estimates indicate that the amount of rainfall that fell during the storm had a return period ranging from 235- to 575-years. Rainfall volume over the entire Cougar Creek watershed is estimated at 9.1 $Mm^3$ (millions of cubic metres) over three days.

Antecedent moisture conditions in the Cougar Creek watershed appear to have been elevated prior to the arrival of the June 19, 2013 storm. Combined with observations of frozen soils at higher elevations and abundant bedrock outcrops, these conditions suggest that a high percentage of the total rainfall generated runoff. Analysis of regional snow pillow data indicates that as much as two thirds of the 42 $km^2$ Cougar Creek catchment may have been covered in snow immediately prior to the rainfall. Analysis of snow data suggests that the additional snowmelt contributed between 12 to 29% of total runoff.

Real-time flow estimates during the June 2013 event are the largest on record for the Bow River at Banff and Waiparous Creek hydrometric stations, although the Waiparous gauge was damaged during the flood and did not record the peak flow. Peak flow estimates were 439 $m^3/s$ for Bow River and 306 $m^3/s$ for Waiparous Creek before its gauge stopped recording. A flood frequency analysis using the measured peak flow data on record at the Banff gauge indicates that the rainfall led to a 200 to 400-year return period flow on Bow River. Adding historical floods, recorded in Calgary and prorated to Banff, the return period of the 2013 flood on Bow River decreases to a 15- to 20-year return period. The Waiparous Creek 2013 flood event had a 40- to 60-year return period given available data.

A preliminary trend analysis of relatively long-term rainfall and streamflow records suggests that more frequent and perhaps more intensive rainfall and small-watershed floods and debris floods should be anticipated in the Canmore region in the future. However, it is challenging to attribute the frequency and magnitude results provided in this report to global warming with certainty.

# TABLE OF CONTENTS

# LIST OF TABLES



# LIST OF FIGURES

## LIST OF APPENDICES



## LIST OF DRAWINGS

# LIMITATIONS

BGC Engineering Inc. (BGC) prepared this document for the account of Town of Canmore. The material in it reflects the judgment of BGC staff in light of the information available to BGC at the time of document preparation. Any use which a third party makes of this document or any reliance on decisions to be based on it is the responsibility of such third parties. BGC accepts no responsibility for damages, if any, suffered by any third party as a result of decisions made or actions based on this document.

As a mutual protection to our client, the public, and ourselves, all documents and drawings are submitted for the confidential information of our client for a specific project. Authorization for any use and/or publication of this document or any data, statements, conclusions or abstracts from or regarding our documents and drawings, through any form of print or electronic media, including without limitation, posting or reproduction of same on any website, is reserved pending BGC's written approval. If this document is issued in an electronic format, an original paper copy is on file at BGC and that copy is the primary reference with precedence over any electronic copy of the document, or any extracts from our documents published by others.

# 1.0 INTRODUCTION

On June 19 to 21, 2013, heavy rainfall in the Canmore area combined with snowmelt at higher elevations initiated flooding, debris floods and debris flows on the Bow River and its tributaries. Extensive damage resulted to buildings, creek crossings, roads, the Trans-Canada Highway, railways and other infrastructure in Canmore and surrounding areas.

In response to these events, the Town of Canmore ("Town") issued a Request for Information (RFI) for specialized engineering expertise in the areas of hydrotechnical and geotechnical engineering, geohazards and debris flows, and GIS and remote sensing. BGC has been retained for forensic analyses of ten creeks within the Town boundary, as well as detailed hazard and risk assessments for Cougar, Three Sisters, Stone and Stoneworks Creeks. As part of the forensic analyses, the Town requested that BGC summarize the hydroclimatic conditions of the June 2013 flood event. An understanding of the hydroclimatic conditions is of importance for the following reasons:

- Understand the severity of the storm in terms of its return period for hazard and risk assessment purposes
- Potentially design an appropriate regional-scale warning system for similar events
- Examine if heavy rainfall events are becoming more frequent as suggested by climate change literature (IPCC, 2012)

This report provides an analysis of regional climate and streamflow data to characterize the June 19-21, 2013 rainstorm in the Canmore area. A primary objective of the analysis is to determine the severity of the 2013 storm and estimate the return period of the associated rainfall and runoff. The present report is structured as follows:

- Section 2 summarizes rainfall data observed at various climate stations near Canmore
- Section 3 summarizes available snowpack data and the contribution of snowmelt to streamflow
- Section 4 summarizes available streamflow data
- Section 5 discusses the potential effects of climate change on future rainfall events and peak flows
- Section 6 provides a summary of results and conclusions.

Appendix A is a report compiled by the Geophysical Disaster Computational Fluid Dynamics Centre (GDCFDC)at the Department of Earth and Ocean Sciences at the University of British Columbia that describes the June 2013 storm's synoptic scale meteorological conditions. It explains how a low-pressure system originating over the Pacific Ocean brought moist air and precipitation to the Bow River watershed.

Appendix B is a report prepared at the Department of Statistics at the University of British Columbia that describes a return level trend analysis using non-stationarity techniques for 3-day rainfall annual maxima recorded at the Meteorological Service of Canada Kananaskis climate station.

Appendix C constitutes a report prepared by the GDCFDC, describing the spatial and temporal trends in synoptic-scale storm events that occurred between 1952 and 2013 and produced heavy precipitation.

# 2.0 RAINFALL

## 2.1. Data Sources

Rainfall was recorded in the Canmore region between June 17 and 23, 2013; however the storm was concentrated between June 19 and 21, 2013. Rainfall records were analyzed from various regional data sources that measured precipitation during the event, including the Marmot Research Basin operated by the University of Saskatchewan, four Alberta Environment and Sustainable Resource Development (AESRD) stations, three Meteorological Service of Canada (MSC) stations, and a weather station operated by a private resident on the Cougar Creek fan, Mr. Ben Gadd (Table 2-1). Drawing 1 is a map of the station locations. Of the stations presented in Table 2-1, the following are considered the best analogues for precipitation and temperature conditions in the Cougar Creek watershed at the time of the storm due to proximity and comparable elevation:

- Kananaskis
- Kananaskis Boundary Auto
- Marmot Basin Stations: Fisera Ridge, Upper Clearing, Hay Meadow
- South Ghost Headwaters.

This report heavily relies on data from the Kananaskis station due to its proximity to the study area and its relatively long and continuous record. Climate stations with long records are sometimes moved and their equipment updated, which may challenge the interpretations of statistical analysis of the data. Table 2-2 outlines known location changes of the Kananaskis station that may affect the data records. This information was provided to BGC by the Meteorological Survey of Canada (MSC). Paul Whitfield, Senior Research Fellow of the Centre for Hydrology, University of Saskatchewan at the Coldwater Laboratory, Kananaskis, is preparing an article that will address the changes to the Kananaskis station over time.

**Table 2-1. Regional rainfall data sources.**

| Data Source | Station Name | Station Location (Lat / Long) | Station Elevation (m asl) | Period of Record[1] | Measurement Frequency[1] | Equipment Type |
|---|---|---|---|---|---|---|
| University of Saskatchewan, Marmot Creek Research Basin | Fisera Ridge | 50° 57' 25" N 115° 12' 16" W | 2325 | 2005–2013[2] | 15 minutes | Tipping buckets & Geonor weighing gauge |
| | Upper Clearing | 50° 57' 23.5" N 115° 10' 31" W | 1845 | 2005–2013[2] | 15 minutes | |
| | Hay Meadow | 50° 56' 39" N 115° 8' 20" W | 1437 | 2005–2013[2] | 15 minutes | |
| Gadd Residence, Cougar Creek Fan | n/a | private | 1355 approx. | 2011-2013 | Hourly[3] | Davis "Vantage Vue" tipping spoon; factory calibration |
| Meteorological Service of Canada | Kananaskis | 51°01'39 " N 115°02'05" W | 1391 | 1939-2013 | Daily | Type B standard gauge |
| | Banff CS | 51° 11' 36" N 115° 33' 08" W | 1396 | 1953-2013 | Daily | Geonor weighing gauge |
| | Bow Valley | 51° 05' 00" N 115° 04' 00" W | 1298 | 1963-2013 | Daily | Geonor weighing gauge |
| Alberta Environment and Sustainable Resource Development | Kananaskis Boundary Auto | 50° 55' 48" N 115° 07' 12" W | 1464 | 2005-2013[4] | Hourly | n/a[5] |
| | South Ghost Headwaters | 51° 12' 45" N 115° 10' 19" W | 1684 | 2005-2013 | Hourly | Ott Pluvio 1000 weighing gauge |
| | Ghost Diversion | 51° 17' 24" N 115° 8' 22" W | 1600 | 1984-2013 | Hourly | Ott Pluvio 1000 weighing gauge |
| | Ghost Ranger Station | 51° 19' 24" N 114° 57' 35" W | 1460 | 1984-2013 | Hourly | Ott Pluvio 1000 weighing gauge |

1. Refers to records available at the time of analysis.
2. Alberta Forestry recorded daily and hourly data from 1962-1987 at comparable locations with different equipment.
3. Only the totals were recorded as well as the peak one hour precipitation amount.
4. The data record likely extends farther into the past; however, the online data host only provides data from 2005. The earlier part of the record was not immediately relevant to this study and was not available by the time the report was issued.
5. Not available by the time the report was issued.

**Table 2-2. Location changes to the Kananaskis climate station.**

| Time Frame | Comments |
|---|---|
| Pre-1950 | No location information available. |
| 1950 | Site was located in 23-24-8-W5M (Dominion Land Survey system), near Canoe Meadows. |
| 1955 – 1962 range | Station was moved 3 km south, 100 m SE of existing location. |
| August 1963 | Station was moved to a knoll where the wind tower is today, approximately 200 m NW of current location |
| November 8, 1976 | Station was moved to current location. |

Average monthly precipitation for the Kananaskis and Banff MSC stations is summarized in Table 2-3. These values are based on the 1971-2000 climate normals published by Environment Canada. Climate normals are not available from the Bow Valley station as the record is too fragmented. Average annual precipitation is about 640 mm at Kananaskis and 470 mm at Banff, with 60% of the precipitation occurring between May and September on average. It is suspected that the Banff station underreports due to the datalogger program used since 2007, and therefore, the average annual precipitation value may be lower than the actual value (J. Pomeroy, pers. comm., 2013).

**Table 2-3. Average monthly precipitation at Kananaskis and Banff (1971-2000 climate normals).**

| Station | Average Monthly Precipitation (mm) | | | | | | | | | | | | Annual Total |
|---|---|---|---|---|---|---|---|---|---|---|---|---|---|
| | Jan | Feb | Mar | Apr | May | Jun | Jul | Aug | Sep | Oct | Nov | Dec | |
| Kananaskis | 29 | 27 | 46 | 53 | 92 | 90 | 69 | 73 | 67 | 36 | 28 | 29 | 638 |
| Banff CS | 28 | 22 | 23 | 32 | 60 | 62 | 54 | 60 | 42 | 29 | 27 | 33 | 472 |

## 2.2. Rainfall Intensity

Table 2-4 provides the maximum 1-day, 2-day and 3-day rainfall totals measured at the regional stations during the June 2013 storm and the maximum hourly rainfall intensity where currently available. Of note is that the 1-day maximum rainfall recorded at Kananaskis (157 mm) is 75% greater than the long-term average rainfall for the month of June. The maximum hourly rainfall intensity and maximum daily rainfall total occurred on different dates during the storm at the various stations. Hourly rainfall data from the three Marmot Basin stations and from the Kananaskis Boundary Auto station show that the storm was at its maximum intensity overnight on June 19/20 (Figure 2-1). The Marmot Basin hourly data were provided by John Pomeroy at the University of Saskatchewan for use in this study, and the Kananaskis Boundary Auto data were obtained with the Alberta Weather Station Data Viewer operated by Alberta Agriculture.

**Table 2-4. Maximum rainfall June 19 to 21, 2013.**

| Station Name | 1-Day Rainfall (mm) | 2-Day Rainfall (mm) | 3-Day Rainfall (mm) | Max Hourly Rainfall Intensity (mm/h) |
|---|---|---|---|---|
| Kananaskis | 157 | 224 | 265 | n/a |
| Bow Valley | 111 | 171 | 219 | n/a |
| Banff | 60 | 77 | 90 | n/a |
| Gadd Residence | 91 | n/a | 147 | 17.4 |
| Kananaskis Boundary Auto | 169 | 230 | 281 | 16.0 |
| South Ghost Headwaters | 115 | 189 | 236 | n/a |
| Ghost Diversion | 101 | 153 | 184 | n/a |
| Ghost Ranger Station | 80 | 109 | 136 | n/a |
| Fisera Ridge | 111 | 184 | 224 | 11.8 |
| Hay Meadow | 122 | 199 | 246 | 13.0 |
| Upper Clearing | 126 | 187 | 225 | 13.3 |

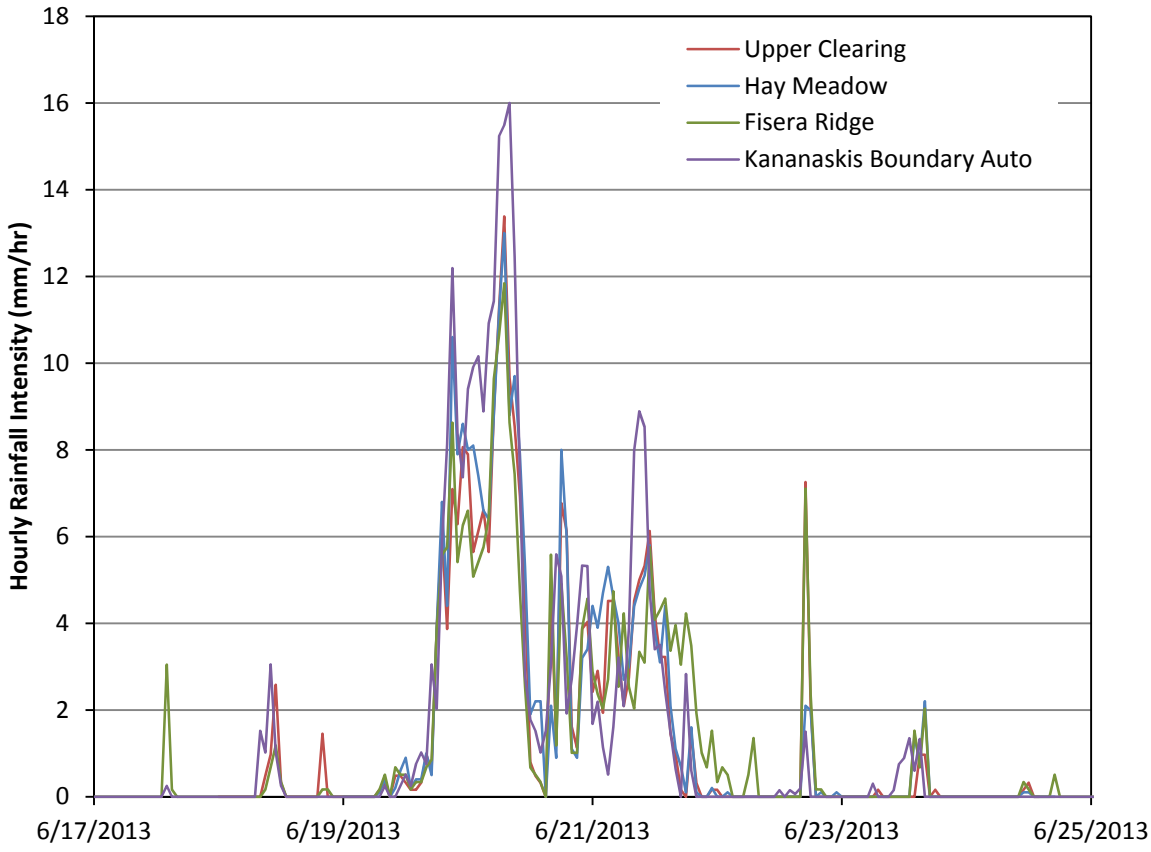


**Figure 2-1. Hourly rainfall intensity at three rain gauges in the Marmot Basin and at Kananaskis Boundary Auto.**

The available hourly rainfall records are too short to develop a reliable Intensity-Duration-Frequency (IDF) curve. However, an IDF curve is available for the Kananaskis station (Figure 2-2). Comparisons of the IDF curve with the maximum 15-minute rainfall intensities measured at the Marmot Basin stations ranged from 4.3 mm to 5.1 mm, and indicate less than a 2-year return period (Figure 2-2). The maximum hourly rainfall intensity recorded at the Upper Clearing Marmot Basin station indicates approximately a 2- to 5-year return period. The one-hour duration as measured at the Kananaskis Boundary Auto station indicates a return period of approximately 5 years, and the two-hour duration relates to a 10- to 25-year return period. The six-hour, 12-hour, and 24-hour each plot in excess of a 100-year return period. These results show that the storm intensity was not particularly rare for rainfall durations of two hours or less. However, the storm was record-breaking for 1-day, 2-day and 3-day cumulative precipitation, as demonstrated by Figure 2-3, Figure 2-4 and Figure 2-5. The return period of the 1-day rainfall at the Kananaskis climate station exceeded 200 years (Figure 2-2).

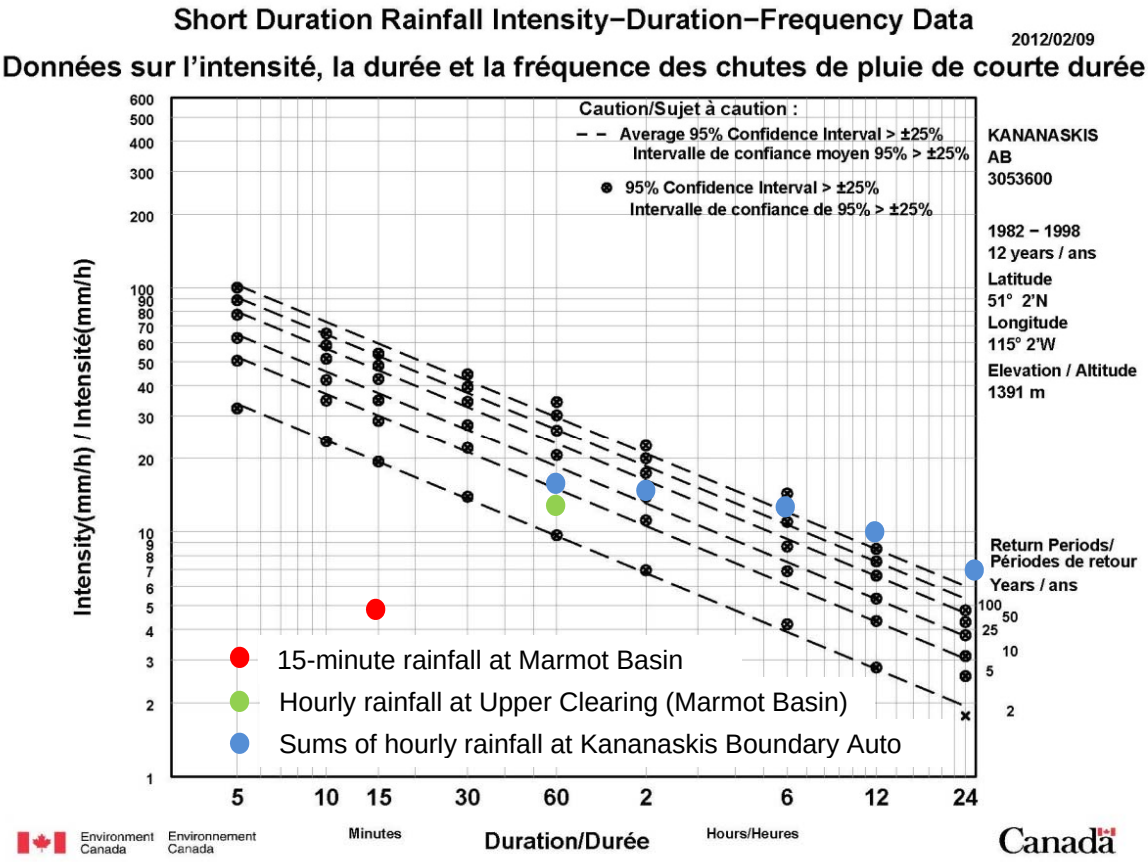


**Figure 2-2. Intensity-Duration-Frequency curve for Kananaskis climate station with June 2013 event rainfall intensities superimposed.**

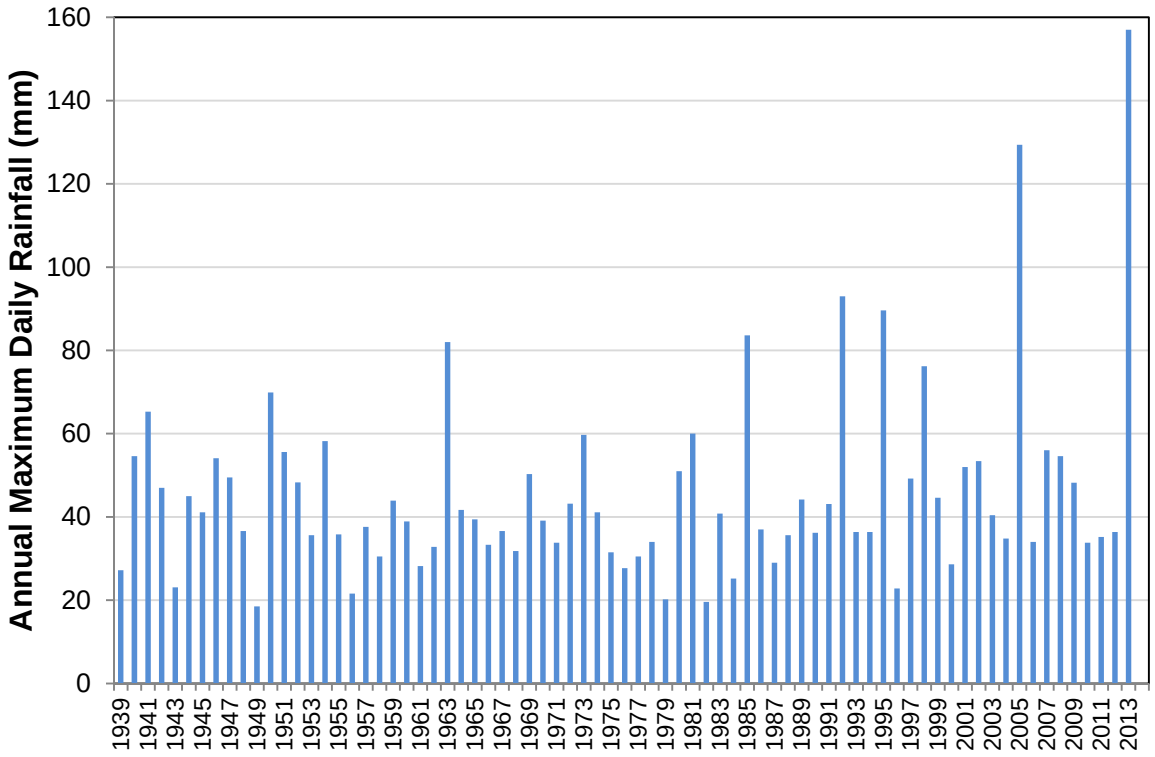


**Figure 2-3. Annual Maximum 1–Day Rainfall at Kananaskis (1939-2013)**

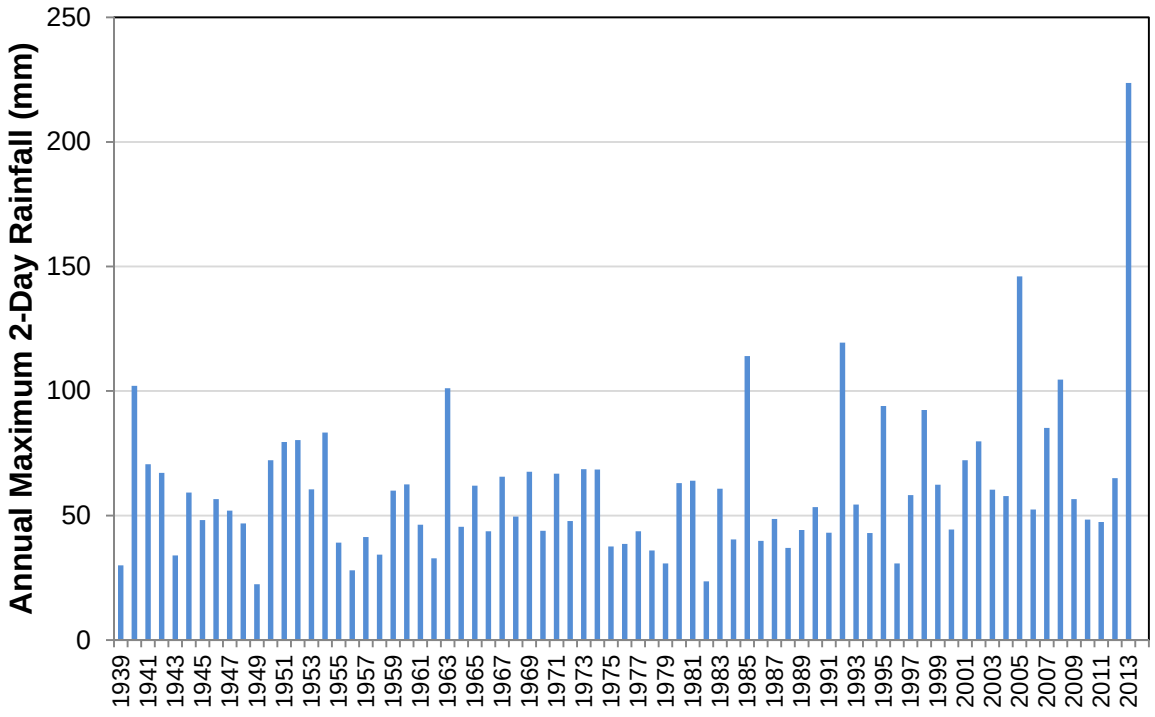


**Figure 2-4. Annual Maximum 2–Day Rainfall at Kananaskis (1939-2013)**

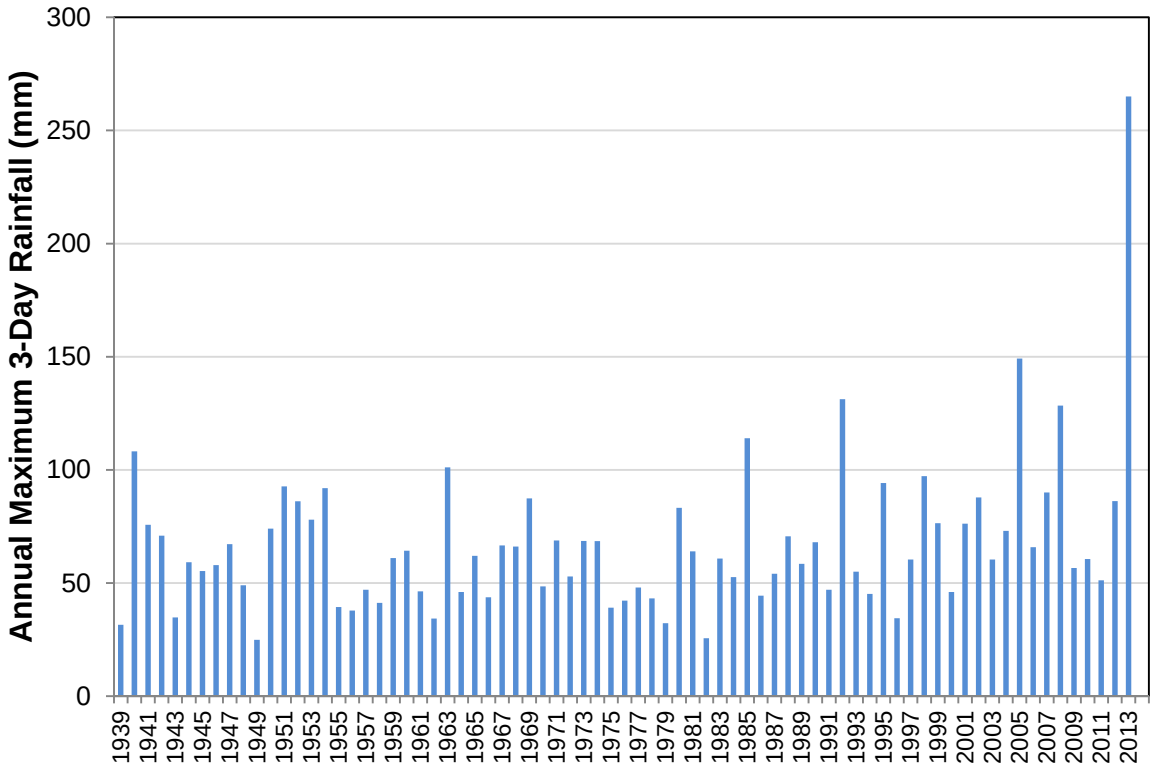


**Figure 2-5. Annual Maximum 3–Day Rainfall at Kananaskis (1939-2013)**

## 2.3. Rainfall Frequency Analysis

The MSC Kananaskis climate station has the longest rainfall record in the region and therefore lends itself for trend and frequency analysis. As described above, this station has been moved several times which may challenge the validity of trend analysis and as such, frequency results estimated with these data should be interpreted with caution.

The data records from the Banff and Bow Valley climate stations are not appropriate for frequency or long term trend analysis. Throughout its period of record, the Banff climate station has been moved several times and instrumentation has been updated. Rainfall and snow readings are also missing from 2007 to present, although total precipitation values are available. In the Bow Valley record, there are multiple periods of missing rainfall, snowfall and precipitation data for several periods greater than a month and up to several years.

Noting the potential caution with the data, rainfall frequency analyses were prepared for the Kananaskis station using the Annual Maximum Series approach and the Generalized Extreme Value (GEV) distribution in the extRemes package for the statistical software *R*. The GEV is a family of distributions comprised of the Gumbel, Frechet and Weibull distributions. Adamowski (1996) demonstrated that the GEV accurately fits annual maxima of precipitation data for all of Canada.

In the present analysis, 1-day, 2-day and 3-day maximum annual rainfall totals were analyzed. The June 2013 rainfall event is the largest on record at Kananaskis station for each of these durations and could be considered an outlier. There is some controversy in the hydrological community regarding the treatment of outliers because of the difficulty fitting a distribution to a sample containing them. Therefore, frequency results produced by both including and omitting the 2013 rainfall event from the input dataset are presented in Table 2-5. Four years with missing data periods during times when maximum annual rainfall was mostly likely to occur were removed from the dataset (1939, 1949, 1951, 1989). Results show that with increasing storm duration, the event becomes rarer.

**Table 2-5. Frequency analysis results for Kananaskis Station rainfall during the June 2013 storm.**

| Duration | Rainfall Total (mm) | 2013 Event Included in Input Dataset | | 2013 Event Omitted from Input Dataset | |
|---|---|---|---|---|---|
| | | Return Period (years) | Lower and Upper 95% Confidence Intervals (mm) | Return Period (years) | Lower and Upper 95% Confidence Intervals (mm) |
| 1-day | 157 | 235 | 112; 265 | 650 | 110; 276 |
| 2-day | 224 | 360 | 156; 387 | 2100 | 148; 423 |
| 3-day | 265 | 575 | 182; 472 | ~9600 | 166; 544 |

## 2.4. Rainfall Distribution and Volume

AESRD regularly generates precipitation maps following notable storm events. The precipitation map for the June 2013 event spans a 72-hour duration and was prepared using 477 weather stations across Alberta (Figure 2-6). The contours were prepared using kriging[1]. Figure 2-6 shows that precipitation fell from approximately the latitudes of Grande Prairie, Edmonton, and Cold Lake southward across the province. The highest rainfall totals were centred in the mountains west of High River, and along the eastern margin of the Rocky Mountains, west of Calgary. The Marmot Basin and Kananaskis areas, approximately 15 km east of Canmore, experienced notably high rainfall totals in the Rockies. The map indicates that these areas are most closely representative of the Cougar Creek area.

Of interest is that the storm was much less severe in Banff, which is located about 20 km to the northwest of Canmore. This observation is in accordance with the rainfall totals presented in Table 2-4 although as previously suggested, it is suspected that the Banff station is underreporting. Weather radar imagery from Strathmore, Alberta shows that the highest rainfall intensities in the Canmore area were experienced from the late hours of June 19 to the early hours of June 20, which is consistent with the hourly interval rainfall measurements (Figure 2-1).

[1] Kriging is a method in which the weights of the values sum to unity. It uses an average of a subset of neighboring points to produce a particular interpolation point.

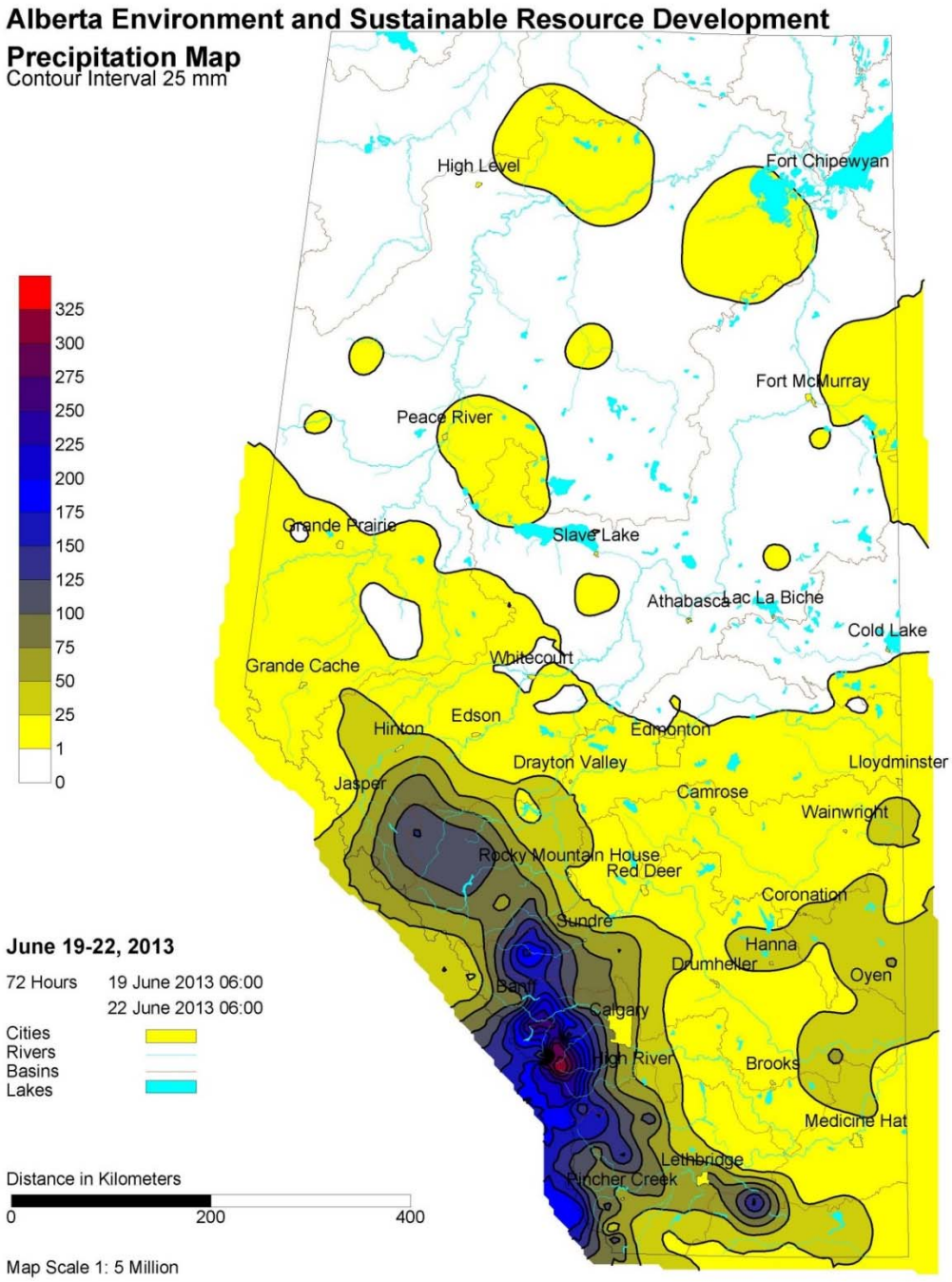


**Figure 2-6. AESRD precipitation map for the June 2013 storm event (http://www.environment.alberta.ca/forecasting/data/precipmaps/precipmaps.html).**

By overlaying the Cougar Creek watershed area over the precipitation map, rainfall totals during this time amounted to approximately 220 mm between 06:00 June 19, 2013 to 06:00 June 22, 2013. This total is consistent with the three-day rainfall totals at the Kananaskis, Bow Valley, South Ghost and Marmot Basin stations, and therefore will be the preferred estimate for the Cougar Creek watershed in the remainder of this report. Using the 220 mm estimate,

the rainfall volume for the entire Cougar Creek watershed is estimated to be 9.1 $Mm^3$ for the 72 hour storm duration.

## 2.5. Antecedent Moisture Conditions

Antecedent moisture refers to the amount of soil moisture in a watershed at any given moment. "Antecedent" further signifies moisture present prior to the arrival of an important hydroclimatic event. The degree of antecedent moisture is an important contributing factor to the amount of runoff produced during a storm. There are no soil saturation measurements available to characterize antecedent moisture in the Cougar Creek basin; however, snowpack and preceding rainfall trends can be used as a proxy for prevailing conditions at the arrival of the June 19, 2013 storm.

Table 2-6 presents average monthly rainfall, snowfall and total precipitation values for November through May, and April, May and June at the long term Kananaskis station. Also, 2013 conditions prior to June 19 are shown for comparison. Rainfall totals in June 2013 prior to the storm were average, given the ratio of the number of pre-storm days in June 2013 to the full month. Rainfall in May was about 30% higher than average. Of particular interest, however, is that snowfall in April was nearly three times higher than the monthly average, and considerably more snow and rain fell over the preceding winter than the long-term average. These results suggest that antecedent moisture conditions prior to the mid June 2013 storm were well above average.

**Table 2-6. Average monthly and 2013 precipitation conditions at Kananaskis.**

| Month | Average Totals | | | 2013 Totals | | |
|---|---|---|---|---|---|---|
| | Rainfall (mm) | Snowfall (cm) | Precipitation (mm) | Rainfall (mm) | Snowfall (cm) | Precipitation (mm) |
| Nov-May | 92 | 250 | 235 | 112 | 320 | 443 |
| April | 12 | 49 | 61 | 1.3 | 142 | 144 |
| May | 60 | 26 | 85 | 78 | 24 | 102 |
| June | 104 | 0.9 | 109 | 60* | 0* | 60* |

* 2013 records shown up to June 18.

Another important contributor to the amount and timing of runoff is the distribution and abundance of seasonally frozen ground. If the ground is frozen, it has a reduced capacity to absorb water. Much like areas underlain by permafrost, rainfall cannot infiltrate through the frozen soil matrix until it is thawed and instead runs off as overland flow. Dr. Pomeroy noted frozen ground in the valley bottoms and at high elevations just prior to the flood, which may have contributed to the volume of the Cougar Creek flood (J. Pomeroy, pers. comm., 2013) though it cannot be quantified reliably.

# 3.0 SNOWPACK

## 3.1. Introduction

In mountainous regions, major peak flows are often attributed to rain-on-snow events. Therefore, snowmelt is an important factor in hydrologic analyses. Several factors influence the distribution and abundance of snowpack including: elevation and basin hypsometry, slope aspect, local wind speed and direction, local precipitation variances and air and ground temperatures. As a result it can be challenging to prepare an accurate characterization of snowpack conditions without actual field measurements in the basin of interest, as is the case at Cougar Creek. This section attempts to characterize the Cougar Creek snowpack and associated contribution to runoff during the June 2013 storm with available information.

## 3.2. Regional Snowpack Measurements

While snowpack is not monitored in the Cougar Creek watershed, it is monitored regionally at both the Marmot Creek research basin and at several locations further south managed by AESRD.

### 3.2.1. Marmot Basin

As well as measuring precipitation, the climate station at Fisera Ridge (Drawing 1) also monitors snowpack thickness with an acoustic signal. Minimal snow remained at the station (elevation 2325 m asl) by June 8 (Figure 3-1); however, approximately 7 cm of snow fell there during the storm event. Snowfall began at 09:00 on June 21, reaching maximum at 16:00 and was melted by approximately 17:00 on June 22. Assuming a fresh snow density of 100 kg/m$^3$, or approximately 10% water, 7 mm of snow water equivalent (SWE) melted and contributed to runoff in the immediate vicinity of the station.

Although the 7 cm snowpack measurement at the Fisera Ridge station indicates that snow accumulated at this elevation during the storm event, the related 7 mm snow melt estimate is considered to be too low and not representative of overall snowmelt conditions in the vicinity of the station. While the station data suggest that there was no snow on the ground prior to the storm, snow was observed to persist in a treed area near the Fisera Ridge climate station at least until June 19, and the Marmot Basin research team measured 90 mm of snowmelt in the vicinity of the station during the storm (pers. comm., J. Pomeroy, 2013). Thus, a snowmelt value of 90 mm is considered the best estimate at Fisera Ridge.

In addition, the Marmot Basin research team also measured up to 240 mm of SWE loss by snow survey in other locations of the basin between June 13 and June 26, 2013. It is expected that most of this loss would have formed snowmelt during the heavy rainfall of June 19-21 (pers. comm., J. Pomeroy, 2013).

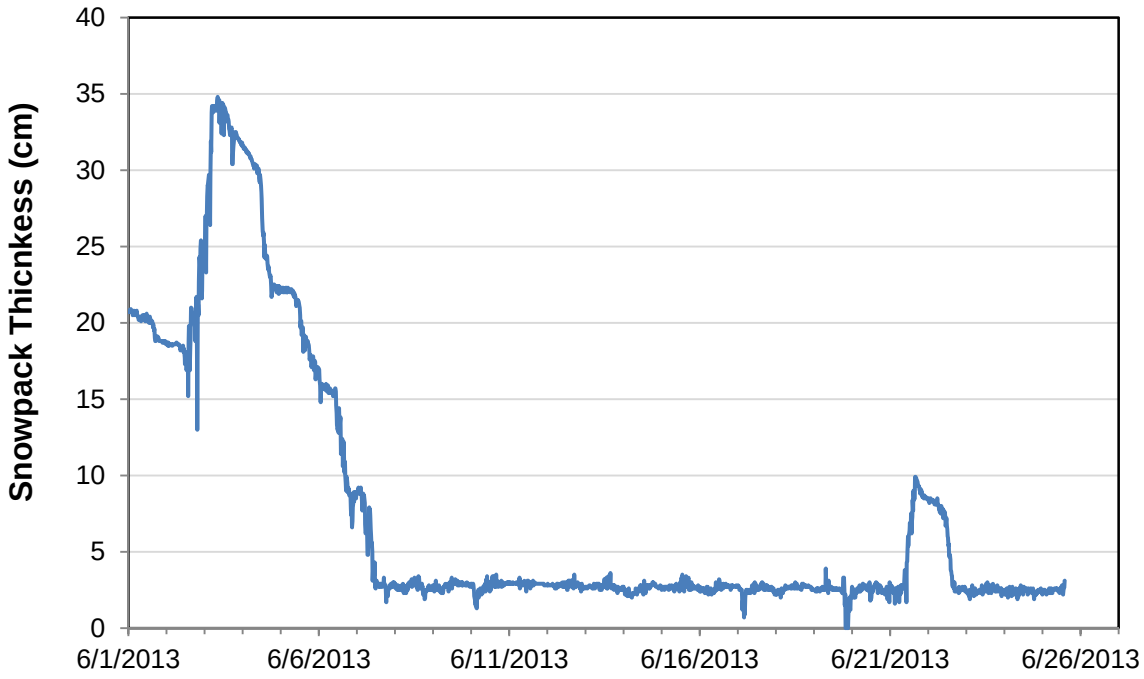


**Figure 3-1. Snowpack thickness measurement in June 2013 measured at Fisera Ridge in Marmot Basin. Note the 2 to 3 cm base level is vegetation between the soil and the acoustic depth gauge.**

### 3.2.2. Regional Snow Pillows

The AESRD operates three regional snow pillows to the south-southeast of Canmore: Three Isle Lake, Little Elbow Summit and Mount Odlum (Drawing 1). Summary information about these snow pillows is provided in Table 3-1.

**Table 3-1. Regional AESRD snow pillow stations.**

| Station Name | Latitude (°) | Longitude (°) | Elevation (m asl) | Distance from Cougar Creek Fan | Period of Record | Years of Data |
|---|---|---|---|---|---|---|
| Three Isle Lake | 50.631 | -115.279 | 2160 | 50 km S | 1985 - 2013 | 29 |
| Little Elbow Summit | 50.822 | -114.989 | 2120 | 48 km SSW | 1979 - 2013 | 34 |
| Mount Odlum | 50.486 | -114.913 | 2060 | 73 km SSW | 1985 - 2013 | 28 |

Both snowpack thickness and SWE are monitored at these stations. SWE is the water content of a melted sample of snow and can be used to infer the contribution of snowmelt to runoff. The SWE snow pillow records during the June 2013 storm are shown with the Fisera Ridge (2325 m asl) snowpack thickness in Figure 3-2. The timing of snowmelt and snowfall during the event correlates well between the stations suggesting that the regional freezing level was at, or lower, than 2120 m asl on June 21. The net SWE loss during the storm (midnight on June 19 to midnight on June 23) at Mount Odlum, Little Elbow Summit and Three Isle Lake

stations, were 54 mm, 51 mm and 42 mm, respectively. However, snow pillows can underreport snowmelt during rain-on-snow events due to ponding issues.

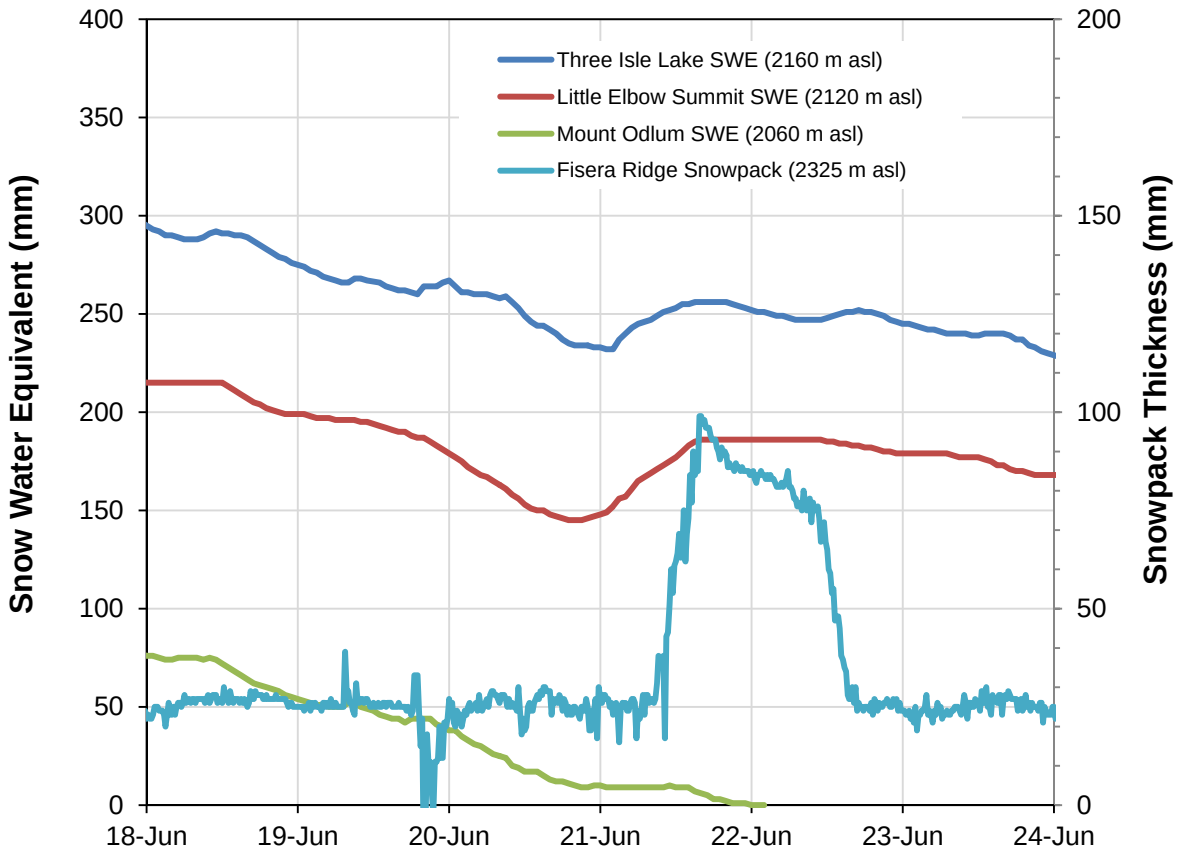


**Figure 3-2. SWE at snow pillows in the vicinity of Cougar Creek and Fisera Ridge snowpack thickness during the June 2013 event.**

### 3.2.3. Synthesis

Over the duration of the June storm of 2013, approximately 90 mm to 240 mm of snowmelt was observed by researchers at the University of Saskatchewan in the Marmot Basin.

A hypsometric curve for the Cougar Creek basin above the fan apex indicates that approximately 26 km$^2$ are located above 2060 m asl, the lowest regional snow pillow elevation with snow at the time of the storm event (Figure 3-3). Assuming that the snowpack below elevation 2060 m in the Cougar Creek watershed was minimal and non-contributory to runoff, the curve suggests that 63% of the 41.9 km$^2$ catchment could have been covered in snow immediately prior to the rainfall. The net SWE losses measured at the three snow pillows and the 90 mm Fisera Ridge measurement were correlated to Cougar Creek catchment area using the respective station elevations, resulting in a weighted average total snowmelt volume estimate over the storm period of 1.2 Mm$^3$, and a range of 0.9 Mm$^3$ to 1.4 Mm$^3$. When summed with the 9.1 Mm$^3$ rainfall volume estimate, the estimated snowmelt could have increased the total water available for runoff by 12%. Assuming a uniform 90 mm of snowmelt above 2060 m,

the snowmelt volume would be 2.4 $Mm^3$, or 21% of the total runoff contribution. Using 60% of the University of Saskatchewan's maximum snowmelt measurement in the Marmot Basin for the period of June 13 to June 26, there would have been a total snowmelt volume of 3.8 $Mm^3$ in the Cougar Creek basin, contributing 29% to total runoff. Table 3-2 provides a summary.

**Table 3-2. Snowmelt contribution to total runoff estimates for Cougar Creek above 2060 m.**

| Data Source | Water Content (mm) | Volume Estimate ($Mm^3$) | Contribution to Total Runoff |
|---|---|---|---|
| Regional Snow Pillows and Fisera Ridge during duration of the June storm | 54, 51, 42, 90 (weighted averaged) | 1.2 | 12% |
| Fisera Ridge during the duration of the June storm only | 90 | 2.4 | 21% |
| Arbitrary 60% of the maximum measurement (241 mm) in the vicinity of Fisera Ridge between June 13 and June 26, 2013 | 145 | 3.8 | 29% |

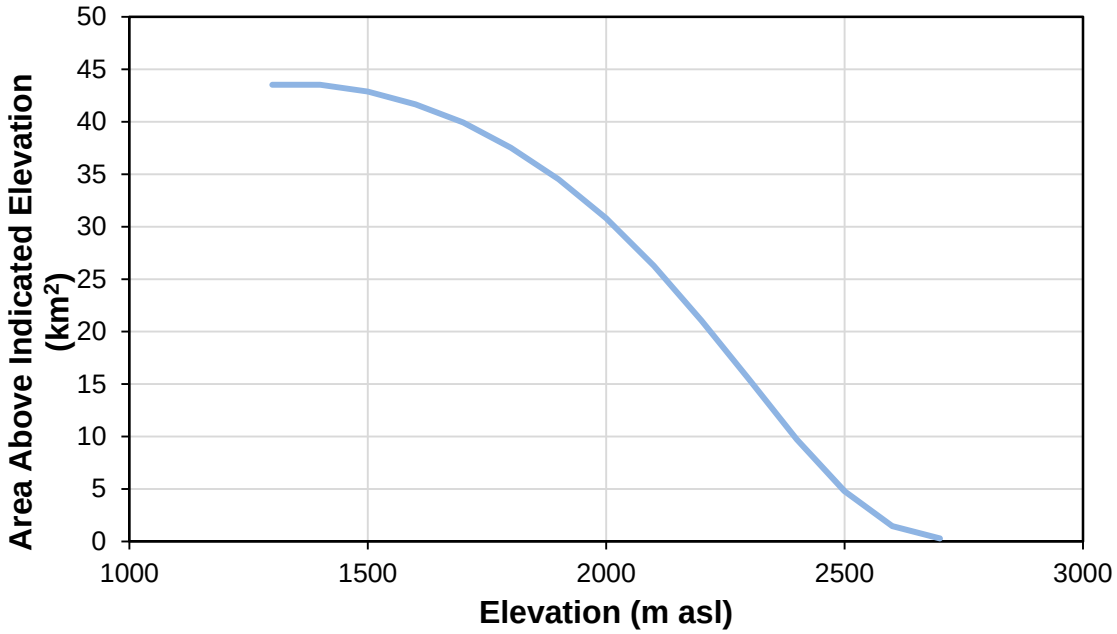


**Figure 3-3. Hypsometric curve for the Cougar Creek catchment above the fan apex.**

## 3.3. Snow Cover Distribution

Two data sources were also investigated to characterize the distribution of the Cougar Creek snowpack before, during, and after the June storm event: the satellite-based Moderate Resolution Imaging Spectroradiometer (MODIS) and the model-based Snow Data Assimilation System (SNODAS).

Snow and ice indices can be derived from MODIS, which is an instrument aboard the Terra (EOS AM) and Aqua (EOS PM) NASA satellites. Terra MODIS and Aqua MODIS view the entire Earth's surface every 1 to 2 days. Daily data of snow distribution are available and can be used to prepare 500 m resolution raster-format daily snow cover maps throughout North America. A shortcoming of MODIS is that it cannot collect data through cloud cover. Unfortunately, there was too much cloud cover over the Cougar Creek watershed throughout June 2013 to utilize MODIS data for the present analysis.

SNODAS is a modeling and data assimilation system developed by the US National Weather Service's National Operational Hydrologic Remote Sensing Center. The system integrates snow data from satellite, airborne, and ground stations platforms with snow mass and energy balance model estimates. The resulting outputs are daily 1 $km^2$ resolution raster-format estimates of snow depth, snowmelt runoff, SWE and other related snow parameters. It is important to note the data are modeled estimates, not measured observations.

SNODAS parameter estimates suggest that roughly 7% of the Cougar Creek watershed had snow cover prior to the storm event (June 18), which ranged in thickness from approximately 14 to 123 cm. This estimate is not in accordance with the regional snow pillow data that suggests two-thirds of the watershed could have had snow cover. Furthermore, the SNODAS estimates indicate that snowfall occurred on June 20 (Table 3-3), which is inconsistent with the Fisera Ridge and snow pillow observations (Figure 3-2). It is also suspect that the SNODAS estimates do not show more snowmelt during the event. Rain-on-snow events typically produce rapid snowmelt due to energy transfer from sensible and latent heat, and longwave radiation to the snowpack and is exacerbated by strong upslope winds (Appendix A).

**Table 3-3. SNODAS Cougar Creek snowmelt runoff estimates.**

| Date | Snowpack Area ($km^2$) | Mean SWE (mm) | Mean Snowmelt (mm) | Mean Snowmelt Water Volume ($Mm^3$) | Cumulative Snowmelt ($Mm^3$) |
|---|---|---|---|---|---|
| June 19 | 2.8 | 172 | 30 | 0.08 | 0.08 |
| June 20 | 2.3 | 187 | 54 | 0.15 | 0.24 |
| June 21 | 2.3 | 162 | 111 | 0.25 | 0.49 |

Clow et al. (2012) indicate that SNODAS performs poorly in alpine areas due to the effects of terrain, vegetation and prevailing wind direction on the redistribution of snow by wind. Windward slopes experience snow scour and leeward slopes experience snow deposition. As the Cougar Creek watershed is on the leeward side of prevailing winds, it is possible that SNODAS under-predicted the snowpack here. However, assuming the daily snowmelt runoff estimates were reasonable, there was potential to contribute 0.49 $Mm^3$ of water to runoff during the June 19 to June 22, 2013, midnight to midnight period. Considering the 9.1 $Mm^3$ rainfall volume estimate, this estimated snowmelt contribution using SNODAS represents an additional 5% of water available for runoff.

Of note is also that much of the Cougar Creek watershed has an overall southerly aspect and many slopes are near or steeper than the angle of repose. Steep slopes do typically discourage heavy snow accumulation due to frequent small avalanches. The overall southerly aspect favours early melt. The combination of these factors may suggest that the snowmelt contribution for the June 2013 storm in the Cougar Creek watershed was closer to the lower estimate of 12%.

### 3.4. Summary

The available snowpack and snowmelt data indicate that the 3-day rainfall estimate of 220 mm in the Cougar Creek watershed was augmented by snowmelt. While up to 63% of the watershed may have been covered in snow prior to the event, the available data at the time of writing suggest additional contribution of snowmelt during the storm was less than the total rain volume (~ 12 to 29% of the total available water). Due to the uncertainties involved in these analyses, BGC used the entire spectrum of estimated snowmelt contribution values in their debris flood hazard analysis (BGC, 2014).

# 4.0 STREAMFLOW

## 4.1. Introduction

This section characterizes the June 2013 event from a hydrologic perspective. Depending on antecedent moisture conditions and the extent of frozen soil, amongst other factors, runoff behaviour and event return period may differ for similar rainfall events. Furthermore, depending on the watershed size, runoff may be sudden with a very "peaky" hydrograph or elongated with a smooth hydrograph.

## 4.2. Streamflow Frequency Analysis Data

The Water Survey of Canada (WSC) operates two real-time hydrometric stations in the vicinity of Canmore: *Bow River at Banff* (05BB001) and *Waiparous Creek near the Mouth* (05BG006) from which data can be used for frequency analysis. Station locations are shown on Drawing 1, while station information is provided in Table 4-1. It is important to realize that while these streams provide valuable data, their drainage areas are roughly 8 to 50 times larger than Cougar Creek. This means that runoff reaction to hydroclimatic input will be dramatically different.

Real time discharge estimates during the June 2013 event were obtained for these stations from AESRD and are considered preliminary at the time of writing. Furthermore, the *Bow River at Banff* WSC peak flow data should be used with caution because the station's stage-discharge curve is outdated according to Paul Whitfield (pers. comm., 2013). Real time discharge estimates are also available for the Highwood River to the south of Canmore but were not analyzed due to limited relevance to conditions near Canmore.

**Table 4-1. WSC hydrometric station information.**

| Station Name | Bow River at Banff | Waiparous Creek | Marmot Creek Main Stem near Seebe |
|---|---|---|---|
| Station ID | 05BB001 | 05BG006 | 05BF016 |
| Latitude | 51°10'20" N | 51°16'58.1" N | 50°57'1.9" N |
| Longitude | 115°34'18.4" W | 114°50'18.3" W | 115°09'10.4" W |
| Drainage Area ($km^2$) | 2,210 | 332.5 | 9.1 |
| Record Period | 1909-2013 | 1966-2013 | 1962-2010 |
| Record Length (years)* | 104 | 47 | 47 |
| Regulation Type | unregulated | unregulated | unregulated |

* Years of peak flow data available for frequency analysis.

The greatest flow estimates during the 2013 storm event measured at the two stations described above are the largest flows on record. Bow River at Banff measured an estimated peak flow of 439 $m^3/s$, while the greatest flow on the Waiparous Creek record was 306 $m^3/s$. This Waiparous Creek discharge value is expected to be less than the actual peak

instantaneous discharge during the flood. The gauge was destroyed by high water and 306 $m^3/s$ was the last value to be reported by AESRD before the gauge went offline. This reading may also be inaccurate due to potential damage to the gauge having already been sustained. Data that are available to characterize the Waiparous Creek flood are summarized in Table 4-2. Of note is the rapid increase in water level between the two automatic records, and the magnitude difference between those and the surveyed high water mark.

**Table 4-2. Waiparous Creek 2013 flood data.**

| Data Source | Measurement Type | Time of Occurrence | Estimated Discharge ($m^3/s$) | Water Level (m) |
|---|---|---|---|---|
| WSC | Automatic | June 21, 2013, 06:00 | n/a | 2.557 |
| AESRD | Automatic | June 20, 2013, 11:00 | 306 | 3.400 |
| WSC | Surveyed high water mark | Unknown | n/a | 4.005* |

* Provisional surveyed high water mark (pers. comm, .D. Lazowski, 2013)

Figure 4-1 and Figure 4-2 plot the annual maximum peak instantaneous flows on record for both of the WSC stations, including 2013 records. In the case where peak instantaneous flow records were missing, linear regression equations were prepared to estimate these values using annual maximum daily flow.

Three known extreme floods occurred on Bow River at Calgary before discharge was recorded at the present-day location of the WSC gauge (05BH004). They occurred in 1879, 1897, and 1902, and had estimated discharges of 2265 $m^3/s$, 2265 $m^3/s$, and 1550 $m^3/s$, respectively (Neill and Watt, 2001). It is assumed that these flood events were also experienced at Banff. Linear regression analysis for the period of time before the Glenmore Dam began operation correlated these three floods to the Bow River at Banff peak flow record. An extreme flood event was also experienced at Banff in 1884, prior to the initiation of discharge measurements (Neill and Watt, 2001) though the magnitude of this event is unknown.

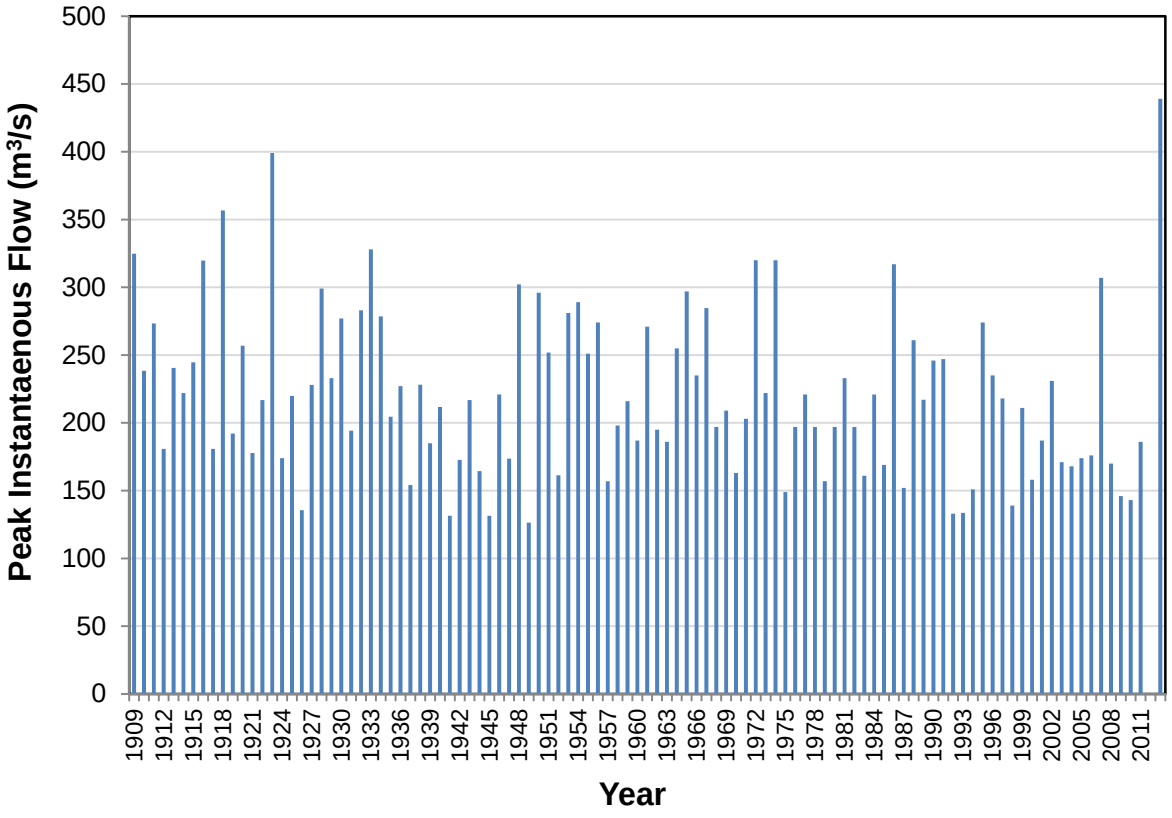


**Figure 4-1. Peak instantaneous flows at Bow River at Banff (1909-2013).**

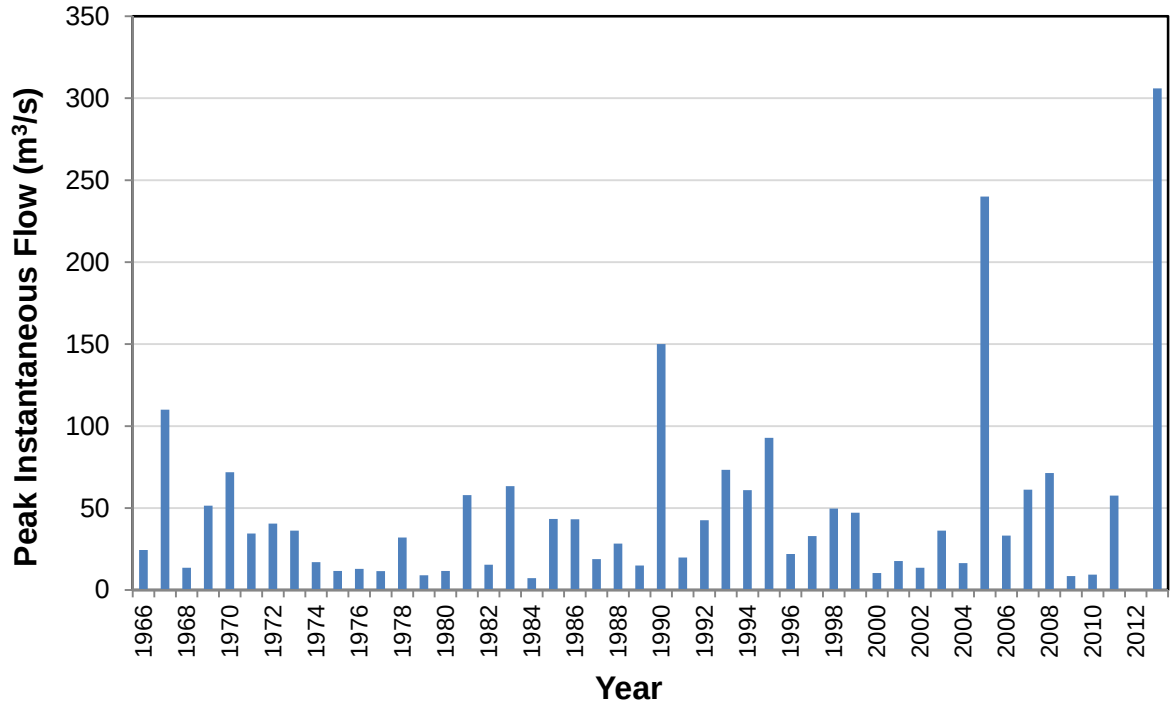


**Figure 4-2. Peak instantaneous flows at Waiparous Creek (1966-2013).**

### 4.3. Streamflow Frequency Analysis Methods and Results

To determine the return period of flooding at the Bow River at Banff and Waiparous Creek gauges, frequency analyses were prepared using the Annual Maximum Series approach. It is expected that the estimates will be refined in the future as preliminary data becomes finalized, at which point a frequency analysis should be repeated.

Two methods were used to address the effect of the 2013 peak flow outlier: with the real-time peak flow estimate (or last available estimate) included in the input peak flow dataset and without, as also described in Section 2.3. In the case of the Bow River at Banff, an additional method was employed: supplementing the dataset with the additional three historical records outside of the measurement period and repeating the analysis with consideration of the effect of the full extended period of record. This was achieved in the flood frequency analysis program HydroFreq by extending the record length for the outlier events and assigning an assumed threshold value. The GEV distribution was used to fit the data to be consistent with the previous analysis using *R*. The threshold was set to 1000 $m^3/s$, a value less than the historical extreme flood events for Bow River at Banff estimated from linear regression analysis with Bow River at Calgary estimates for the same events:.

Results appear in Table 4-3 and indicate that the June 2013 rainfall led to a relatively extreme streamflow on the Bow River (200 to 400-year return period) when using the WSC measurement period (1909-2013), and a less rare event when the historical flood discharge estimates were included in the dataset (~15 to 20-year return period). The lesser return period estimate is consistent with a lack of flooding evidence on the landscape in the Canmore region at the time, and is considered more representative. At Waiparous Creek, the June 2013 event was estimated at a 40- to 60-year return period. The reader should be cautioned that the runoff formation processes for the Bow River and Waiparous Creek would have been different between catchments during flood and therefore, result in a differing peak flow response.

The Waiparous Creek condition would have been more similar to that in Cougar Creek as it's watershed is only 8 times larger than that of Cougar Creek (as opposed to the 50 times in the case of Bow River). It likely also had a higher return period than that estimated in this analysis given the data limitations pertaining to the gauge damage described above. Further peak flow trend analysis could address the potential limitation of runoff mechanisms differing from year-to-year and thereby affecting the validity of lumping all peak flow estimates into a single population. This may necessitate splitting the data record into solely rainfall-generated floods and floods generated by snowmelt. Splitting the data further into hybrids (rain-on-snow events) may decrease the sample size below a reasonable limit given that the record only extends back to 1966.

**Table 4-3. Frequency estimates for regional real-time peak flows during the June 2013 event.**

| Dataset | Drainage Area ($km^2$) | 2013 Peak Discharge ($m^3/s$) | Time of Peak | Return Period (years) | |
|---|---|---|---|---|---|
| | | | | Peak in dataset | Peak not in dataset |
| *Bow River at Banff* [05BB001] Post-1909 | 2210 | 439 | June 21, 2013, 16:00 | 175 | 425 |
| *Bow River at Banff* [05BB001] Including historical data | 2210 | 439 | June 21, 2013, 16:00 | 15-20 | 15-20 |
| *Waiparous Creek* [05BG006] | 332 | 306 | June 20, 2013, 11:00 | 38 | 58 |

A third WSC hydrometric station, *Marmot Creek Main Stem Near Seebe* (05BF016), is located in close proximity to Canmore (Drawing 1). This station is likely the most appropriate analog for Cougar Creek. However, real-time data are not available from this station and the instrumentation was damaged during the June 2013 event by a debris flow. Therefore, data were not recorded that could be used to characterize the event (pers. comm., J. Pomeroy, 2013). Future research at the University of Saskatchewan Centre for Hydrology will seek to characterize the Marmot Creek event.

# 5.0 CLIMATE CHANGE

## 5.1. Introduction

Anthropogenic greenhouse gas emissions have led to a marked increase in global temperatures over the past 50 to 60 years. IPCC (2013) states that "It is *extremely likely* that human influence has been the dominant cause of the observed warming since the mid-20th century". Amongst the climate science community, there is no credible doubt that greenhouse gas emissions are the primary driver for global warming observed in the last few decades. This conclusion is important because without an understanding of the dominant climate forcing factors, prediction is impossible.

The more pertinent question for this report is how this observed warming is translating into possible changes in the frequency and or magnitude of rainfall events or rain-on-snow events in the Rocky Mountain front of southern Alberta. The following text and analysis are by no means a comprehensive analysis of climate change effects on flooding or debris flooding, but provides some initial considerations that ought to be accounted for in the risk management of steep mountain creeks.

The IPCC (2013) and the Special Report of the Intergovernmental Panel on Climate Change (Managing the risks of extreme events and disasters to advance climate change adaptation) (IPCC, 2012) agree that there have been statistically significant trends in the number of heavy precipitation events in some regions and that it is likely the number of heavy precipitation events has increased in more regions than it has decreased since 1950. Notably, the IPCC (2013) mentions that the confidence of this statement is highest in North America, where the most consistent trends towards heavier precipitation are found. For example, DeGaetano (2009) showed a 20% reduction in the return period for extreme precipitation of different return levels over 1950 to 2007 in the continental United States. Also of note, Pryor et al. (2009) showed a significant trend towards increased annual total precipitation, number of rainy days and intense precipitation with a focus on the Great Plains and Northwestern American Midwest, which would also include southern Alberta. Modelling by Valeo et al. (2008) demonstrated that changes in precipitation regimes may lead to nearly doubling of freshet flood peaks in the Elbow River watershed.

It should be recognized while such general trends have been identified, climate undergoes various cycles of differing wave length. For example, the Pacific Decadal Oscillation (PDO) is a climate change pattern that is based on sea surface temperatures in the northern Pacific Ocean. In Western Canada, the warm or positive phase is associated with warmer than average temperatures and greater than average precipitation totals, while the cool or negative phase is associated with the opposite. The pattern cycles on a scale of approximately 20 to 35 years. The last marked phase change occurred around 1977 and involved a shift from a cool phase to a warm phase. Although there has been no distinct trend in PDO index values since 1997, negative values have been measured since 2008. St. Jacques et al. (2010) found that a strong negative relationship exists between the PDO and streamflow in south and central

Alberta. When in a cool PDO phase, streamflow was higher than average. This trend did not exist for all stations, which indicates that there is uncertainty in the linkage to PDO. However, when the PDO was removed from a trend analysis, mean daily flows at the *Bow River at Banff* gauge were found to be decreasing over the period of record (St. Jacques et al., 2010).

BGC has conducted a preliminary assessment of potential trends in rainfall and streamflow for the Canmore area. This assessment is discussed in Sections 5.2 and 5.3.

## 5.2. Rainfall Trend Analysis

BGC retained extreme value statisticians at the University of British Columbia to repeat the 3-day rainfall frequency analysis but with an assumption of non-stationarity to detect and quantify a possible trend This trend was then included in the rainfall frequency analysis. The full report appears in Appendix B.

This work demonstrated a linear trend in the rainfall time series. Assuming a continuation of the observed linear trend, an exceedance of the June 2013 event is expected to occur within 242 years (Interpretation 1), and is expected to happen once in the next 294 years (Interpretation 2). In other words, under the assumption of data non-stationarity, the 575-year return period of the 3-day rainfall at the Kananaskis station would decrease to approximately 300 years. Following the same line of argument, by the year 2300, the 3-day rainfall observed during the 2013 Cougar Creek event could have decreased to a 100-year return period event.

This trend analysis also demonstrated that (under the assumption of a continuation of the linear trend), a 100-year return period 3-day rainfall could increase by 10%, a 500-year return period 3-day rainfall event by approximately 30%, and a 1000-year return period 3-day rainfall by over 60%.

It must be noted that these analyses ignore the unknown forcing mechanism for the observed trend and assume that the linear trend will continue. Both these assumptions can be criticized. Moreover, the analysis was completed for only one station and would have to be repeated for numerous stations in the area to demonstrate that the observed trend is not a legacy of the meteorological station's record or localized effects. Paul Whitfield[2] notes "The Kananaskis station has been relocated several times and the precipitation measurement system has been changed in addition. The precipitation record from 1939 to present contains several inhomogeneities as a result and any trend analysis that does not properly consider these is likely to be suspect". Furthermore, Whitfield is unaware of an analysis that indicates there is a trend in annual precipitation extremes.

To further test the assumption of linear trends in extreme rainfall time series, BGC repeated the trend analysis using 3-day rainfall data from the Ghost Diversion and Ghost Ranger climate stations. Both station records reach back to 1984 (Figure 5-1 and Figure 5-2). A linear trend

[2] Senior Research Fellow, Centre for Hydrology, University of Saskatchewan. Emeritus Scientist, Environment Canada (retired).

analysis was performed after log-transforming data recorded at both stations because they were not normally distributed. Both stations showed a significant linear trend for the 3-day precipitation data series. In a hypothesis test, the p-values were p=0.04 and p=0.01 for Ghost Diversion and Ghost Ranger, respectively, and less than a significance level of 0.05.

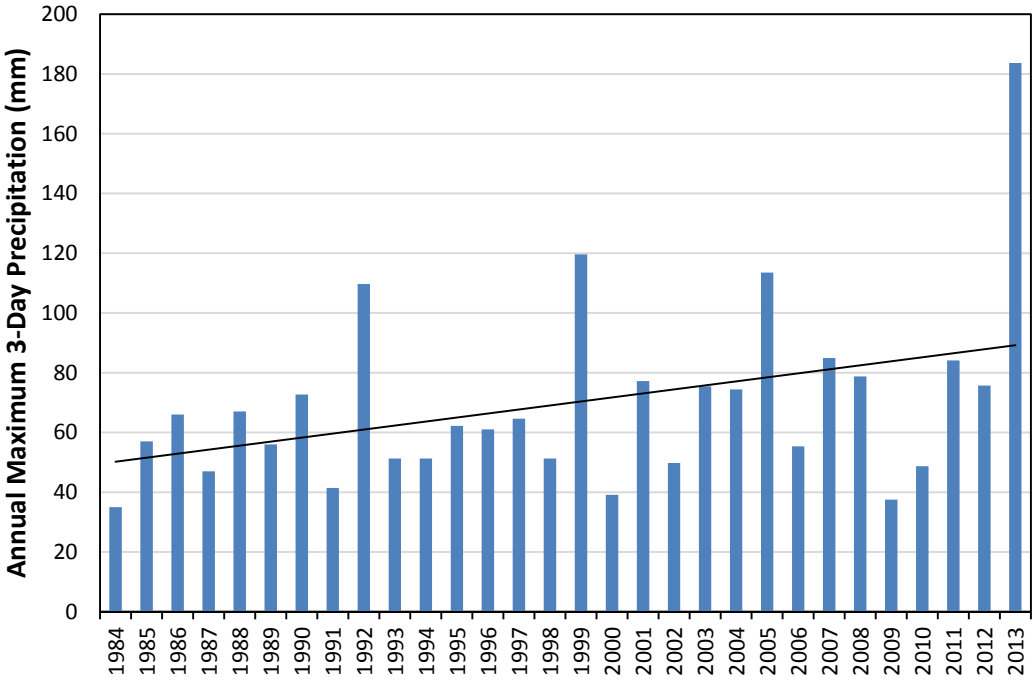


**Figure 5-1. Ghost Diversion Station Annual Maximum 3-Day Precipitation**

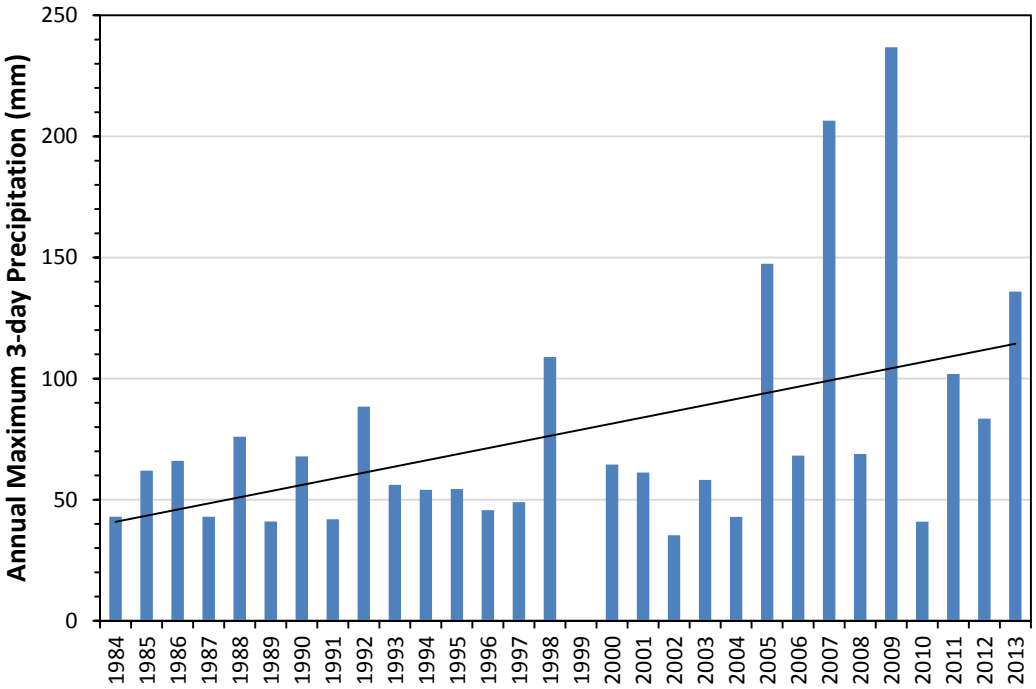


**Figure 5-2. Ghost Ranger Station Annual Maximum 3-Day Precipitation**

While the above analyses do not replace a more thorough regional trend analysis, they do point towards trends in maximum 3-day rainfall over their respective observation periods within the area affected most by the June 2013 storm. The hypothesis of a linear trend in extreme precipitation should therefore be upheld and should be acknowledged in risk-based decision making.

BGC initially evaluated potential trends in maximum annual 1-day rainfall as observed at the Kananaskis climate station (Figure 5-3). This figure shows an increasing linear trend for the entire data series (black). However, a visual examination of the time series indicates that this trend was less pronounced to non-existing for roughly the first three quarters of the record, followed by more significant changes in the last quarter. Thus, the data were split and trend lines replotted showing a strong upwards trend after approximately 1990, interrupted only by the 2000 to 2005 segment during which annual rainfall maxima return to the average. Furthermore, if peaks over an arbitrary 60 mm threshold are considered, a strong trend, again starting in the late 1980s or early 1990s, can be discerned (Figure 5-3).

To further illustrate this observation, the 5-year means were calculated and plotted (Figure 5-4). This figure supports the earlier conclusion and demonstrates that the upward trend began in the five year increment from 1989 to 1993 which continued to the present, except from the five year period from 1999 to 2003. This increase may suggest that starting around 1990 rainfall intensities have increased well above the long-term 1-day average of 46 mm.

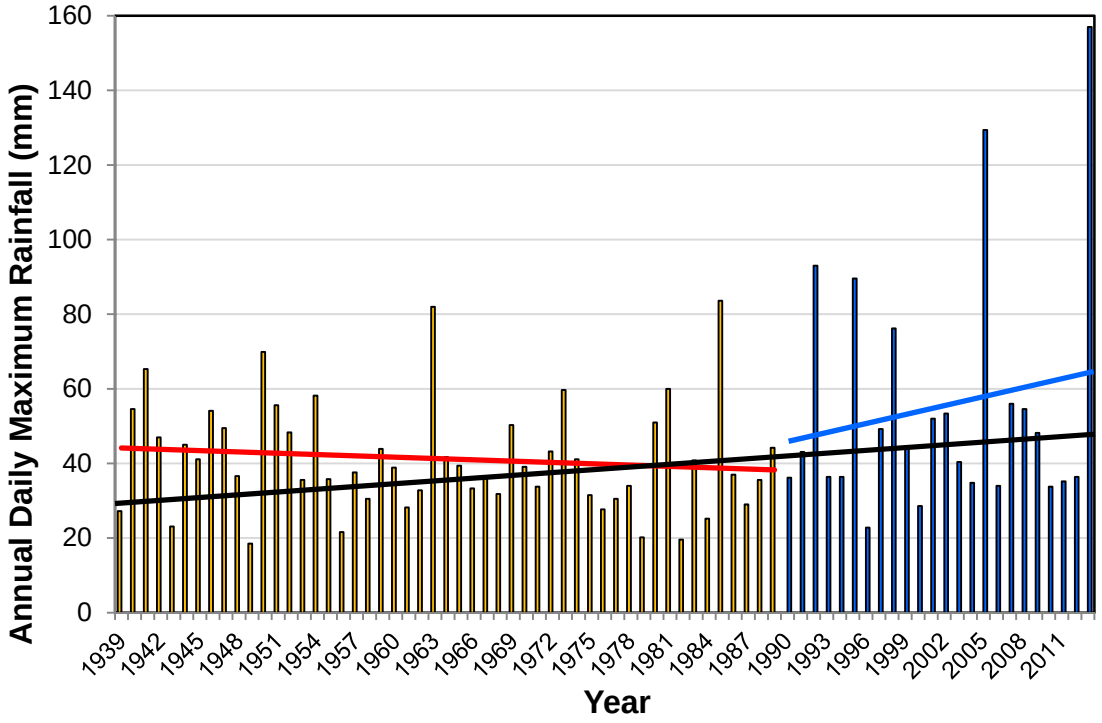


**Figure 5-3. Time series of maximum annual daily rainfall for the Kananaskis climate station with a linear trend line for the entire data series (black line) as well as trend lines for the periods 1939 to 1989 (red line) and 1990 to 2013 (blue line).**

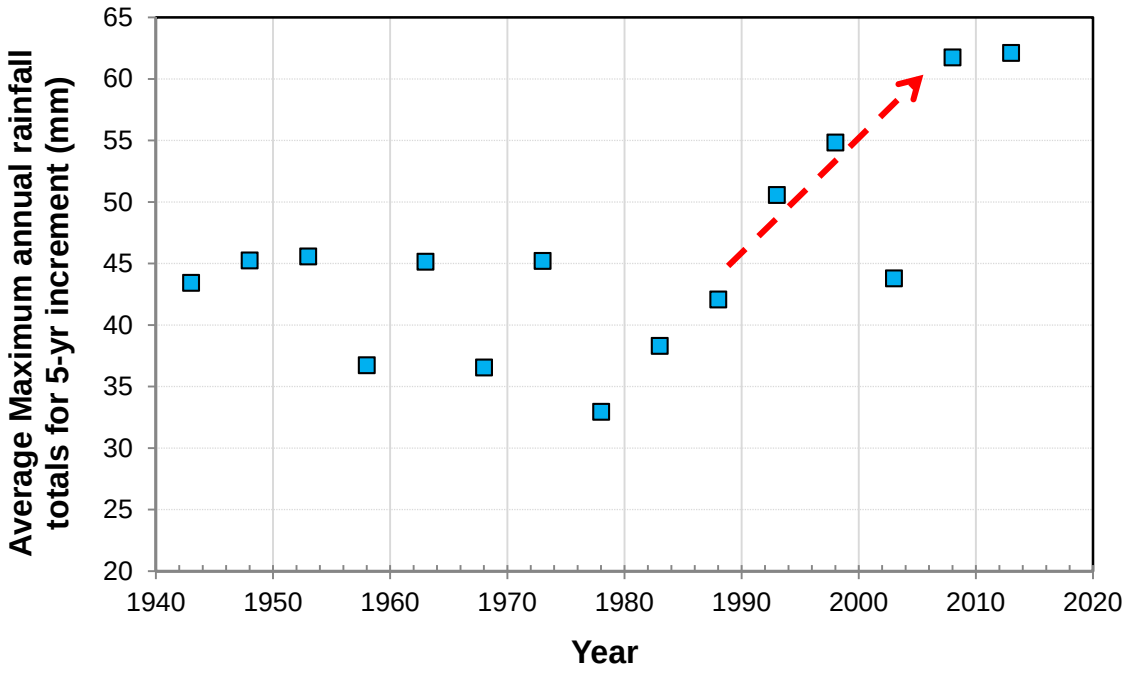


**Figure 5-4. Five year averages of the maximum annual daily rainfalls for the Kananaskis climate station showing a trend towards above-average rainfall totals after approximately 1990.**

An additional analysis was conducted to examine if the frequency of extreme rainfall events has changed over time. Again, the Kananaskis station was used for the analysis due it its continuous and long record. Exceedances for maximum daily rainfall were counted for 20 to 70 mm. Upward trends were identified for each threshold. Figure 5-5 shows the exceedance counts for 50 mm daily rainfall. It appears that prior to the 1990s, there was no year in which there was more than one exceedance of this threshold. After 1995, however, two or more exceedances are observed six times. This result may suggest that there is no smooth trend but an increase in the number and severity of extreme events.

A combination of climate change model and theory with the admittedly precursory analysis presented herein, suggests that more and perhaps more intensive rainfall and small-watershed floods and debris floods should be anticipated.

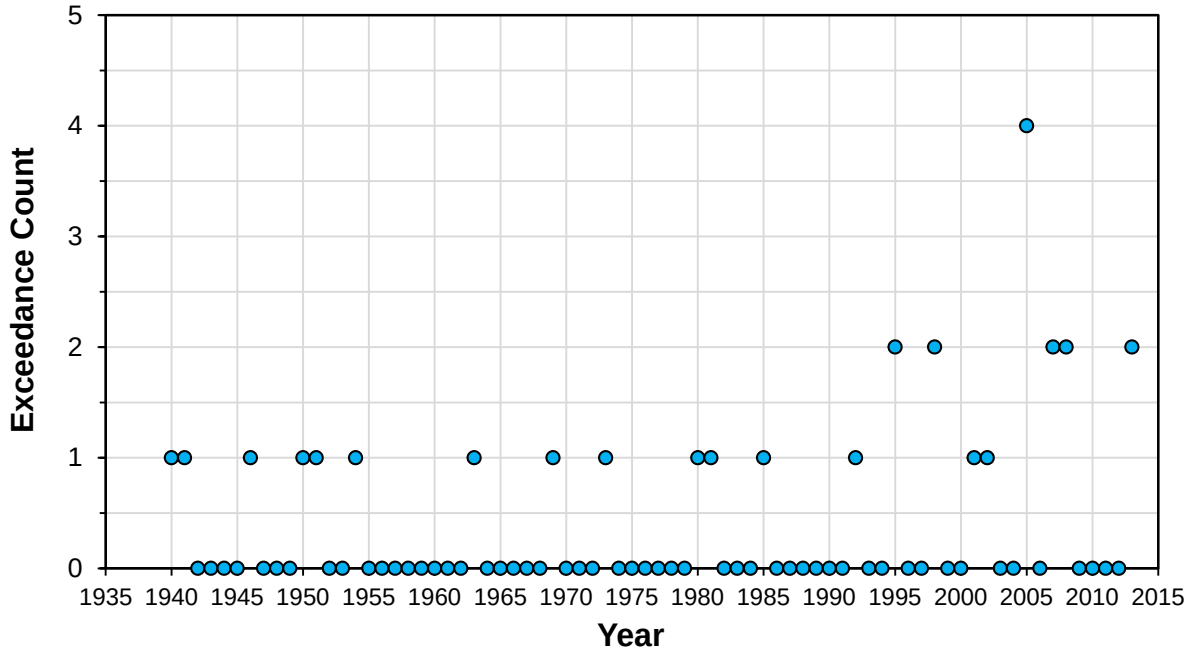


**Figure 5-5. Exceedance counts of incidents of greater than 50 mm of daily rainfall at Kananaskis.**

The Town of Canmore retained the Geophysical Disaster Computational Fluid Dynamics Center at the University of British Columbia to conduct further analysis of a changing hydroclimate in the study area. The study compared the June 2013 storm with historical storms that produced greater than 50 mm of precipitation. The objective was to determine whether there is a spatial or temporal trend in past synoptic-scale low pressure systems that led to heavy precipitation events. The key findings of this study show that heavy precipitation events (>50 mm) are approximately twice as likely to occur today (3-year return period) as they were 30 years ago (6-year return period). Furthermore, no correlation was noted between heavy precipitation events and the El Niño Southern Oscillation (ENSO) and PDO climate patterns. Appendix C provides the full report.

## 5.3. Streamflow

The previous analysis focused on rainfall only and does not discuss streamflow or trends in snowpack which may be equally important when discussing the effects of climate change on peak flows in mountainous creeks. BGC plotted the time series of Waiparous Creek (Figure 5-6) and Bow River (Figure 5-7) annual peak instantaneous flows to gain preliminary insights on possible trends in peak runoff. Caution should be used in interpretation of these results due to variation in runoff mechanisms (rainfall and rain-on-snow), meaning that the data are not from the same statistical population.

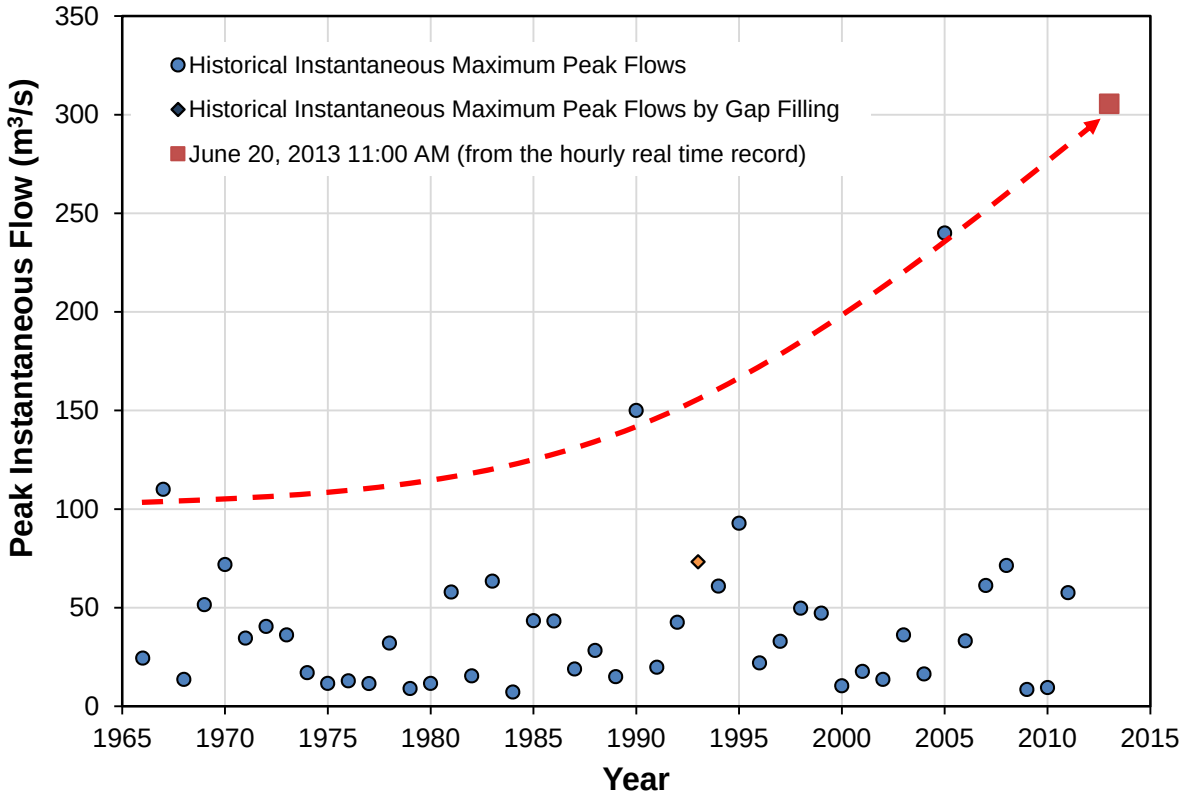


**Figure 5-6. Time series of peak instantaneous flow at Waiparous Creek (05BG006).**

Waiparous Creek (333 km$^2$ watershed) demonstrates an increase in episodic and singular extreme peak flow events over an arbitrary threshold of 100 m$^3$/s, while the time series of flows over less than this threshold has remained relatively stationary over the observational period. In contrast, no upward trend can be discerned in extreme runoff events (defined here above an arbitrary threshold of 300 m$^3$/s) at the Bow River gauge with a watershed area of 2210 km$^2$. The difference between the two creeks may be that Bow River is largely nival and thus responds mostly to trends in snowpack and temperature during the spring runoff, whereas Waiparous Creek may respond more readily to heavy rain even in absence of heavy snowpacks.

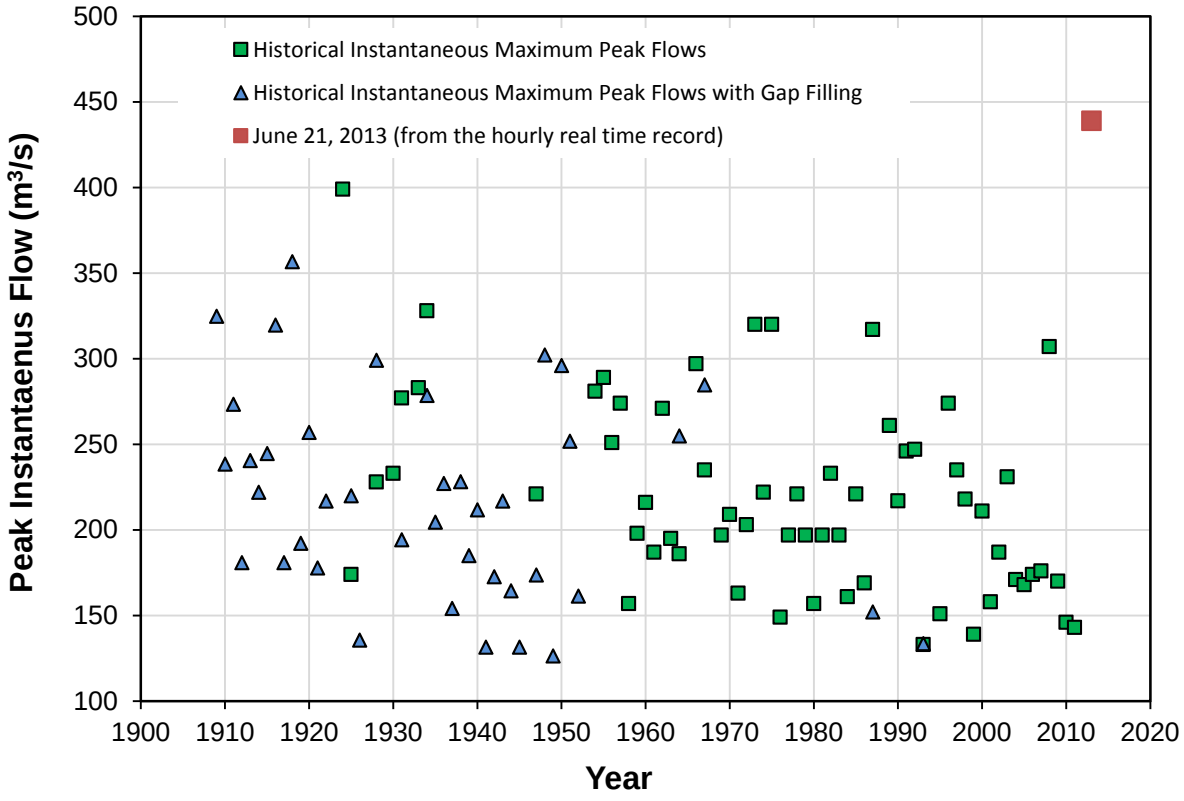


**Figure 5-7. Time series of peak instantaneous flow at Bow River at Banff (05BB001)**

This analysis is precursory as it is based on only one weather station and two streamflow gauges. Further analysis ought to determine if data non-stationarity is becoming a factor that should be considered in the design of short and/or long-term mitigation measures. It should be re-emphasized in this context, that there are two dominant failure mechanisms for debris floods on Cougar Creek (BGC, 2013):

- Mobilization of bedload through the exceedance of a critical discharge
- Landslide dam outbreak floods.

It is difficult enough to associate global warming with ambiguous trends in the frequency and/or magnitude of extreme hydroclimatic events. The determination of how far climate change may influence the frequency of magnitude of landslides in the Cougar Creek watershed adds another layer of uncertainty. This brings its effects on landsliding into the realm of speculation given the different types and hydroclimatic triggers of landslides that prevail in the Cougar Creek watershed.

# 6.0 CONCLUSION

The June 19 – 21, 2013 storm was a very rare event because of its long duration and associated total rainfall. The 1-day, 2-day and 3-day rainfall totals for this storm at Kananaskis, the nearest long-term climate station to Cougar Creek, were the highest on record since observations began in 1939. However, the event was not extreme in terms of short term maximum hourly rainfall intensity, where similar intensities have occurred frequently in the region over the period of record.

Antecedent moisture conditions in the Cougar Creek watershed appear to have been high prior to the storm. This condition, combined with observations of frozen soils at higher elevations, suggests that a high percentage of the total rainfall occurred as storm runoff. Snowmelt contribution estimates range from approximately 12% to 29% of the total rainfall. Contributions from Marmot Basin could be an appropriate analog for Cougar Creek conditions. However, BGC's analysis suggests that the flood event was rainfall-dominated and could have produced similar damage had there not been a snowpack.

The storm produced a long-duration flood which transported considerable volumes of bedload and caused massive bank erosion. Peak instantaneous flows recorded on WSC hydrometric stations on the Bow River and on Waiparous Creek are the largest on record, although the Waiparous gauge was damaged during the flood and did not record the peak. A flood frequency analysis indicates that the rainfall led to a relatively extreme streamflow on the Bow River (200 to 400-year return period) considering the measured peak flow data on record only, and a less rare event when incorporating historical data into the analysis (~ 15- to 20-year return period). The Waiparous Creek 2013 flood event had a 40- to 60-year return period given the available data.

A preliminary trend analysis of relatively long-term rainfall and streamflow records suggests that more frequent and perhaps larger total volume rainfall and small-watershed floods and debris floods could be anticipated in the Canmore region in the future. However, these results were prepared with limited data and methods, and therefore one cannot attribute the frequency and magnitude results provided in this report to climate change with certainty. Nonetheless, a continuation of the observed trends would, over time, jeopardize the results of the frequency-magnitude analysis (BGC, 2014) as that analysis is based on long term data stationarity. In light of the uncertainty of a continuing trend of extreme events it may be prudent to allow for adjustments in the design or maintenance requirements over time for creek mitigation works in the region.

## 7.0 CLOSURE

We trust the above satisfies your requirements at this time. Should you have any questions or comments, please do not hesitate to contact us.

Yours sincerely,

**BGC ENGINEERING INC.**
**per:**

ISSUED AS DIGITAL DOCUMENT. SIGNED HARDCOPY ON FILE WITH BGC ENGINEERING INC.

Ashley Perkins, M.Sc., P.Geo. (BC, AB)
Hydrologist

ISSUED AS DIGITAL DOCUMENT. SIGNED HARDCOPY ON FILE WITH BGC ENGINEERING INC.

Matthias Jakob, Ph.D., P.Geo. (BC, AB)
Senior Geoscientist

Reviewed by:

Hamish Weatherly, M.Sc., P.Geo. (BC, AB)
Senior Hydrologist

AP/MJ/HW/jc/cm

# REFERENCES

Adamowski, K., 1996. Regional rainfall distribution for Canada. Atmospheric Research, 42: 75-88.

BGC Engineering Inc., 2013. Cougar Creek, Forensic Analysis and Short-Term Debris Flood Mitigation. Final Draft submitted to the Town of Canmore. September 30, 2013.

Clow, D.W., L. Nanus, K.L. Verdin, and J. Schmidt, 2012. Evaluation of SNODAS snow depth and snow water equivalent estimates for the Colorado Rocky Mountains, USA. Hydrological Processes, 26: 2583-2591.

DeGaetano, A.T., 2009. Time-Dependent Changes in Extreme-Precipitation Return-Period Amounts in the Continental United States. Journal of Applied Meteorology and Climatology, 48: 2086-2099.

Gadd, B., 2013. Eyewitness: Photos from a flash flood in Alberta. The Tyee. June 26, 2013. http://thetyee.ca/Blogs/TheHook/2013/06/26/CougarCreekFlood/#disqus_thread

IPCC, 2012. Managing the Risks of Extreme Events and Disasters to Advance Climate Change Adaptation. A Special Report of Working Groups I and II of the Intergovernmental Panel on Climate Change [Field, C.B., V. Barros, T.F. Stocker, D. Qin, D.J. Dokken, K.L. Ebi, M.D. Mastrandrea, K.J. Mach, G.-K. Plattner, S.K. Allen, M. Tignor, and P.M. Midgley (eds.)] Cambridge University Press, Cambridge, UK, and New York, NY, USA 582 pp.

IPCC, 2013. Working Group I Contribution to the IPCC Fifth Assessment Report Climate Change 2013: The Physical Science Basis Summary for Policymakers.

Neill, C.R., and W.E. Watt, 2001. Report on Six Cases of Flood Frequency Analyses. Prepared for: Alberta Transportation, Transportation and Civil Engineering Division, Civil Projects Branch. April, 2001.

Pryor, S.C., J.A. Howe, and K.E. Kunkel, 2009. How spatially coherent and statistically robust are temporal changes in extreme precipitation in the contiguous USA? International Journal of Climatology, 29: 31-45.

St. Jacques, J-M., D.J. Sauchyn, and Y. Zhao, 2010. Northern Rocky Mountain stream flow records: Global warming trends, human impacts or natural variability? Geophysical Research Letters, vol. 37.

Valeo, C., Xiang, Z., Bouchart, F.JC., Yeung, P. and M.C. Ryan, 2013. Climate change Impacts in the Elbow River watershed. Canadian Water Resources Journal 32(4): 285-302.

# APPENDIX A
# DESCRIPTION AND ANALYSIS OF THE WEATHER LEADING TO THE FLOODING IN CANMORE, ALBERTA, IN JUNE 2013

# Description and Analysis of the Weather leading to the Flooding in Canmore, Alberta, in June 2013

**Part 1 of Weather Analysis Project for**
**Canmore's Mountain Creek Hazard Mitigation**

Town of Canmore
Contract No. _____
15 Aug 2013 – 31 Mar 2014
Submitted to Manager of Engineering: **Andy Esarte**
902-7th Avenue, Canmore, Alberta, T1W3K1
phone: 403-678-1545; email: AEsarte@canmore.ca


**Principal Investigator:**
Prof. Roland Stull, PMet, CCM, CFII
Earth, Ocean & Atmos. Sci. Dept.
University of British Columbia
2020-2207 Main Mall, Vancouver, BC V6T 1Z4
phone: 604-822-5901, fax: 604-822-6088
email: rstull@eos.ubc.ca

**Report Created by:**
Dr. Rosie Howard
Earth, Ocean & Atmos. Sci. Dept.
University of British Columbia
2020-2207 Main Mall, Vancouver, BC V6T 1Z4
phone: 604-822-3591, fax: 604-822-6088
email: rhoward@eos.ubc.ca


**27 Aug 2013**

## Overview


Three low-pressure systems interacted to cause the heavy precipitation at Canmore. The resulting complex of storms was able to tap large moisture supplies from air originating over the Pacific and Gulf of Mexico, and was able to move this humid air toward the east side of the Rockies. There, winds with a significant component from the east pushed the humid air upslope, triggering extensive clouds, precipitation, and embedded thunderstorms. Moisture leaving the atmosphere as rain was replaced by a continual inflow of more humid air in the "conveyer belt" of winds from the south and east, enabling the heavy precipitation to continue for several days.


## 1. Introduction

On Wednesday 19 June 2013, heavy rain developed over southwest Alberta (AB), Canada, contributing to extreme flooding on the Bow River and its tributaries in Canmore and Calgary. By 20 June 2013, massive evacuations were underway, with mudslides and bridge washouts in places. The event resulted in fatalities, destroyed homes and roads, and displaced tens of thousands of residents in southwest Alberta.

This report explains the weather-map (*synoptic-scale*) patterns that led to this event, covering the period 18 - 21 June 2013. For this analysis, we considered weather-analysis maps, water-vapour satellite imagery, the Canadian Precipitation Analysis (CaPA) from Environment Canada (CaPA, 2013), groundwater level, and snowpack. The CaPA analyses (shown in figures below) combine rainfall observations with a sophisticated weather prediction model to produce the rainfall estimates.

## 2. Storm Development Day by Day — An Outline of Events

### 18 June 2013

- An old low-pressure system (*extratropical cycl*one) was off the Oregon coast, with winds ahead of the low moving moist air from over the Pacific into southern AB (Fig. 1).
- Generally warm temperatures were present in southern AB. (Warm air can hold more water vapour than cold air.)
- A second, stronger low-pressure system existed to the south in Utah (having originating in Colorado) and was moving northwards.

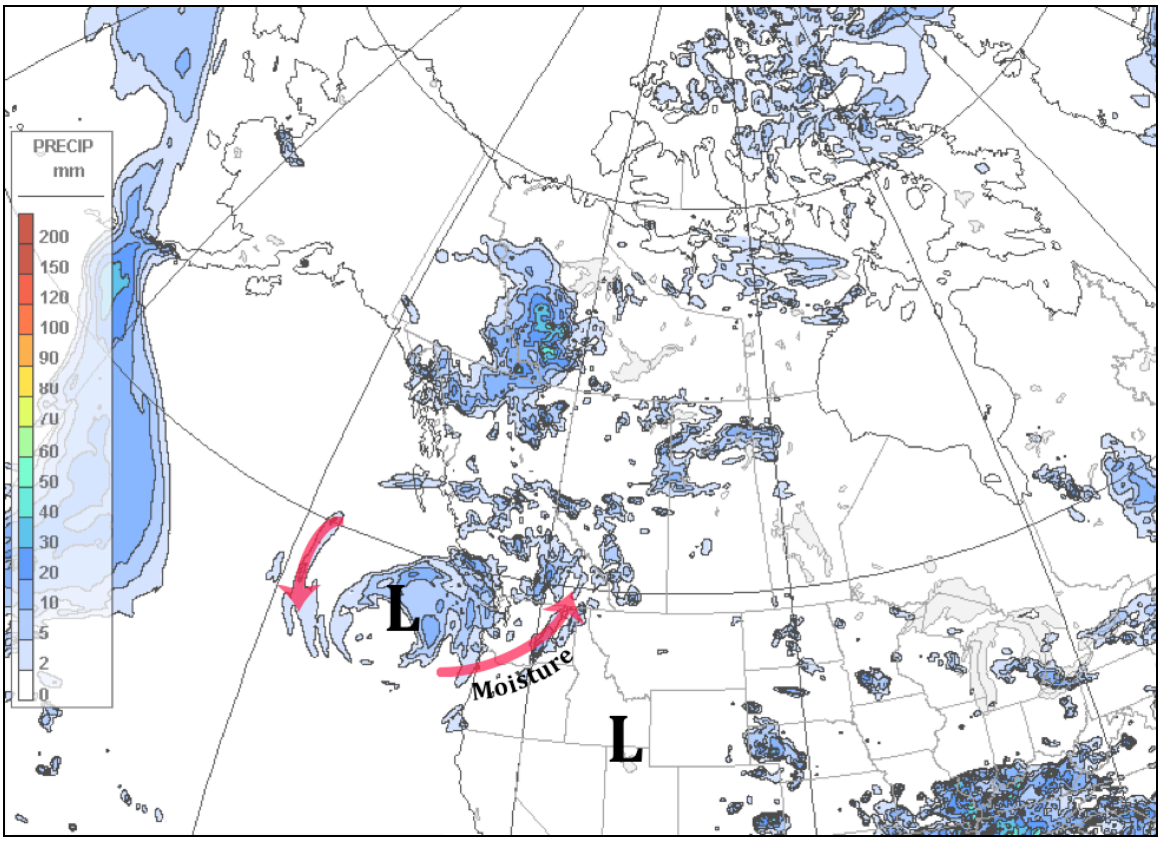


**Figure 1. Map showing 24-hour accumulated precipitation (mm) valid at 5am on 18 June 2013. "L" symbols represent low-pressure systems, and red arrows show the prevailing direction of flow, with moisture moving into southern AB.**
**(Source of background map: http://loki.qc.ec.gc.ca/DAI/CaPA/index.html).**

**19 June 2013**

- The old low-pressure system was moving very slowly eastward, and continued to bring more moisture inland towards AB (Fig. 2) from over the Pacific.
- The second low-pressure system was strengthening and moving northwards, now on the Idaho-Montana border, resulting in very warm moist air carried by increasing wind speeds toward southern AB. This warm humid air originated from over the tropical waters of the Gulf of Mexico.
- The combined effect of these two lows was to create a conveyer belt of fast-moving warm humid air.
- As that air was pushed toward the Alberta Rockies from the east, the upslope conditions caused heavy rain to develop over southwest AB (Fig. 2).

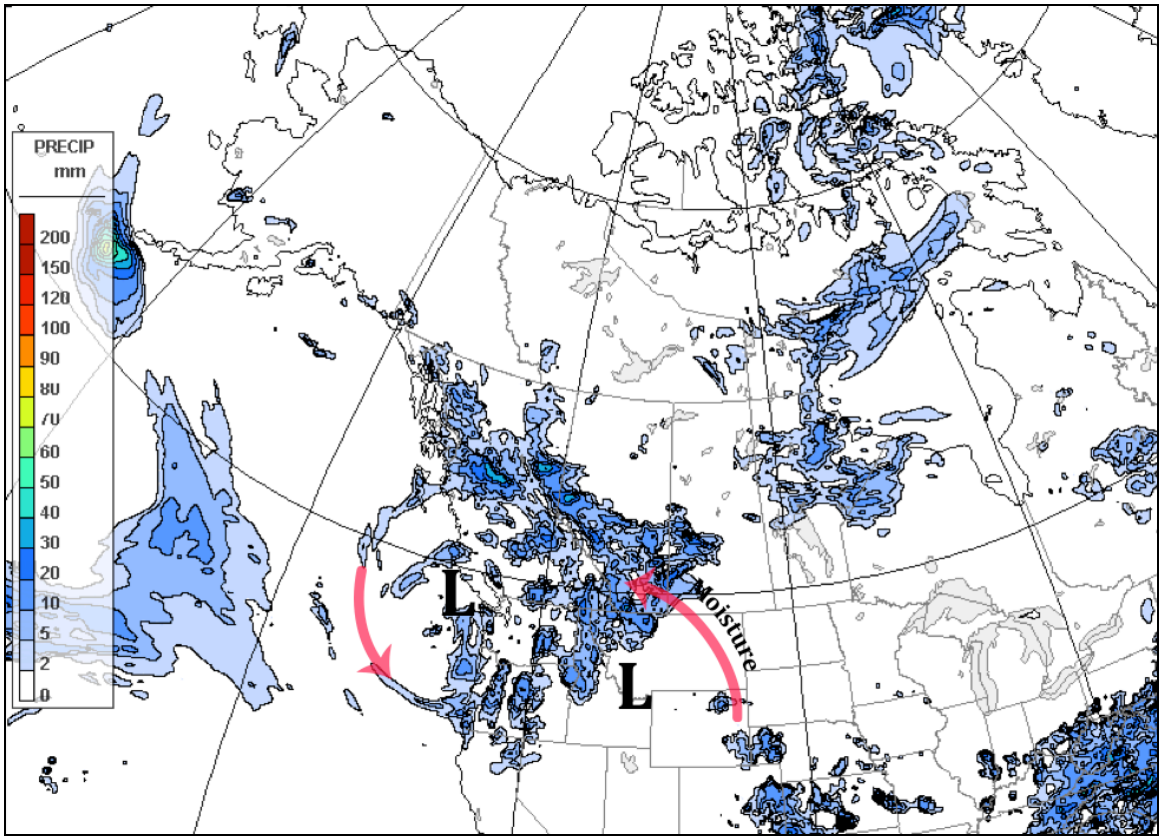


**Figure 2. As for Fig. 1, except valid at 5am on 19 June 2013.**
**(Source of background map: http://loki.qc.ec.gc.ca/DAI/CaPA/index.html).**

**20 June 2013**

- The old low pressure system near coast was weakening, but still bringing more Pacific moisture inland where the other Low could tap into it (Fig. 3).
- The inland low-pressure system (i.e., the second low from Fig. 2) was now weakening and moving further eastwards, but continuing to bring moisture from the Gulf of Mexico and US plains states towards southern AB.
- A **new** (3rd) surface low-pressure system was born in southern AB by consolidating the energy from the two older lows. This 3rd low is marked with a red "X" in Figure 3.
- Very moist southeasterly/easterly flow across southern AB, fed by a moist airmass over southwest prairies and central US (Fig. 3). Direction of flow becomes perpendicular to Rocky Mountains, resulting in enhanced precipitation due to strong upslope conditions (*orographic precipitation*).
- Heavy rain continues in southwest AB.

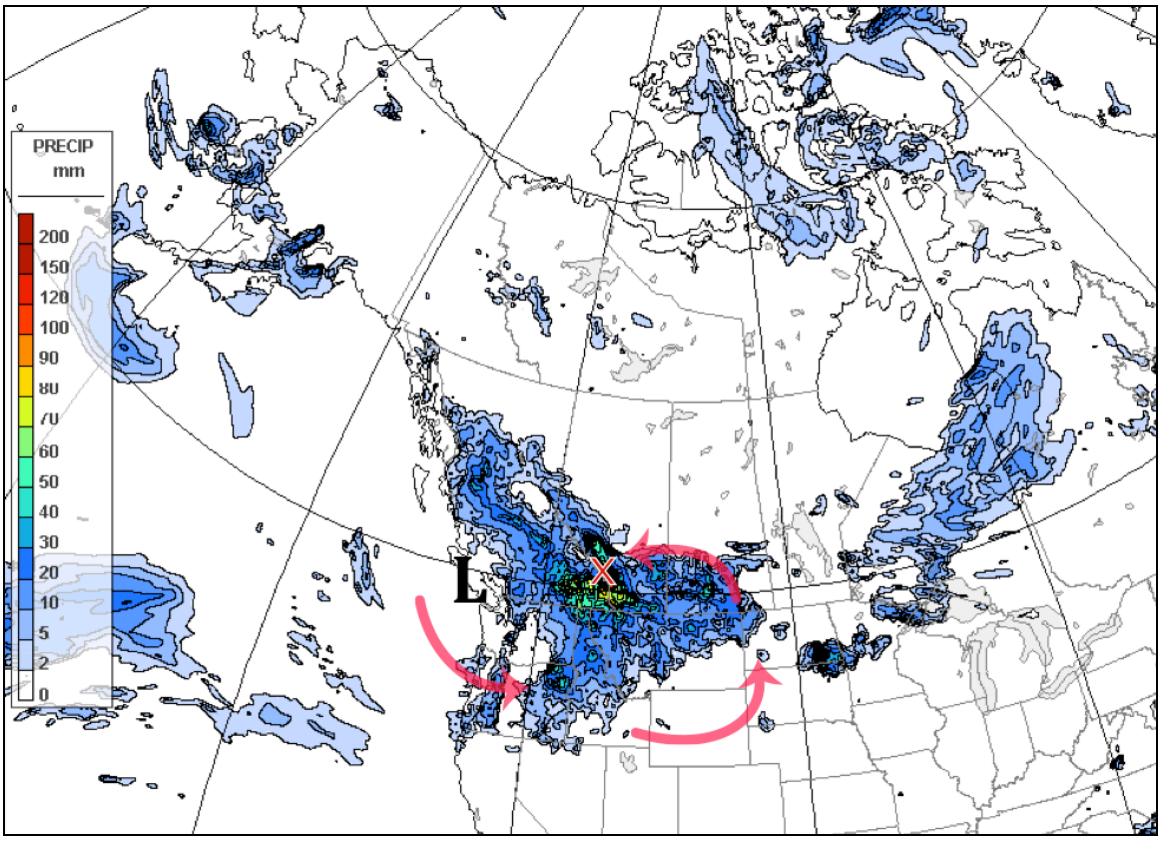


**Figure 3. As for Fig. 1, except valid at 5am on 20 June 2013. Red "X" indicates new low pressure system directing moisture into AB and towards the mountains.**
**(Source of background map: http://loki.qc.ec.gc.ca/DAI/CaPA/index.html).**

**21 June 2013**

- While the storms are weakening, moist air flowing from the northeast (fig. 4) continued to move humid air upslope over southwest AB.
- Rain continued to accumulate over southwest AB, but rainfall rates were gradually decreasing.

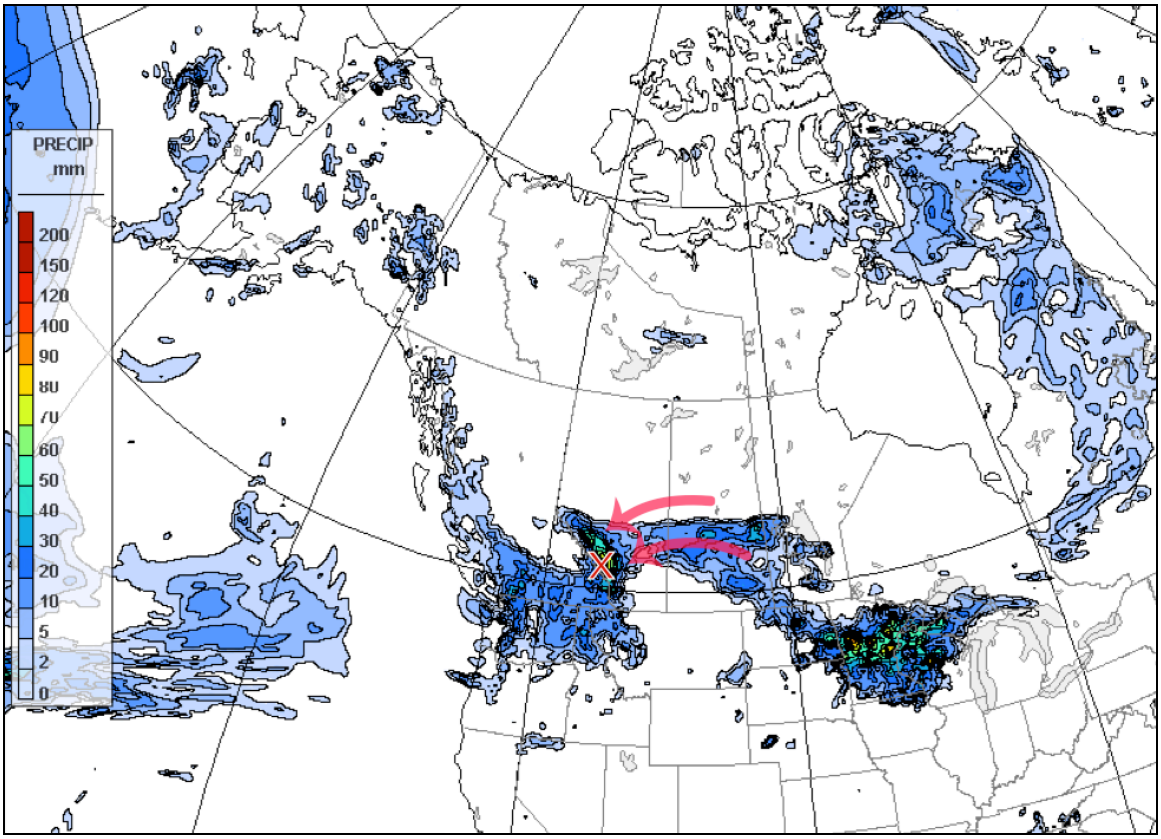


**Figure 4. As for Fig. 1, except valid at 5am on 21 June 2013. Red "X" denotes pivotal region where flow converges with mountains.**
**(Source of background map: http://loki.qc.ec.gc.ca/DAI/CaPA/index.html).**

## 3. Summary and other contributing factors

- Slow moving low-pressure system crossing Washington, northern ID and northwest MT, steadily bringing Pacific moisture inland towards southern AB.
- Flow into southwest AB rotated from southwesterly to northeasterly, with the pivot point (red "X") located directly over the Bow River watershed, meaning precipitation persisted there throughout the four-day period (Fig. 5).
- Contribution of additional moisture from Central and Midwest US. That moisture had originated over the Gulf of Mexico.

- Initially warm surface/near-surface temperatures (able to hold lots of moisture) and the upslope wind direction enhanced deep storm clouds with heavy precipitation (*convection*) over southwest AB.
- Snowpack still present in the Rockies caused high runoff due to frozen ground underneath, and rain-on-snow caused rapid snowmelt, adding water to runoff. Groundwater levels were already higher than average (Tim Ashman, 2013, BC Hydro, personal communication).

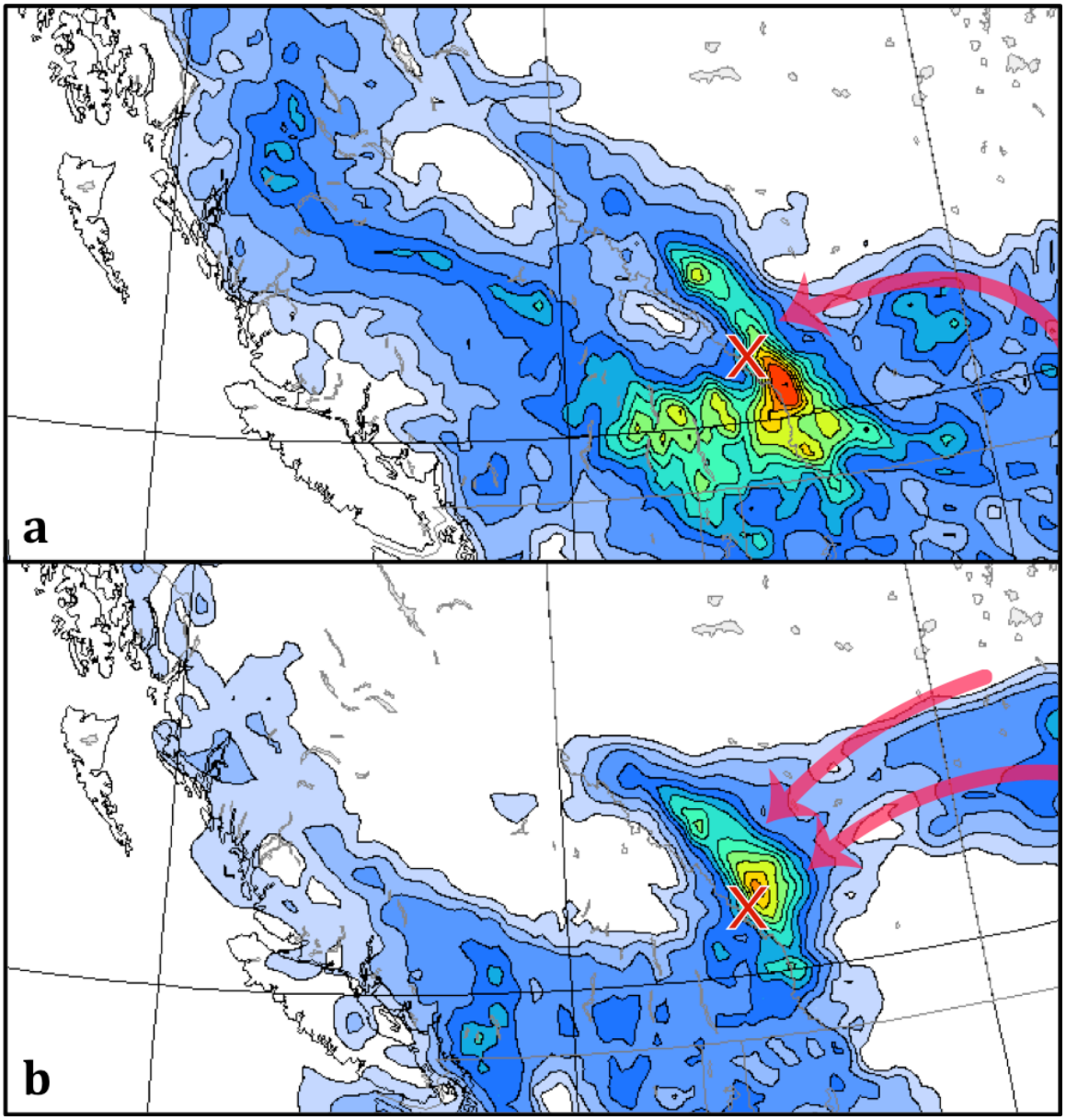


**Figure 5. Zoomed images of figs. 3 and 4 (a and b, respectively), showing precipitation and flow over southern BC and AB.** **(Source of background map: http://loki.qc.ec.gc.ca/DAI/CaPA/index.html).**

## Reference

CaPA, cited 2013: Canadian Precipitation Analysis. [Available online at http://loki.qc.ec.gc.ca/DAI/CaPA/index.html].

# APPENDIX B
# RETURN LEVEL ANALYSIS OF KANANASKIS RAINFALL

# Return Level Analysis of Kananaskis Rainfall

Prepared by: Vincenzo Coia and Natalia Nolde
Department of Statistics
The University of British Columbia

For BGC Engineering Inc., Vancouver

October 22, 2013

## 1 Model Selection

The objective of this report is to provide an analysis of return levels of annual 3-day maximum rainfall in the Canmore area. The data are collected from the Kananaskis climate station since 1939. In the draft "Cougar Creek Forensic Analysis" report, a return level analysis is performed by fitting a Generalized Extreme Value (GEV) distribution to the data, but assuming the fitted distribution is unchanging every year (i.e. is *stationary*). However, this leads to the question of whether to consider the June 2013 rainfall event as an outlier.

An alternative approach is recommended in this report which relaxes the stationarity assumption of the fitted GEV distribution (to become *non-stationary*). This can be done by adding a trend on one or more of the GEV distribution's three parameters – these are the location parameter, which shifts the entire distribution; the scale parameter, which stretches the distribution; and the shape parameter, which determines the tail behaviour of the distribution. Typically, no trend is fit to the shape parameter which is thought to be inherent to the underlying phenomenon, so only a trend in the shape and scale parameters will be considered.

To determine an appropriate form for the trend, a "forward selection" approach is used, which progressively adds higher-order terms if they are deemed significant by a likelihood ratio test[1], beginning from a stationary model. To start, a linear term is added to the location parameter. Comparing this model to the stationary model shows that the linear location trend is significant at the 0.05 level ($p$-value = 0.037). Keeping the linear location trend, a linear trend to the scale parameter is added, but is not significant at the 0.05 level ($p$-value = 0.375), so we will keep the scale parameter constant in the model. Adding a quadratic term to the location parameter is also insignificant ($p$-value = 0.125), so the location parameter will be kept with a linear trend. This leaves us with a final model having a linear trend in location, and no trend in the scale and shape parameters.

Finally, we should check whether the chosen model fits the data well. This can be done by checking the "Residual Probability Plot" or the "Residual Quantile Plot", after standardizing the data to follow a standard Gumbel distribution (see Figure 1). Since the modelled probabilities and quantiles are close to those suggested by the data (as indicated by closeness to the diagonal line), the model can be considered a reasonable fit. One concern may be the last point in the Quantile Plot (corresponding to the June 2013 rainfall event), but it is not enough to seriously doubt the model's fit.

## 2 Analysis

The return period and return level analyses under non-stationarity are very different from the stationary case. This section will first discuss the consequences of a non-stationary distribution in Section 2.1 on risk, then will perform the return period and return level analyses in Sections 2.2 and 2.3, respectively.

[1] The likelihood ratio test approximates the distribution of the test statistic (the deviance) by a Chi-squared distribution. Since the sample size ($n = 75$) is large, this approximation is expected to be acceptable.

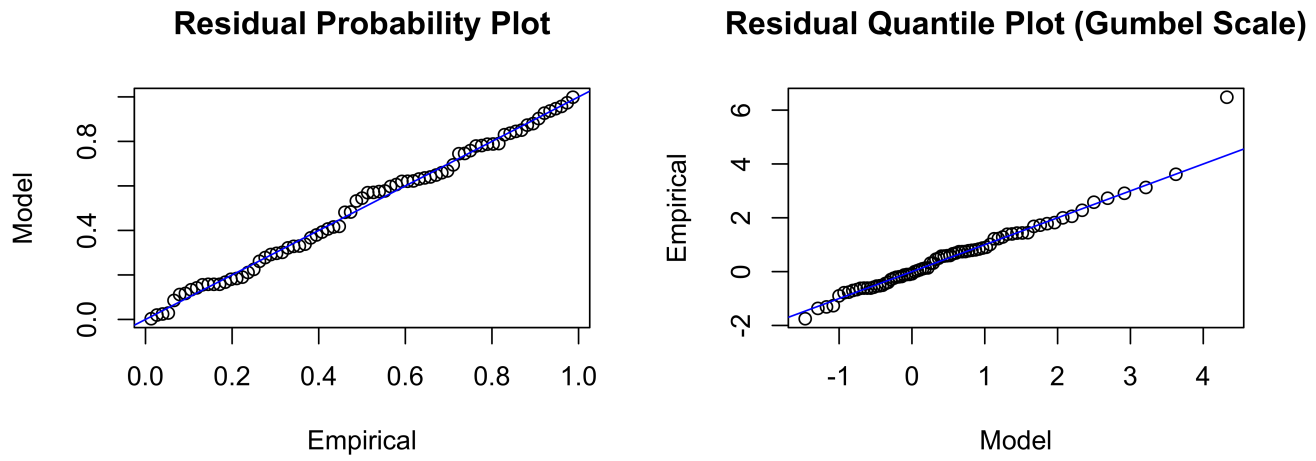


Figure 1: Goodness of fit plots of the chosen model. The plots compare the probabilities (left) or quantiles (right) suggested by the model versus the data (empirical). The standard Gumbel distribution is used to compared to the standardized data.

## 2.1 Changing Risk

A major consequence of adding a trend to the model is that the risk changes over time. However, it is dangerous to assume that the fitted trend will continue into the future. The linear trend is an approximate fit to a more complicated true trend for the study period only. As such, the fitted trend becomes less reliable the further into the future it is fit. In the absence of additional physical information on the possible evolution of the trend, the analyses in this report all assume the fitted trend (in the location parameter) continues indefinitely.

To get a sense of the changing risk, Figure 2 shows how the return level changes each year for a few given risk levels. Note that, if the linear trend (in the location parameter) is assumed to continue, then the return period for the return levels cannot be computed as the reciprocal of risk, which requires trendless data. On the other hand, we *can* interpret the risk reciprocal as the return period if we wish to examine the scenario where the trend "freezes" at some year, that is, the model parameters suddenly stop changing. Considering the dangers of extrapolating the trend, freezing the trend in 2013 would yield the "best case scenario" providing the smallest return levels one could hope for, assuming the trend is never reversed in the future. Freezing the trend at 2013 gives an estimated 750-year return level of 272mm with 95% confidence interval [138mm, 406mm].

## 2.2 Return Period Analysis

The return period for a given rainfall level can either be interpreted as **the expected wait time until that level recurs** (Interpretation 1), or as **the amount of time to pass where a recurrence event is expected to occur once** (Interpretation 2). In the former interpretation, the recurrence event is expected to occur at the end of the interval, whereas the event can occur at any time in the interval in the latter definition. If no trend is present, these interpretations are equivalent. Since the recurrence probability changes each year, the return periods will also change depending on the reference year (i.e. the year one begins "waiting"). Figure 3 displays the return period for the June 2013 rainfall event, depending on the reference year, for both interpretations as well as a comparison to the stationary case. Starting the wait in 2013, and assuming the linear trend (in the location parameter) continues, an exceedance of the June 2013 event is expected to occur in 242 years (Interpretation 1), and is expected to happen once in the next 294 years (Interpretation 2).

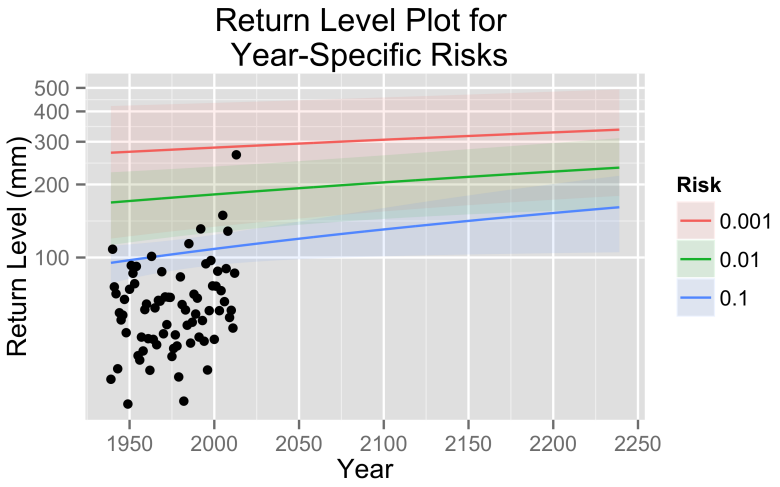


Figure 2: The year-specific return level over past and future years, for a few levels of risk (i.e. probability of exceedance) along with 95% confidence intervals (derived using the Delta method). Note that the risks cannot be thought of as return periods under the fitted trend. The Kananaskis data are shown as dots.

## 2.3 Return Level Analysis

Analogous to the return period, the return level can be interpreted as **the rainfall level for which an exceedance is expected at the end of a given period,** (Interpretation 1), or as **the rainfall level that is expected to occur once during a given period** (Interpretation 2). Under the assumption of stationarity, these interpretations are equivalent. As is the case with the return period, the return level will depend on the reference year. See Figure 4 for the return level plots for both interpretations. Estimated return levels from the 2013 perspective can be found in Table 1.

| Return Period | Interpretation 1 | Interpretation 2 | Stationary Model |
|---|---|---|---|
| 100 years | 204mm | 196mm | 178mm |
| 500 years | 343mm | 319mm | 246mm |
| 1000 years | 466mm | 435mm | 279mm |
| 10,000 years | 2456mm | 2418mm | 419mm |

Table 1: Estimated return levels under both interpretations, beginning the wait time in 2013. The linear trend is assumed to hold at least for the next 10,000 years. The results from the stationary model are also included for comparison.

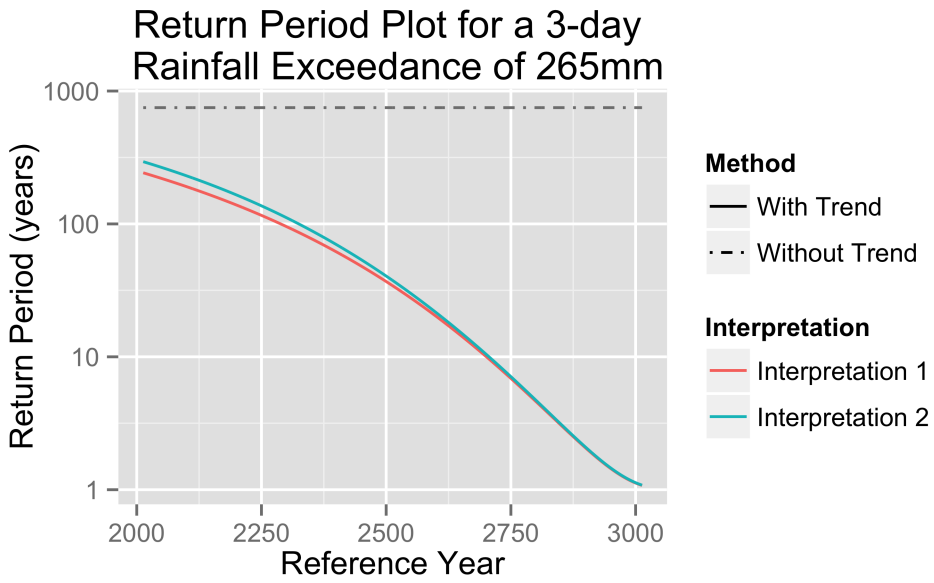


Figure 3: The return period of the June 2013 rainfall event as influenced by the reference year. Both interpretations are included, as well as the results from fitting a stationary GEV model.

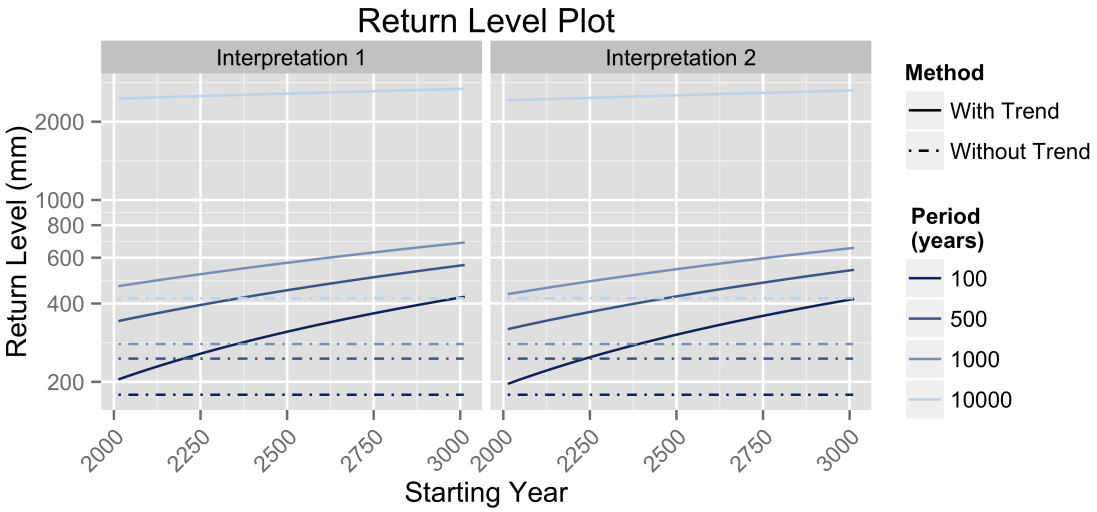


Figure 4: The return levels as influenced by the reference year. The stationary cases (dot-dashed lines) are also included.

# APPENDIX C
# INTERCOMPARISON OF THE JUNE 2013 SOUTHWEST ALBERTA RAINSTORM WITH PAST HEAVY PRECIPITATION EVENTS

# Intercomparison of the June 2013 Southwest Alberta rainstorm with past heavy precipitation events

**Part 2 of Weather Analysis Project for**

**Canmore's Mountain Creek Hazard Mitigation**

March 14, 2014

Town of Canmore
Contract No._____
15 Aug 2013 – 31 Mar 2014
Submitted to Manager of Engineering: **Andy Esarte**
902-7th Avenue, Canmore, Alberta, T1W 3K1
phone: 403-678-1545; email: AEsarte@canmore.ca


**Principal Investigator:**
Prof. Roland Stull, PMet, CCM, CFII
Earth, Ocean & Atmos. Sci. Dept.
University of British Columbia
2020-2207 Main Mall
Vancouver BC, V6T 1Z4
phone: 604-822-5901, fax: 604-822-6088
email: rstull@eos.ubc.ca

**Report created by:**
Dr. Rosie Howard
Earth, Ocean & Atmos. Sci. Dept.
University of British Columbia
2020-2207 Main Mall
Vancouver BC, V6T 1Z4
phone: 604-822-5901, fax: 604-822-6088
email: rhoward@eos.ubc.ca


## Executive Summary


Heavy precipitation caused severe flooding in Canmore and surrounding area in June 2013, affecting tens of thousands of residents in southwest Alberta. Precipitation data was used to identify similar events (18 total for the period 1952–2013), to investigate whether

the synoptic conditions causing them have changed, and whether there is any relationship with large-scale climate signals.

Reanalysis data from the National Centers for Environmental Prediction/National Center for Atmospheric Research was used to score each event according to the main mechanisms that are known to lead to heavy precipitation in southwest Alberta. Since no correlation was found between precipitation amounts and the resulting scores, we conclude that several different combinations of synoptic weather features can cause heavy precipitation.

The scoring system served to classify the storms. Most heavy precipitation events are caused by an upper-level quasi-stationary low-pressure system, with the next most important factors being subtropical moisture source(s), easterly upslope flow, thunderstorms, and frontal precipitation. There is a potential shift in the large-scale pattern, with half the storms after 1990 tapping a subtropical moisture source, four of which included moisture from both the Pacific and the Gulf of Mexico. Some disparity between the scoring and precipitation amounts can be attributed to the subjective nature of the scoring system, as well as the fact that thunderstorms (instability) are not well-modelled by the coarse-resolution reanalysis data.

The return period of heavy precipitation events has decreased from about 6 years in the 1980s to about 3 years presently, meaning that the probability of a heavy precipitation event occurring this year is roughly 1/3.

Very little correlation was found between El Niño Southern Oscillation/Pacific Decadal Oscillation and heavy precipitation events. While there is evidence in the literature for relationships between climate signals and precipitation response in southwest Canada, these mainly exist in the winter and for more stratified than convective storms. All heavy precipitation events in this study occurred between April and September, and since thunderstorms contributed substantially to precipitation totals, the lack of correlation is not surprising.

# 1. Introduction

In June 2013, heavy precipitation occurred in southwest Alberta (AB), Canada, causing extreme flooding on the Bow River, affecting Banff, Canmore, Calgary, and other residential areas. A first report summarizing the synoptic weather conditions leading to this event determined that during the period 18–21 June 2013, three low-pressure systems interacted to bring very humid air to Southwest AB. This moisture originated from both the Pacific and the Gulf of Mexico, and the local prevailing (easterly) wind direction triggered orographic clouds, heavy up-slope precipitation, and embedded thunderstorms.

This report compares the June 2013 storm with past storms in order to determine whether there has been a long-term change in the large-scale configuration of storms producing heavy precipitation on the eastern slopes of the AB Rockies. Namely, we attempt to determine whether past synoptic conditions leading to heavy precipitation events show any trend, temporally and spatially.

# 2. Data

### *a. Precipitation data*

Historical precipitation data (EnvironmentCanada 2013) from the three Environment Canada (EC) automatic weather stations closest to the town of Canmore (Banff, Bow Valley, and Kananaskis; see fig. 1) are used. Table 1 outlines the locations and data records for each station, located on or near the eastern slopes of the Rockies. We define a threshold for heavy precipitation events where total rainfall $\geq$ 50 mm/(2 days).

We focus on the synoptic scale, the scale of low-pressure systems and their associated fronts. The predictability of convective, isolated thunder showers (i.e. mesoscale) is less than that of frontal or organized precipitation, so we chose events where at least two of the three stations had recorded a heavy precipitation event for the same time period or within one day

of each other, in order to exclude thunderstorms. This criteria produced 18 cases (or "heavy precipitation events") spanning the years 1952–2013 (fig. 2 and table 2). In an attempt to account for instrument changes and inaccuracies over this long period, the Adjusted and Homogenized Canadian Climate Dataset was considered, outcomes of which are discussed in appendix A.

There were 4 cases with total rainfall $\geq$ 50 mm/(2 days) at all three stations, and the remaining 14 cases had the heavy rain at two stations with some rain at the third "drier" station. Precipitation totals for each of the 18 cases lie between 50–100 mm per event, except for those occurring in 2005 and 2013 which have greater amounts (fig. 3). In general, of the three stations, Kananaskis had the most precipitation per event. All cases occurred between April and September (none in July), with the most occurring in May (4 cases) and June (10 cases).

### *b. Reanalysis data*

Analysis of the June 2013 storm was produced using surface and mid-troposphere (50 kPa, roughly 5.5 km above mean sea level) weather analysis maps from EC (see report 1). Similar maps allowing comparison were only available from 2007 onwards, so instead we used data from the National Centers for Environmental Prediction/National Center for Atmospheric Research (NCEP/NCAR) reanalysis project (Kalnay et al. 1996).

This is a global data assimilation system complete with land surface, ship, rawinsonde, aircraft, satellite, and other observations, producing analyses of atmospheric fields over the period 1950–present. We chose six fields to compare with the analysis plots for the June 2013 storm (Godfrey 2010; NCEP/NCAR 2014): geopotential heights at 50 kPa, mean sea level pressure, wind speed and direction interpolated to a near-surface reference pressure of 100 kPa, best 4-layer lifted index (a measure of atmospheric stability), precipitable water, and corrected precipitation rate. Definitions and details of each variable are given in appendix B. Multiple plots (using the available 00Z and 12Z times) covering each event were analyzed in

order to view the development of features, e.g. storm speed, lowest pressure centre, moisture source, prevailing winds, etc.

# 3. Data analysis

### *a. Spatial analysis*

Heavy precipitation in the AB Rockies can be brought about by one or a combination of the following factors (G. West, 2014, pers. comm.):

- **Closed low at 50 kPa** advecting Pacific moisture towards the Canadian Rockies. Deeper and slower-moving closed lows tend to bring the largest amounts of precipitation, having more time to both destabilize the atmosphere and transport moisture. A typical storm will move from southwest to southeast British Columbia (BC) in about 12 hours, but these quasi-stationary storms tend to linger around Washington and Oregon. They are typical in May and June.

- Quasi-stationary surface low-pressure system or troughing in lee of Rocky Mountains, leading to **easterly upslope flow** in the AB Rockies. These systems have been observed transporting monsoonal moisture from southern US, even the Gulf of Mexico (e.g. the June 2013 Canmore storm).

- Progressive (faster-moving) low-pressure system with associated **frontal precipitation**.

- **Thunderstorms** either embedded in fronts and/or triggered by upslope flow.

With these features in mind, each of the 18 heavy precipitation events was "scored" according to which factors they included, as follows (scoring points are in parentheses):

a. Upper-level low (1), slow-moving (+1), low centre $\leq$ 5,500 m (+0.5).

b. Upper-level trough (1).

c. Surface closed low (1), quasi-stationary and centred over Canmore (+0.5), low centre $\leq$ 99.8 kPa (+0.5), surface trough with axis near Canmore (+0.5).

d. Surface trough with front (1) (can score with c **or** d, not both).

e. Easterly component to flow at upper level (0.5), and/or at lower level (0.5).

f. Precipitable water: $\geq$ 20 kg m$^{-2}$ during greatest storm precipitation (1), and/or from a subtropical source: Gulf of Mexico (0.5) and/or Pacific (0.5).

g. Atmospheric stability (to represent thunderstorms): lifted index $<$ 0°C (0.5) or lifted index $<$ −3°C (1).

For example, the April 2003 storm scored 2.5 for feature 'a', having a slow-moving upper-level low with centre reaching 5,350 m (fig. 4). The June 1952 storm scored 2.5 for feature 'c', having a surface low pressure system lingering over Canmore, with central pressure 99.5 kPa, and a surface trough with the axis near Canmore also contributing during the storm (fig. 5). Figure 6 illustrates that the June 2001 storm scored 0.5 for having an easterly component to the near-surface wind, and the June 2012 storm scored 2 points for having precipitable water content $\geq$ 20 kg m$^{-2}$, with its origins being both the subtropical Pacific and the Gulf of Mexico (fig. 7). The maximum score possible for one storm is 10.

Following this analysis, the storms could be classified somewhat, setting them apart according to their main mechanisms and contributing factors: upper-level low, upper-level low + subtropical or monsoonal moisture $\geq$ 20 kg m$^{-2}$, upper-level low + subtropical moisture $\geq$ 20 kg m$^{-2}$ from Pacific **and** Gulf of Mexico, frontal, and main mechanism unclear.

The scoring system was an attempt to quantitively find a correlation between spatial features and the heavy rainstorm frequency or precipitation amount, but there is none obvious (fig. 8). Namely, several different types of synoptic weather systems can cause heavy precipitation near Canmore. Despite the attempt to include thunderstorms by using the

lifted index, this is not well-modelled nor well-resolved by the coarse resolution reanalysis data (see appendix B), thereby contributing to this lack of correlation.

15 of 18 cases have upper-level closed lows, spanning all months in which the storms occurred, with 11 of them being quasi-stationary, and 1 of those associated with the passage of a frontal system. The deeper upper-level lows (low centre $\leq$ 5,500 m) all occurred between April and June, and the deeper surface lows (low centre $\leq$ 99.8 kPa) all occurred in May and June. Progressive frontal systems accounted for 3 cases, and despite tending to score lower, associated precipitation amounts were comparable to storms having different mechanisms, so they should not be discounted.

The storms that entrained large amounts of subtropical moisture occurred mostly since 1990, these being the highest scoring cases. This shows a potential shift in the large-scale pattern, bringing more moisture from the south (subtropics). However, the pattern is not completely new, because the 1952 case included subtropical moisture. Also, there are four storms, including the June 2013 storm, in which moisture was advected from both the subtropical Pacific Ocean and the Gulf of Mexico. This did not occur before 1990 (for these cases).

Judging by the spatial analysis of large-scale features, the June 2013 event was not unique, with similar storms occurring in 1990, 1995, 1998, 2005, and 2012. As discussed, one explanation for the greater precipitation amounts in 2013 is thunderstorms. These are not well accounted for in this analysis. Also, the scoring system is rather subjective and definitely does not account for all the variance.

Temporal analysis on the precipitation data is carried out in the next section.

### *b. Temporal analysis*

The return period, $RP$, of a heavy precipitation event can be calculated using the following equation:

$$RP = \frac{N}{\sum_{i=1}^{N} f_i} \tag{1}$$

where $f_i$ is the event frequency for $N$ years ($i$ = 1,$N$). Using all precipitation data in the period 1952–2013, we computed $RP$ for 1981–2013, with a sliding window of $N = 30$ years (the standard time period to define a climatological average) using a 1-year interval (fig. 9). From 1982–1989, $RP = 6$ years, meaning that the probability of a heavy precipitation event occurring in one of those years is 1/6. From 2007–2013, $RP \leq 3$ years, and there is a clear downward trend in between these two time periods. This implies that heavy precipitation events are now approximately twice as likely to occur as they were 30 years ago.

### *c. Investigation into the correlation of heavy precipitation events with natural climate cycles*

#### 1) El Niño Southern Oscillation

El Niño Southern Oscillation (ENSO) events have historically been related to regional extremes in weather, such as hurricanes, droughts, and floods (Hanley et al. 2003). ENSO events tend to last 6–18 months, their fingerprint is seen mainly in the tropics, and the mechanisms are relatively well understood (Mantua and Hare 2002).

Several indices are commonly used to classify ENSO events, including averaged sea-surface temperature (SST) anomalies over at least six different regions in the tropical Pacific, to the surface atmospheric pressure-based index, as well as the multivariate ENSO index (MEI), which includes sea-level pressure, zonal and meridional surface wind components, SST, surface air temperature, and total cloud fraction. Based upon analysis of these indices, ENSO can be classified into three phases: warm (El Niño), cold (La Niña) and neutral.

To determine a warm (cold) phase, Trenberth (1997) recommends using data from the region bounded by 5°N–5°S, 120°–170°W known as Niño 3.4, with the Japanese Meteorological Agency (JMA) definition that 5-month running means of monthly SST anomalies must be greater than (less than) a certain threshold for at least six consecutive months. The MEI approach claims to provide a more complete and flexible description of ENSO than with using just one variable (Wolter and Timlin 2011). The correlation coefficient between the Niño 3.4 and the MEI indices is $r = 0.88$, giving confidence in their use yet showing enough difference to assess both.

The Niño 3.4 SST anomalies and MEI indices (5-month running means) are calculated for the entire period (1952–2013) (fig. 10). Threshold values used to classify the ENSO phase are determined using the upper quartile to define an El Niño event, and the lower quartile to define a La Niña event (Hanley et al. 2003). [The upper (lower) quartile for the Niño 3.4 SST anomalies is 0.57°C (−0.56°C), and the upper (lower) quartile for the MEI indices is 0.62 (−0.59) (dimensionless).]

The heavy precipitation events are also plotted in figure 10. With the Niño 3.4 data, 12 precipitation events occurred during a neutral ENSO phase, 4 at the end of an El Niño, in April, May or June, and 2 during the onset of a La Niña, in August and September. With the MEI data, 15 precipitation events occurred during a neutral phase, 2 at the end of an El Niño in May and June, and 1 in the 14th month (August) of a cold phase which persisted for 34 months.

Based upon this analysis, there is no direct correlation between ENSO phase and southern AB heavy precipitation events as defined in this study. When a heavy precipitation event did coincide with El Niño conditions, it was at the end of the warm phase during springtime. Similarly, when a precipitation event coincided with La Niña conditions, it was during the onset of the cold phase in August or September. However, all precipitation events occurred between April and September, with 14 of 18 events in May or June, so the ENSO data does not necessarily add to their predictability, since they are expected at this time of year

anyway.

### 2) Pacific Decadal Oscillation

The Pacific Decadal Oscillation (PDO) can be observed by regime shifts in ENSO indices. Events persist for 20–30 years, the effects are mainly seen in the extratropics, particularly the North Pacific [it is strongly correlated with the Aleutian Low (Mantua et al. 1997)], and finally the mechanisms causing PDO variability are not well known (Mantua and Hare 2002). Regimes are commonly reported in the literature as follows: warm phase from 1925–1946 (prior to the dates used in this study, 1952–2013), cold phase from 1947–1976 (Bonsal and Shabbar 2011; Gan et al. 2007; Mantua and Hare 2002; Zhang et al. 1997), warm phase from 1977 onwards, with possible flip to cold phase in 1998 (Gan et al. 2007). It remains to be seen whether 1998 marks the beginning of 20–30 year cold phase (Mantua and Hare 2002).

The PDO Index uses North Pacific Ocean (poleward of 20°N) SST anomalies from 1900–1993 (Mantua 2000). Monthly mean global average SST anomalies are removed. The correlation coefficient between the 5-month running mean PDO and MEI (Niño 3.4) indices is $r = 0.63$ ($r = 0.51$) so we chose to compare the PDO and MEI indices (fig. 11). The regime shift to warm PDO phase in 1977 can be observed, as well as a sharp change in 1998.

Several periods within the phases determined in the literature could be considered significant shifts, e.g. in 1957–1958. The subsequent warm period lasted only a few years which is perhaps why it has received little emphasis in previous studies (Zhang et al. 1997). Strongly negative values at the end of the 1980s and early 1990s are also generally ignored in the modal classification of the PDO.

There appears to be no correlation between the literature-defined PDO epochs above and heavy precipitation events. Six events occur during the initial cold (negative) phase. Despite a break in precipitation events that seems to correspond with the proposed 1977 regime shift, 4 events occur between 1990 and 1998, while the PDO index is still positive. The remaining 8 events happen during what the literature considers a PDO cold phase. Judging by the

PDO index alone, 9 events occur during a warm phase, and 9 during a cold phase.

The apparently random spread of heavy precipitation events throughout all ENSO/PDO modes (since 1952) agrees with the findings of Gan et al. (2007) and Bonsal and Shabbar (2011), that relationships between ENSO/PDO and Canadian climate are strongest during the winter, and that the more consistent impacts are on temperature variables, and to a lesser extent precipitation. In particular, Gan et al. (2007) found that no single climate index can explain more than 30% of interannual precipitation variability in southwest Canada.

Their study region extended from BC across to Manitoba and they included complete precipitation records (not just heavy rain events) from 21 weather stations. With this in mind, accurate seasonal predictions of highly nonlinear precipitation processes are unlikely, using climate indices alone. This is supported by Yarnal and Diaz (1986), who claim that teleconnection patterns mainly capture the large-scale features of variability while local changes in anomaly centres can result in large differences in western North American climate.

Several studies claim that there is an enhancing effect on precipitation response in Canada when ENSO and PDO warm or cold phases coincide (Bonsal and Shabbar 2011; Gan et al. 2007; Mantua et al. 1997). This is not evident for the 18 heavy precipitation events in this study, since only 3 of them were during a potential "enhanced" ENSO and PDO phase, 1 cold and 2 warm (August 1974, and May and June 1998, respectively). There are several other occasions when potential enhancing occurs (fig. 11) but heavy precipitation events do not, such as 1957, 1977, 1983, 1987, to name a few.

Aside from occurring predominantly in winter, correlations between ENSO/PDO and precipitation appear to be with more stratiform than convective storms (Yarnal and Diaz 1986). Since thunderstorms are not well accounted for in this study, and precipitation amounts (fig. 3) do not correlate well with the large-scale analysis scoring system (fig. 8), this speculation could help explain why very little correlation is seen between ENSO/PDO and the 18 heavy precipitation events.

# 4. Summary and Conclusions

### *a. Summary*

Precipitation data from three southern AB stations were used to identify 18 heavy precipitation events, with total precipitation $\geq$ 50 mm/(2 days), from 1952–2013. All cases occurred between April and September, with most storms in May and June. Precipitation amounts per storm were between 50–100 mm, except for three cases, two in 2005 and one in 2013 (this was the June 2013 event, precipitation at Kananaskis exceeded 270 mm).

Reanalysis maps of geopotential height, mean sea-level pressure, wind speed and direction, best 4-layer lifted index, precipitable water, and corrected precipitation rate, were used to intercompare these storms and score them based upon features known to bring heavy precipitation to southern AB. As a result of this classification scoring, most heavy precipitation events occurred due to a slow-moving upper-level closed low.

Also, the deepest low-pressure systems (considering upper and lower levels) occurred between April and May. Since 1990, there is a more regular occurrence of storms tapping moisture from the subtropics, and in particular, new occurrences (for this data) of storms sourcing moisture from both the subtropical Pacific Ocean and the Gulf of Mexico (the highest scoring storms, which includes the June 2013 event). 50% of cases since 1990 included subtropical moisture, as opposed to 39% for the entire 62-year period.

More progressive frontal systems as the main mechanism were rare (3 cases), but brought as much, sometimes more, precipitation as slower-moving storms, so should not be ignored. Some of the disparity between the scoring and precipitation amounts can likely be accounted for by thunderstorms that were not modelled or resolved by the coarse-resolution reanalysis data (this could also be the reason that no storms scored a maximum of 10 points, e.g. the June 2012 storm scored 9 but lacked instability according to the reanalysis data).

The return period of the heavy precipitation events was calculated with a 30-year sliding window and a 1-year interval. A downward trend is observed, from about 6 years in the

1980s to about 3 years from 2007–2013.

Two El Niño Southern Oscillation indices (El Niño 3.4 and MEI) were calculated to determine ENSO phases for the period 1952–2013, but no obvious correlation with heavy precipitation events was found. For the precipitation events that coincided with an ENSO phase (only 6 cases for El Niño 3.4 data), they were either at the end of a warm phase or the onset of a cold phase. However, these times are during spring or autumn when we can expect heavy precipitation events to occur anyway.

There is also no obvious correlation between the Pacific Decadal Oscillation and heavy precipitation events. Some correlation between PDO and precipitation in southwest Canada is reported in the literature for winter and for more stratiform than convective storms.

### *b. Conclusions and further work*

- Most heavy precipitation events that have occurred in southern AB are caused by an upper-level quasi-stationary closed low, as opposed to any other mechanism. The next most important factors are subtropical moisture source(s), and easterly upslope flow/instability. All of these contributed to the June 2013 event.

- There is evidence of a change in the large-scale pattern, with more storms tapping moisture from the subtropics since 1990, in particular from both the Pacific Ocean and the Gulf of Mexico.

- Heavy precipitation events, as defined in this study, are about twice as likely to occur now (having a return period of about 3 years) as 30 years ago.

- A correlation cannot be found between heavy precipitation events and large scale climate signals, specifically the ENSO and the PDO. When they did coincide with ENSO, the timing was consistent, so this is worth investigating further.

- It is not appropriate to use climate indices alone to capture the variability in the

spring/summer heavy precipitation events in this study, many of which have a strong convective component.

This study is somewhat limited by defining heavy precipitation events, thereby reducing available precipitation data substantially. With regards to correlation with climate signals, we suggest that future work includes more precipitation data (more stations and possibly no thresholds) to investigate this thoroughly, and this is beyond the scope of the analysis here.

In addition, further work could include analysis of a higher-resolution dataset in an attempt to better include thunderstorms (instability). The higher resolution data currently available (North American Regional Reanalysis) only dates back to 1977, so it was not included in this study, as this would have reduced the (already small) number of heavy precipitation cases.

We also recommend that a high-quality automatic weather station be installed at Canmore. It would aid in documenting high-precipitation/flood events and could have other advantages for the Town regarding road maintenance, health, and other issues.

*Acknowledgments.*

For the use of NCEP/NCAR reanalysis data, we thank Dr. Christopher Godfrey, the University of North Carolina Asheville, and the National Centers for Environmental Prediction/National Center for Atmospheric Research. NCEP Reanalysis data was provided by the NOAA/OAR/ESRL PSD, Boulder, Colorado, USA, from their website at http://www.esrl.noaa.gov/psd/.

Regarding the use of EC Climate Data Online: the website is official work that is published by the Government of Canada, and the reproduction has not been produced in affiliation with or with the endorsement of the Government of Canada.

Thanks to Matthias Jakob of BGC Engineering Inc. for spearheading this project, and to Andy Esarte at Canmore, AB, for organizing the funding for this work.

# APPENDIX A

## Adjusted and Homogenized Canadian Climate Data

The Adjusted and Homogenized Canadian Climate Dataset (AHCCD) was created for use in climate research. Adjustments are applied to original station data to account for shifts due to instrument changes and observing procedures. Mekis and Vincent (2011) describe the corrections to precipitation records, in particular due to wind undercatch, evaporation, and gauge-specific problems.

Of the three stations in this study, only Banff is included in the AHCCD, and only monthly rain records are available up to 2007. For the 12 months within the AHCCD that contain heavy precipitation events (some months had more than one event), the mean absolute difference between original rain record and adjusted totals is 7.3 mm, with a standard deviation of 2.2 mm. Since this discrepancy is small and we do not know when within the month the correction is applied, we chose to use the original Banff record, which contributed to identifying 8 of the 18 heavy precipitation events.

# APPENDIX B

## Definitions and details of reanalysis variables

a. Geopotential heights (m) at at altitude of roughly 5.5 km, where pressure is 50 kPa. Designated a class A variable by NCEP/NCAR, which is the most reliable class, strongly influenced by observational data.

b. Mean sea level pressure (hPa) (class A).

c. Wind speed (m $s^{-1}$) and direction interpolated to a near-surface reference pressure of 100 kPa (class A).

d. Best 4-layer lifted index (°C) (Galway 1956; DeRubertis 2006). Designated a Class B variable, meaning there are observational data directly affecting the value but the numerical weather prediction (NWP) model has a very strong influence on the analysis value. The lifted index, an indication of atmospheric stability, is based upon the difference between the temperature at 50 kPa and the temperature of a parcel of air lifted to 50 kPa. The more negative the temperature difference is, the greater the chance of thunderstorms (the warmer the parcel is than the environment). For the best 4-layer lifted index, the lifted index is found by lifting from 4 different levels between the surface and 1600 m altitude, and the "best" or most unstable value is kept. This can eliminate times when the surface value may misrepresent the true (deep-layer) instability. Factors leading to a low lifted index value are cold air aloft, large low-level moisture, and a warm surface temperature, for which the latter two variables may not be well modelled in the reanalysis.

e. Precipitable water (kg $m^{-2}$). This is the amount of water vapour in an atmospheric column, integrated between the surface and 10 hPa (∼40 km) (Class B).

f. Corrected precipitation rate (cm $day^{-1}$). Designated a Class C variable, which is not directly affected by observations but derived solely from model fields forced by data assimilation to remain in balance with the atmosphere. Due to this class being more unreliable and smoothing by the NWP model, precipitation data was only used to build confidence in the EC data as to the timing of the heavy precipitation events. Accuracy in rainfall intensity for the NCEP/NCAR data was neglected.

# APPENDIX C

## Other definitions

- Z = Zulu time = coordinated universal time (UTC). UTC = MST + 7 hours.
- mb = millibars, an outdated pressure unit used on some old weather maps.

  1000 mb = 1000 hPa = 100 kPa.

# REFERENCES


Bonsal, B. and A. Shabbar, 2011: Large-scale climate oscillations influencing Canada, 1990–2008. Tech. rep., Canadian Councils of Resource Ministers.

DeRubertis, D., 2006: Recent Trends in Four Common Stability Indices Derived from U.S. Radiosonde Observations. *J. Climate*, **19 (3)**, 309–323, URL http://dx.doi.org/10.1175/JCLI3626.1, doi: 10.1175/JCLI3626.1; M3: doi: 10.1175/JCLI3626.1; 31.

EnvironmentCanada, 2013: National Climate Data and Information Archive Website. URL http://www.climate.weatheroffice.gc.ca/climateData/canada_e.html, URL http://www.climate.weatheroffice.gc.ca/climateData/canada_e.html.

Galway, J. G., 1956: The lifted index as a predictor of latent instability. *Bull. Am. Meteorol. Soc.*, **37**, 528–529.

Gan, T. Y., A. K. Gobena, and Q. Wang, 2007: Precipitation of southwestern Canada: Wavelet, scaling, multifractal analysis, and teleconnection to climate anomalies. *J. Geophys. Res. Atmos.*, **112 (D10)**, n/a–n/a, URL http://dx.doi.org/10.1029/2006JD007157.

Godfrey, C., 2010: NCEP Reanalysis Plotter. URL http://www.atms.unca.edu/cgodfrey/reanalysis/reanalysis.shtml, URL http://www.atms.unca.edu/cgodfrey/reanalysis/reanalysis.shtml.

Hanley, D. E., M. A. Bourassa, J. J. O'Brien, S. R. Smith, and E. R. Spade, 2003: A Quantitative Evaluation of ENSO Indices. *J. Climate*, **16 (8)**, 1249, URL http://search.ebscohost.com/login.aspx?direct=true&db=a2h&AN=9465131&site=ehost-live&scope=site, m3: Article.

Kalnay, E., et al., 1996: The NCEP/NCAR 40-Year Reanalysis Project. *Bull. Am. Meteorol. Soc.*, **77 (3)**, 437–471, URL http://dx.doi.org/10.1175/1520-0477(1996)077<0437:TNYRP>2.0.CO;2, doi: 10.1175/1520-0477(1996)0772.0.CO;2; M3: doi: 10.1175/1520-0477(1996)0772.0.CO;2; 13.

Mantua, N., 2000: The Pacific Decadal Oscillation. URL http://jisao.washington.edu/pdo/, URL http://jisao.washington.edu/pdo/.

Mantua, N. and S. Hare, 2002: The pacific decadal oscillation. *Journal of Oceanography*, **58 (1)**, 35–44, URL http://dx.doi.org/10.1023/A%3A1015820616384, j2: Journal of Oceanography.

Mantua, N. J., S. R. Hare, Y. Zhang, J. M. Wallace, and R. C. Francis, 1997: A Pacific Interdecadal Climate Oscillation with Impacts on Salmon Production. *Bull. Am. Meteorol. Soc.*, **78 (6)**, 1069–1079, URL http://dx.doi.org/10.1175/1520-0477(1997)078<1069:APICOW>2.0.CO;2, doi: 10.1175/1520-0477(1997)0782.0.CO;2; M3: doi: 10.1175/1520-0477(1997)0782.0.CO;2; 27.

Mekis, E. and L. Vincent, 2011: An Overview of the Second Generation Adjusted Daily Precipitation Dataset for Trend Analysis in Canada. *Atmos. Ocean*, **2**, 163–177.

NCEP/NCAR, 2014: NCEP/NCAR Reanalysis 1 Data. URL http://www.esrl.noaa.gov/psd/data/gridded/data.ncep.reanalysis.html, URL http://www.esrl.noaa.gov/psd/data/gridded/data.ncep.reanalysis.html.

Trenberth, K. E., 1997: The Definition of El Niño. *Bull. Am. Meteorol. Soc.*, **78 (12)**, 2771–2777, URL http://dx.doi.org/10.1175/1520-0477(1997)078<2771:TDOENO>2.0.CO;2, doi: 10.1175/1520-0477(1997)0782.0.CO;2; M3: doi: 10.1175/1520-0477(1997)0782.0.CO;2; 25.

Wolter, K. and M. S. Timlin, 2011: El Niño/Southern Oscillation behaviour since 1871 as

diagnosed in an extended multivariate ENSO index (MEI.ext). *Int. J. Climatol.*, **31 (7)**, 1074–1087, URL http://dx.doi.org/10.1002/joc.2336.

Yarnal, B. and H. F. Diaz, 1986: Relationships between extremes of the Southern oscillation and the winter climate of the Anglo-American Pacific Coast. *J. Climatol.*, **6 (2)**, 197–219, URL http://dx.doi.org/10.1002/joc.3370060208.

Zhang, Y., J. Wallace, and D. Battisti, 1997: ENSO-like Interdecadal Variability: 1900–93. *J. Climate*, **10**, 1004–1020, URL http://dx.doi.org/10.1175/1520-0442(1997)010%3C1004:ELIV%3E2.0.CO;2, iD: 3255.

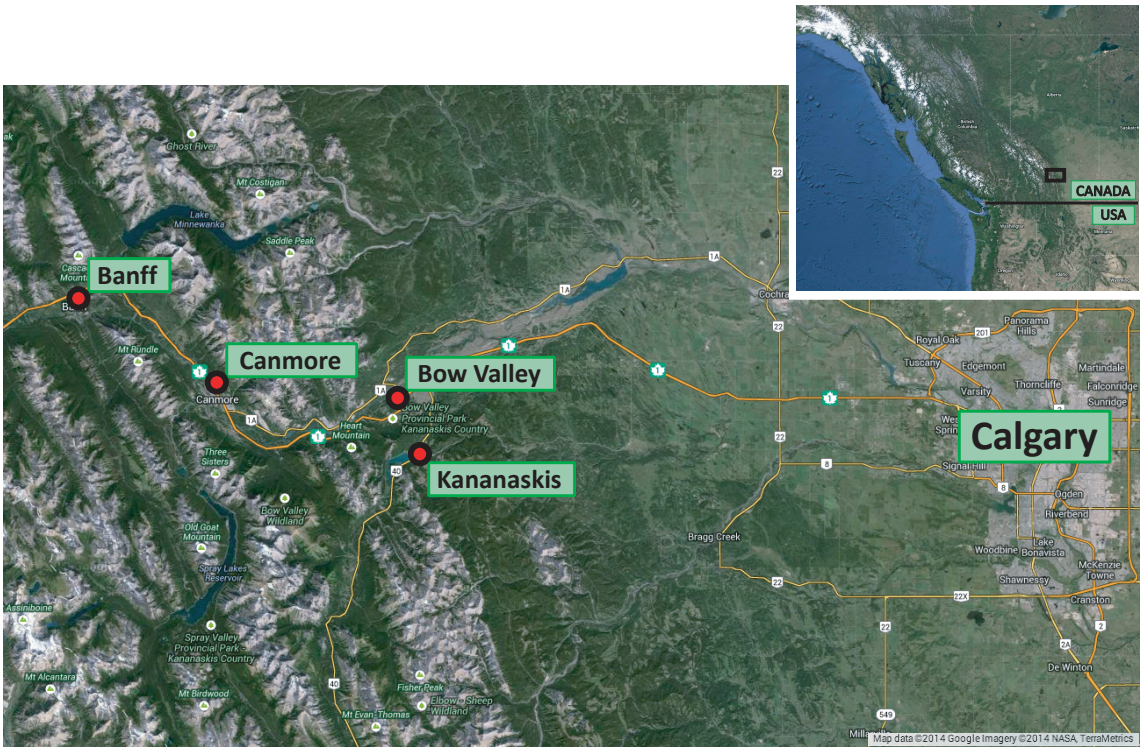


FIG. 1. Map showing locations affected by the June 2013 storm and local Environment Canada weather station locations (Banff, Bow Valley, and Kananaskis) providing monthly and daily precipitation data. (Map data from 2014 Google Imagery.)

TABLE 1. Automatic weather stations near Canmore providing historical monthly and daily precipitation data. Banff and Bow Valley stations were moved during the record, but within close enough proximity to the old station to be considered a continuous record for the purposes of this report.

| Station name | Latitude (N) | Longitude (W) | Elevation (ASL) | Record |
|---|---|---|---|---|
| Banff | 51°11'00" | 115°34'00" | 1383.7 m | 1887–1995 |
| Banff CS | 51°11'36" | 115°33'08" | 1396.9 m | 1995–present |
| Bow Valley Prov. Park | 51°05'00" | 115°04'00" | 1318.0 m | 1967–1990 |
| Bow Valley | 51°05'00" | 115°04'00" | 1297.5 m | 1993–present |
| Kananaskis | 51°01'39" | 115°02'05" | 1391.1 m | 1939–present |

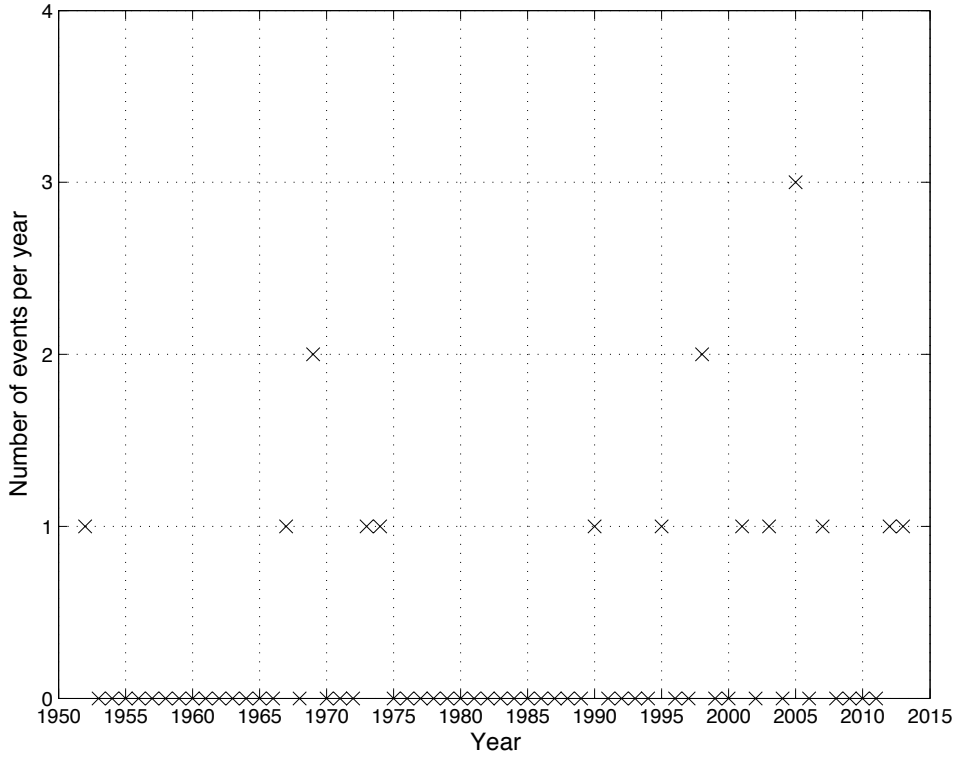


FIG. 2. Frequency of heavy precipitation events per year for the Canmore area, using historical data from Banff, Bow Valley, and Kananaskis stations, between 1952–2013. A heavy precipitation event is defined by total rainfall $\geq$ 50 mm/(2 days) for at least two of the three stations.

TABLE 2. Dates and details of each heavy precipitation event. Storms that had total rainfall $\geq$ 50 mm/(2 days) at all three stations are in bold. Values in parentheses are precipitation totals during the storm that do not reach an excess of 50 mm in the required 2 days for this study. Also noted are some examples of important mechanisms and factors contributing to each storm. For the data in this table, surface lows were centred near to Canmore, easterly flow was present at upper and lower levels, and large amounts of moisture came from the subtropics (Pacific Ocean and Gulf of Mexico). UL = upper-level.

| Year | Dates | Rain total per storm (mm) | | | Main mechanisms and contributing factors | | | | | |
|---|---|---|---|---|---|---|---|---|---|---|
| | | Banff | Bow Valley | Kananaskis | UL low | UL trough | Surface low | Easterly flow | Moisture | Front |
| 1952 | June 21–23 | 54.8 | - | 86.1 | × | | × | | × | |
| 1967 | May 29–30 | (29.2) | 55.1 | 65.6 | × | × | | × | | |
| 1969 | June 23–24 | (17.0) | 62.4 | 67.6 | | × | | | | × |
| 1969 | June 27–28 | (23.1) | 62.5 | 59.2 | × | × | | | | |
| 1973 | May 24–26 | 50.1 | (52.3) | 68.6 | | × | | | | × |
| 1974 | August 11–13 | (35.3) | 57.6 | 63.5 | | × | | | | |
| 1990 | May 24–25 | 51.4 | 73.0 | (44.0) | × | × | × | × | × | |
| 1995 | September 4–6 | (26.8) | 63.4 | 94.2 | × | × | | | × | |
| 1998 | May 26–28 | (31.0) | 51.0 | 73.4 | × | × | | | × | |
| 1998 | June 17–19 | (13.1) | 64.0 | 94.6 | × | | | | | × |
| 2001 | June 2–7 | (6.6) | 57.8 | 73.2 | × | × | | × | | |
| **2003** | **April 24–25** | **57.8** | **58.4** | **60.4** | × | | | | | |
| 2005 | June 5–8 | (52.6) | 120.3 | 137.0 | × | | | | | |
| **2005** | **June 16–18** | **106.8** | **119.4** | **149.2** | × | | | | × | |
| 2005 | September 8–10 | 51.2 | (63.8) | 102.8 | × | × | | | | |
| 2007 | June 15–17 | (30.6) | 78.2 | 90.0 | × | | | | | |
| **2012** | **June 4–6** | **69.5** | **64.7** | **86.2** | × | × | × | × | × | |
| **2013** | **June 18–21** | **90.9** | **219.3** | **272.4** | × | | × | × | × | |

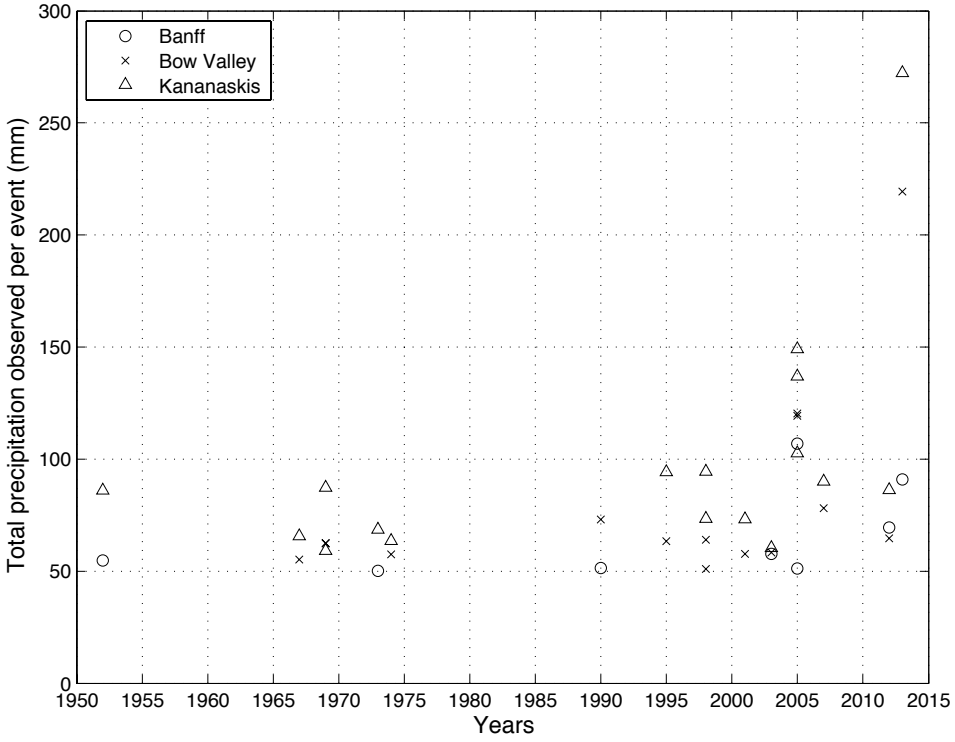


FIG. 3. Precipitation totals at each station, Banff, Bow Valley, and Kananaskis, for the 18 heavy precipitation cases. Note that some years have more than one heavy precipitation event.

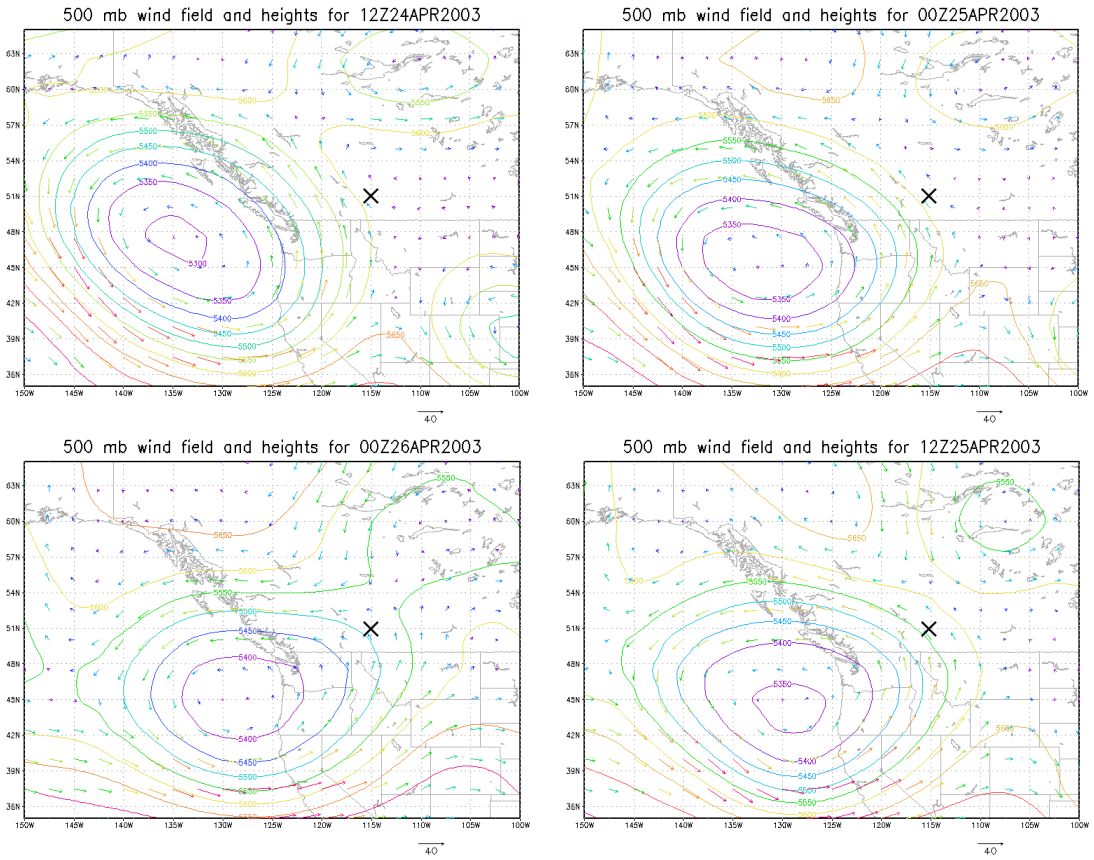


FIG. 4. 50 kPa geopotential heights (contours in metres) and wind direction (vectors) for the April 2003 storm, clockwise from top left: 12Z on 24 April 2003, 00Z on 25 April 2003, 12Z on 25 April 2003, and 00Z on 26 April 2003. A quasi-stationary upper-level low-pressure system is shown, scoring 2.5 points by the scoring system in the text. Canmore is situated at approximately 51°N, 115°W, as indicated with ×.

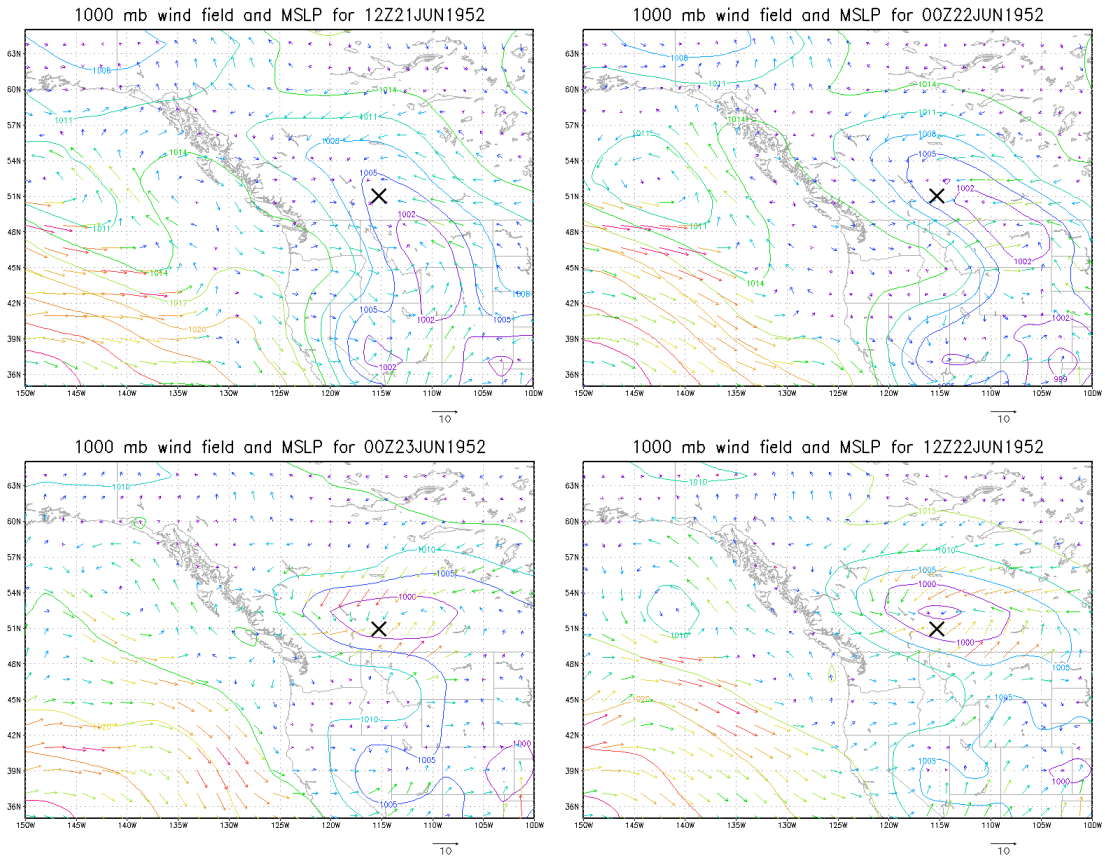


FIG. 5. Mean sea-level pressure (contours in hPa) and wind direction (vectors) for the June 1952 storm, clockwise from top left: 12Z on 21 June 1952, 00Z on 22 June 1952, 12Z on 22 June 1952, and 00Z on 23 June 1952. Surface troughing in the lee of the Canadian Rockies is shown, with a quasi-stationary surface low-pressure system, scoring 2.5 points. Canmore is situated at approximately 51°N, 115°W, marked with ×.

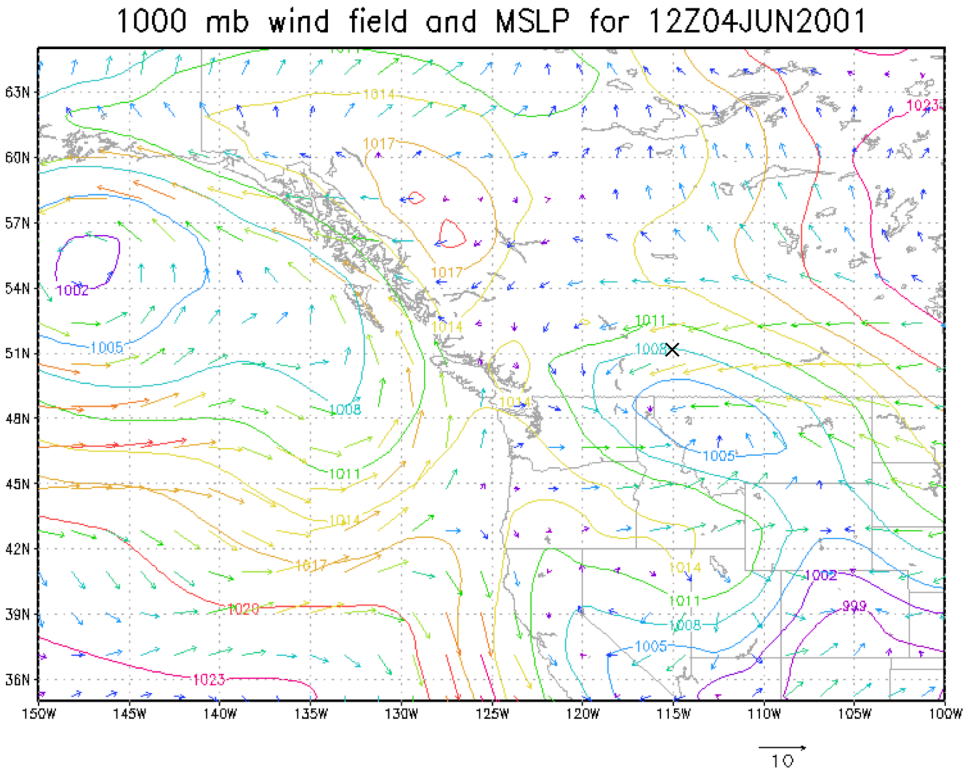


FIG. 6. Mean sea-level pressure (contours in hPa) and wind direction (vectors) for the June 2001 storm (shown here at 12Z on 4 June 2001). An easterly component to the surface winds is evident in the Canmore area and to the lee of the Canadian Rockies, scoring 0.5. Canmore is situated at approximately 51°N, 115°W, marked with ×.

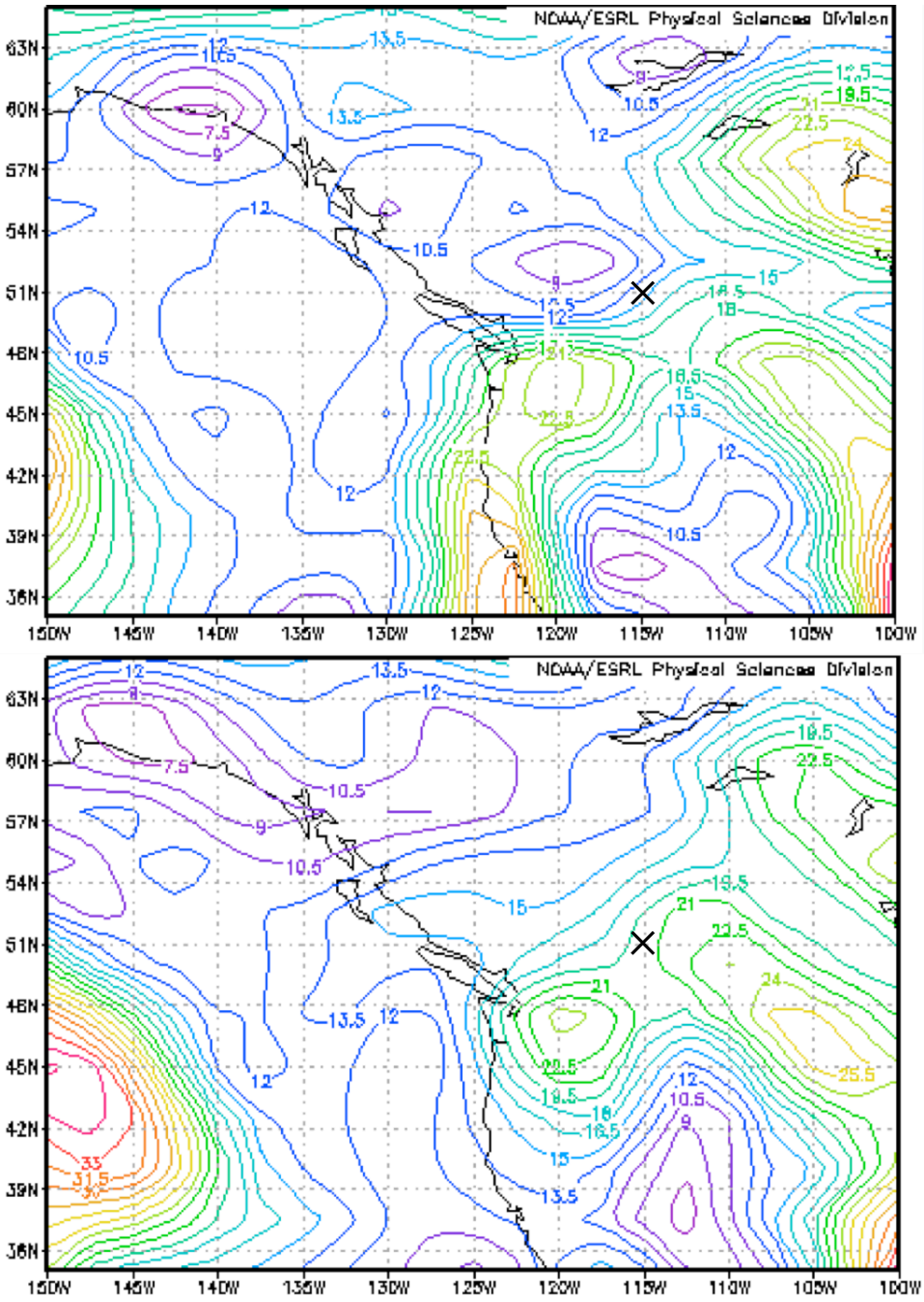


FIG. 7. Precipitable water content (contours in kg $m^{-2}$) for the June 2012 storm. Top: 12Z on 4 June 2012, bottom: 00Z on 5 June 2012 (12 hours later). Canmore is situated at approximately 51°N, 115°W (indicated by ×), with the moisture source advected towards it from the subtropical Pacific and the Gulf of Mexico.

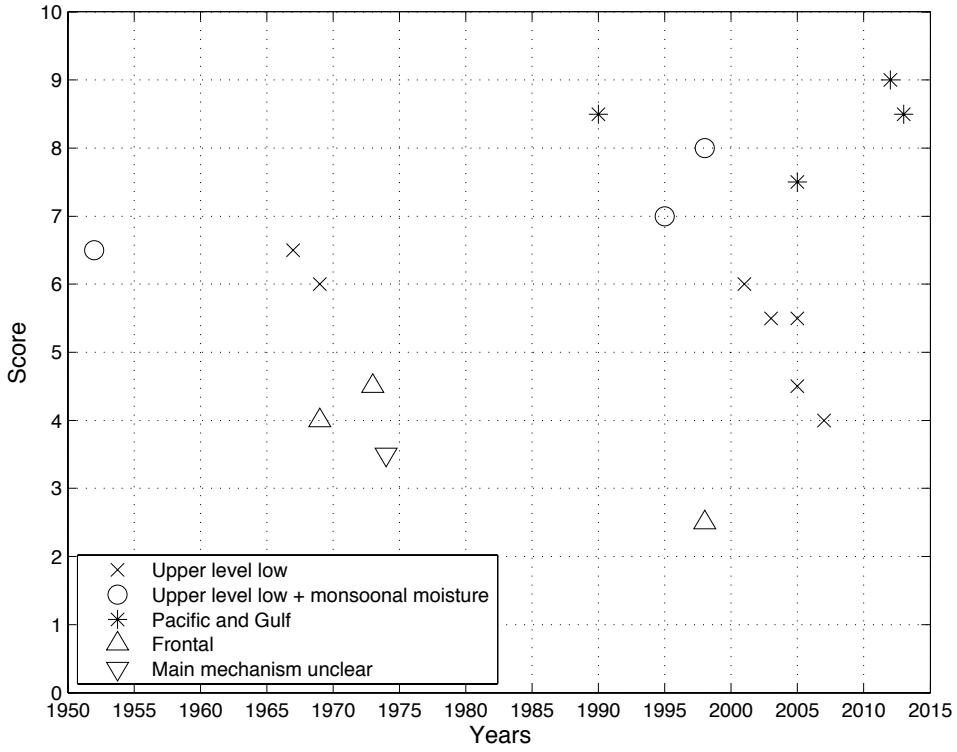


FIG. 8. Total score of each heavy precipitation event according to the rating in the text, plotted by category: upper-level low (crosses), upper-level low plus subtropical moisture greater than 20 kg $m^{-2}$ (open circles), upper-level low plus subtropical moisture greater than 20 kg $m^{-2}$ from Pacific **and** Gulf of Mexico (asterisks), frontal (upward triangles), and main mechanism unclear (downward triangle).

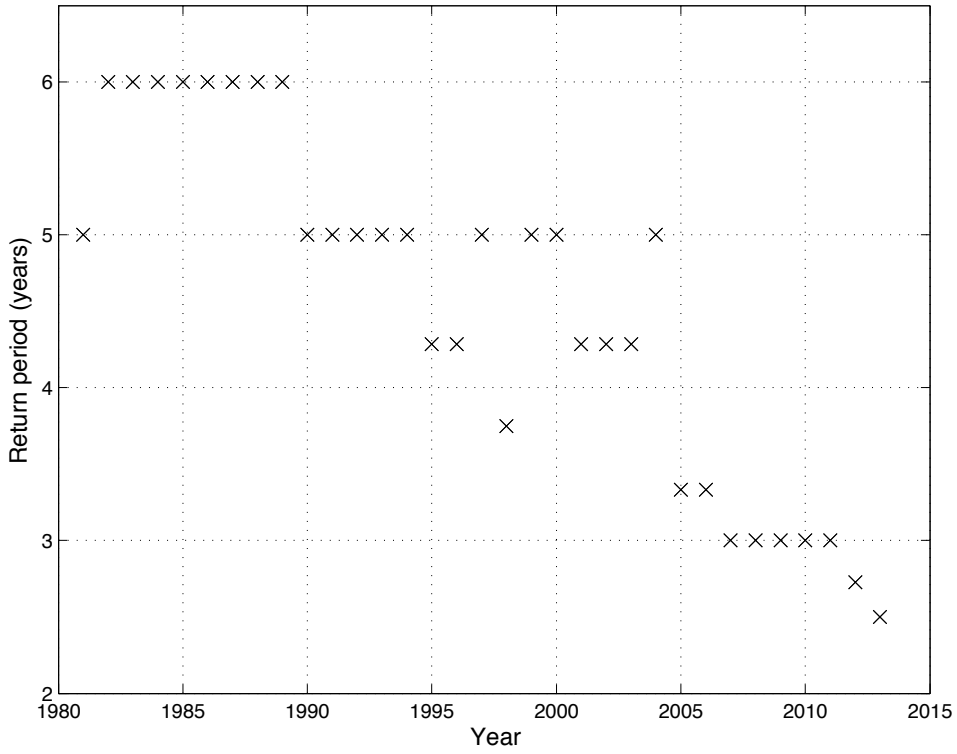


FIG. 9. Return period for heavy precipitation events (as defined in the text) using data from 1952–2013, 18 events in total. Sliding window size is 30 years with a 1 year interval. Each $\times$ corresponds to an average over the 30-year window, ending at the year marked by the $\times$.

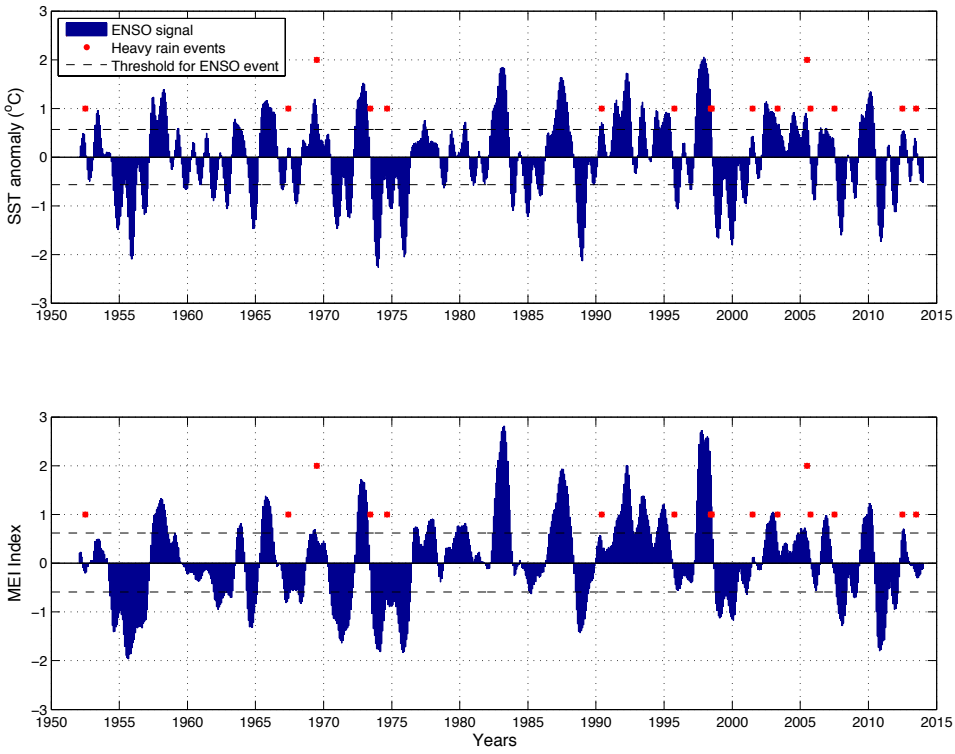


FIG. 10. Time series of the Niño 3.4 index (top panel) and the MEI index (bottom panel) in blue, with upper and lower quartiles (dashed lines) showing thresholds for determining a warm or cold ENSO phase, respectively. The count of southern AB heavy precipitation events is shown with red dots.

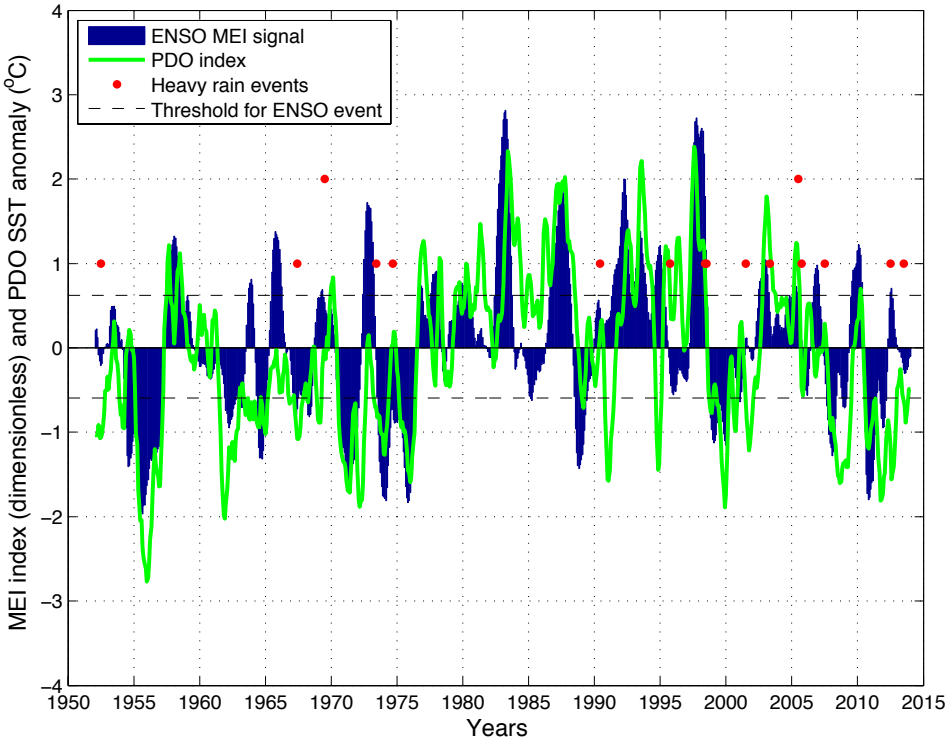


FIG. 11. Time series of the MEI (blue) and PDO (green) index, with upper and lower quartiles (dashed lines) showing thresholds for determining a warm or cold ENSO phase, respectively. The count of southern AB heavy precipitation events is shown with red dots.

# DRAWINGS

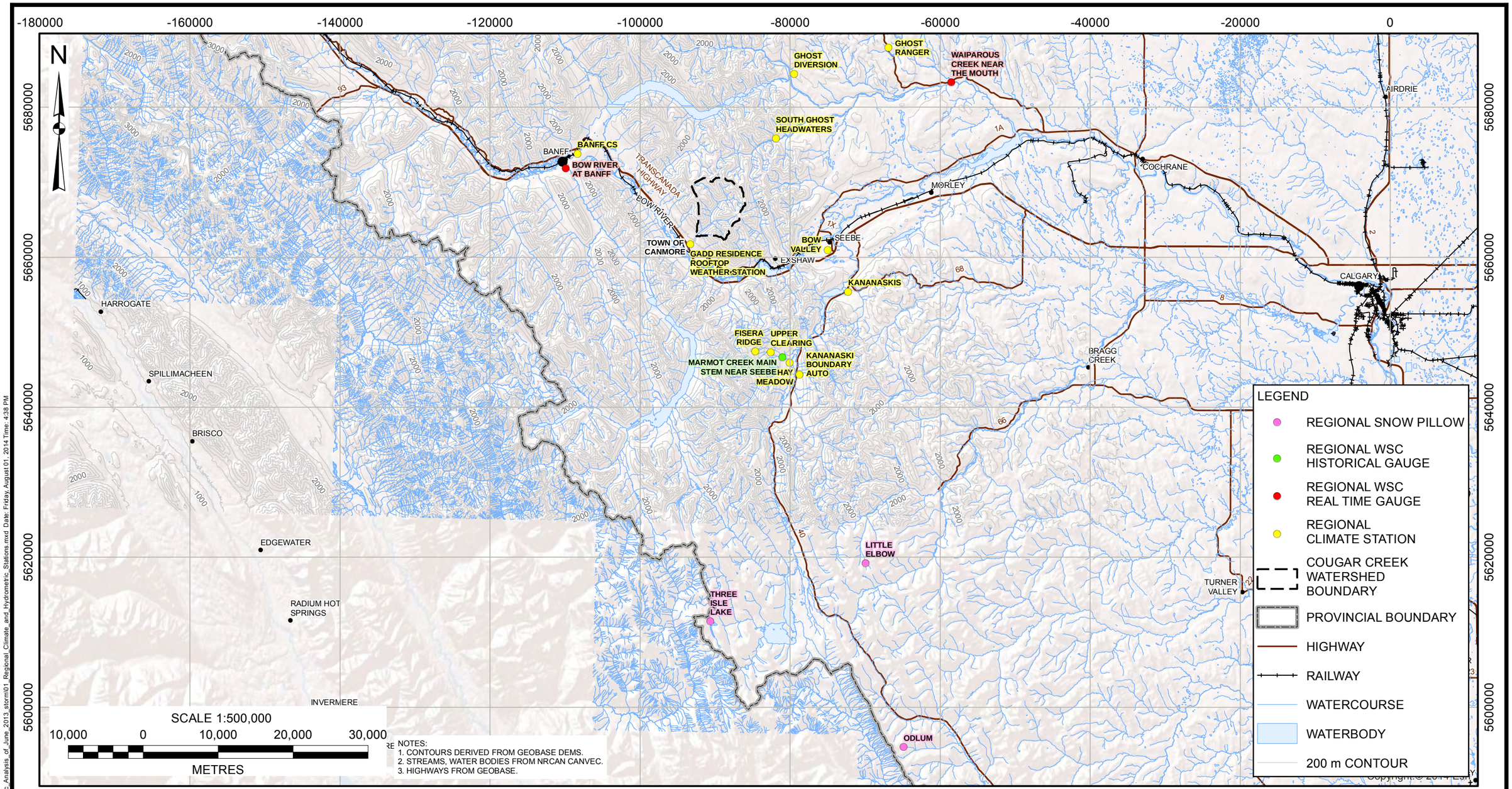




| REV. | DATE | REVISION NOTES | DRAWN | CHECK | APPR. |
|---|---|---|---|---|---|
| | | | | | |

| | |
|---|---|
| SCALE: | 1:500,000 |
| DATE: | AUG 2014 |
| DRAWN: | LL,JS |
| DESIGNED: | AP |
| CHECKED: | HW |
| APPROVED: | JC |

PROFESSIONAL SEAL:

BGC ENGINEERING INC.
AN APPLIED EARTH SCIENCES COMPANY

CLIENT: TOWN OF CANMORE

PROJECT: HYDROCLIMATIC ANALYSIS OF THE JUNE 2013 STORM

TITLE: REGIONAL CLIMATE AND HYDROMETRIC STATIONS

| PROJECT No.: | DWG No.: | REV.: |
|---|---|---|
| 1261001 | 01 | |

X:\Projects\1261001\Workspace\20130930_Hydroclimatic_Analysis_of_June_2013_storm\01_Regional_Climate_and_Hydrometric_Stations.mxd Date: Friday, August 01, 2014 Time: 4:38 PM

DWG TO BE READ WITH BGC REPORT TITLED "HYDROCLIMATIC ANALYSIS OF THE JUNE 2013 STORM" DATED AUGUST 2014